

The enterovirus 71 particle: An evolutionary approach to investigate structure and function with implications for drug and vaccine development.

James Thomas Kelly

Submitted in accordance with the requirements for the degree of Doctor of

Philosophy

Supervisors

Nicola J Stonehouse, David J Rowlands

Industrial Supervisors

Nicolas Burdin, Jeffery Almond

The University of Leeds

School of Molecular and Cellular Biology

September, 2015

The candidate confirms that the work submitted is his own and that appropriate credit has been given where reference has been made to the work of others.

This copy has been supplied on the understanding that it is copyright material and that no quotation from the thesis may be published without proper acknowledgment.

The right of James Thomas Kelly to be identified as Author of this work has been asserted by him in accordance with copy right, Designs and patens Act 1988.

© 2015 The University of Leeds James Thomas Kelly.

Acknowledgements

First and foremost I would like to thank my supervisors Nic Stonehouse and Dave Rowlands, who have both been a tremendous help throughout the whole of my PhD. Both have given me invaluable help and guidance, in lab work, presentation skills and writing. Thank you both for your patience and guidance, it has helped make my PhD both a rewarding and enjoyable (mostly!) experience.

I would like to thank the whole of the Stonelands group past and present for all help and advice given, many enjoyable conversations, and general tomfoolery. With a special thanks to Clare Nicol for helping training me and all other help and advice that she had given me over the last 4 years. I would also like to thank Oluwapelumi Adeyemi and Morgan Herod for the always enjoyable and very intensely speculative discussions about how any minor result or anomaly in an experiment could lead to the next break through Nature paper. Of course Eleni and Joe must get a special mention just for being adorable.

Thank you to all project students I have taught (Amy, Joe, Ross and Lauren) for the hard work they put in and for generally being a pleasure to teach.

Thank you to the members the virology lab and lab 8.54. Especially Becky Surtees for many an attempted conversation over the loud drum of a TC hood.

Thank you to Liz Fry, David Stuart and Luigi DeColibus, for giving me the opportunity to expand on my structural knowledge, and the comments and feedback they have given me on various aspects of my work.

I would also like to thank all the friends I have made over my time in Leeds who have helped make it a very enjoyable experience, especially for the Friday night pub sessions and lunch time conversations.

I would like to thank Amy Radcliffe Lauren Elliott, Luigi De Colibus, Özlem Cesur, Joseph Ward, Oluwapelumi Adeyemi and Jingshan Ren, for the work and they have done that has contributed to my thesis.

I would like to thank all the teachers I have had over the years who have taught me and helped and encouraged me into science, especially my undergraduate and master supervisor Michael Ginger.

Finally I would like to thank my family and girlfriend for their ongoing support throughout my PhD.

Abstract

The capsid plays many important roles in the virus life cycle, including host cell recognition, cell entry, uncoating and protection of viral RNA. In this thesis, artificial selection, use of inhibitory compounds and structural analysis have been combined to further understand aspects of these multiple roles.

The VP1 pocket is a hydrophobic cavity in the capsid that harbours a fatty acid, known as the pocket factor. The presence of this fatty acid can increase capsid stability and its release is required for the virus to uncoat. Certain compounds are able to bind to the pocket and displace the natural fatty acid (causing a further increase in capsid stability) and can inhibit infection by making the virus so stable that it is unable to uncoat. Novel compounds, termed NLD and ALD, have been designed *in silico* based upon the previous best EV71 pocket binding inhibitor GPP3. These were shown to inhibit EV71 infection in cells, with NLD being more than one order of magnitude more potent than the previous best EV71 pocket-binding inhibitor. Resistance towards these compounds was studied to reveal a double mutation in VP1 (I113M and V123L). Mapping the mutations to the EV71 crystal structure revealed that they were located in the VP1 pocket, and modelling predicted that they would prevent NLD and the natural pocket factor from binding. Further characterisation of the resistant isolate revealed that the mutations were thermally- and genetically-unstable.

Further investigation on thermal stability involved selection of a thermally-stable virus. This generated viruses with a double mutation in the VP1 pocket (V179A and

L183V). These mutations were predicted to increase the size of the VP1 pocket, and were shown to affect the way the virus interacts with the natural pocket factor. The effects of a variety of different pocket factors on the heat stability of WT EV71, the thermostable mutant, and the inhibitor-resistant mutant were analysed.

In addition, work was conducted to assess the effect of pH on uncoating. For uncoating it is known that EV71 must be incubated at a low pH in the presence of its major receptor SCARB2. To investigate the effects of this, EV71 was incubated at a low pH during infection. This was shown to reduce the virus titre, and repeated exposure to this condition selected for a VP1 mutation (N104S). This residue is predicted to be involved in binding to SCARB2, and the mutant virus was shown to differ in susceptibility to compounds that affect entry and uncoating.

Abbreviations

BEV ; bovine enterovirus

CAR; Coxsackie and adenovirus receptor

CVA16; Coxsackievirus A16

CVB3; Coxsackievirus B3

DAF; decay accelerating factor

DMSO; Dimethyl sulfoxide

EC50; half maximal effective concentration

ERAV; Equine Rhinitis A Virus

EV1; Echovirus 1

EV71; Enterovirus 71

FMDV; foot-and-mouth disease virus

HAV; hepatitis A virus

HBsAg; hepatitis B surface antigen

HBV; hepatitis B virus

HEVA; human enterovirus A

HFMD; hand, foot, and mouth disease

HPV; human papillomavirus

HRV; Human rhinovirus

HS; heparan sulphate glycosaminoglycan

Hsp; heat shock protein

IC50; half maximal inhibitory concentration

kcal; kilocalorie

Lpro; leader protease

MTT; 3-(4,5-Dimethylthiazol-2-Yl)-2,5-Diphenyltetrazolium Bromide

NP40; nonyl phenoxypolyethoxylethanol Tergitol-type NP-40

OD; Optical density

OPV; Oral Polio Vaccine

PAGE; Polyacrylamide gel electrophoresis

pH; $\log_{10} [H^+]$

PSGL1; P-selectin glycoprotein ligand-1

PV; poliovirus

QMPLD; quantum mechanics-polarised ligand docking

RCF; Relative centrifugal force

RD; Rhabdomyosarcoma

RPM; Revolutions per minute

s.e.m; standard error of the mean

SCARB2; scavenger receptor class B, member 2

SDS; sodium dodecyl sulfate

SVDV; swine vesicular disease virus

TCID; tissue culture infective dose

TEM; Transmission electron microscopy

UTR; untranslated region

v/v; volume over volume

VDPP; vaccine-derived paralytic poliomyelitis

VLP; virus like particle

w/v; Weight over volume

$\Delta\Delta G$; Change in Free folding energy

Table of Contents

Acknowledgements.....	iii
Abstract.....	v
Abbreviations.....	vii
Table of Contents.....	x
Table of Figures.....	xvi
Table of Tables.....	xix
Chapter 1 Introduction.....	2
1.1 Hand, Foot, and Mouth Disease.....	2
1.2 The Picornavirus life cycle.....	5
1.2.1 Genome and capsid structure.....	5
1.2.2 Receptors and Cell entry of picornaviruses.....	10
1.2.3 Co-receptors.....	12
1.2.4 Viral uncoating.....	13
1.2.5 The EV71 capsid and its involvement in cell entry and uncoating.....	15
1.3 Capsid-binding inhibitors.....	22
1.3.1 Resistance against pocket binding compounds.....	26
1.4 Vaccines.....	27
1.4.1 Attenuated vaccines.....	27
1.4.2 Inactivated vaccine.....	29

1.4.3	Pathogen free vaccines: subunit and virus-like particle (VLP) vaccines	31
1.5	Project objectives	36
Chapter 2	Materials and methods	38
2.1	General Buffers, media and reagents.....	38
2.1.1	Luria-Bertoni (LB) Broth	38
2.1.2	10xTBE (Tris-borate-EDTA) buffer pH 8.3	38
2.1.3	6x DNA loading buffer	38
2.1.4	10x <i>Sodium dodecyl sulphate - Polyacrylamide gel electrophoresis</i> (SDS-PAGE) running buffer.....	39
2.1.5	SDS-PAGE stacking gel.....	39
2.1.6	15 % SDS-PAGE resolving gel.....	39
2.1.7	Coomassie blue protein stain.....	40
2.1.8	Cell growth medium (Suspension/microcarrier)	40
2.1.9	Coomassie de-stain solution	40
2.1.10	Tris EDTA (TE) buffer	40
2.1.11	Cell growth medium (Flask)	41
2.1.12	<i>Radio labelling medium</i>	41
2.1.13	Radio-immuno precipitation assay (RIPA) buffer	41
2.1.14	Enhanced chemiluminescence (ECL).....	41
2.1.15	10 x Transfer buffer.....	42

2.1.16	<i>Phosphate-buffered saline (PBS) TWEEN</i>	42
2.1.17	RNA loading buffer	42
2.1.18	Crystal violet stain	43
2.1.19	Blocking buffer	43
2.1.20	Gel dry down buffer	43
2.1.21	Virus re-suspension buffer	43
2.1.22	pH 5.6 buffer	44
2.1.23	Carbonate Coating buffer	44
2.1.24	ELISA Dilution Buffer	44
2.1.25	ELISA Wash Buffer	44
2.1.26	ELISA Assay diluent	44
2.1.27	Antibodies	44
2.1.28	Lipids	45
2.2	Cell culture.....	46
2.2.1	Cell lines used.....	46
2.2.2	Maintenance of cell culture Flasks.....	47
2.2.3	Microcarrier cultures	47
2.2.4	Revival of frozen cells.....	48
2.2.5	Preparation of preserved cell stocks.....	48
2.2.6	Virus infection T175	48

2.2.7	Tissue culture infective dose 50 (TCID ₅₀) assay.....	49
2.2.8	Inhibition of pocket binding inhibitors IC ₅₀ curves	49
2.2.9	Drug inhibition curves knocking down host cell pathways.....	49
2.2.10	Time courses	51
2.2.11	Drug selection	51
2.2.12	pH selection.....	51
2.2.13	Heat selection	51
2.2.14	Heat stability curves.....	52
2.2.15	Radio labelling.....	52
2.3	Gel Electrophoresis methods	53
2.3.1	Agarose gel electrophoresis.....	53
2.3.2	RNA gels	53
2.3.3	SDS-PAGE	53
2.3.4	Western blotting	54
2.3.5	Gel dry down	55
2.4	Cloning.....	55
2.4.1	Transformation of competent cells	55
2.4.2	RNA Extraction	56
2.4.3	RNA Transcriptions.....	56
2.4.4	Reverse transcriptions	56

2.4.5	PCR	56
2.4.6	TOPO cloning.....	56
2.4.7	Sequencing	56
2.5	Purification	58
2.5.1	Purification of Virus through a sucrose gradient (A)	58
2.5.2	Purification of Virus through a sucrose gradient B	58
2.5.3	Nycodenz.....	59
2.5.4	³ H Palmitic acid	59
2.5.5	Scintillation counting.....	60
2.6	Immunoprecipitation	60
2.7	ELISA	60
2.8	PyMol.....	61
Chapter 3	EV71 Compounds – In vitro characterisation and selection of resistant isolates	63
3.1	Characterisation of viral inhibition and cellular cytotoxicity	66
3.2	Selection of resistant mutants	73
3.3	Fitness cost of inhibitor resistant mutations.....	79
3.4	Chapter summary	84
Chapter 4	Growth, cell entry and uncoating of EV71	88
4.1	Cells and purification	92
4.1.1	Optimisation of viral growth	92

4.1.2	Replication kinetics of WT EV71 in Vero cells	95
4.1.3	Viral purification and empty capsid production	100
4.2	A mutant with an altered uncoating phenotype.....	115
4.3	Discussion and future work.....	126
Chapter 5	Heat stability of EV71 and ways to increase it.....	131
5.1	Capsid stability.....	134
5.1.1	Long term stability of EV71/CVA16.....	134
5.1.2	Evolution of an EV71 isolate with increased thermal stability	136
5.1.3	Determination of heat stability mutations	141
5.1.4	Effect of different pocket factors on the thermostability of WT EV71 and isolates with VP1 pocket mutations.....	143
5.1.5	Binding of pocket factors to virus	148
5.1.6	Effect of pocket factors in other enteroviruses	150
5.2	The potential use of antibodies and/or purified receptor to distinguish between heated and native empty particles.....	155
5.2.1	Immunoprecipitation of EV71 using capsid antibodies D6 and A9 ...	155
5.2.2	Use of ELISA in combination with EV71 receptors and antibodies to detect native EV71 antigenicity	157
5.3	Discussion	159
Chapter 6	Concluding remarks and future perspective.....	166
Chapter 7	Bibliography.....	177

Appendix	192
----------------	-----

Table of Figures

Figure 1.1. Lesions typical of HFMD. (Accessed: 09/03/2016)	3
Figure 1.2 Schematic of the enterovirus genome.....	6
Figure 1.3. Diagram of the icosahedral pseudo-T=3 capsid of EV71.	10
Figure 1.4.....	16
Figure 1.5. Acid induced conformational change in SCARB2 creates a connection between its own hydrophobic tunnel and the EV71 hydrophobic VP1 pocket.....	20
Figure 1.6 The enterovirus pocket.	25
Figure 3.1 Structures of different 3-(4-pyridyl)-2-imidazolidinone derivatives with anti-EV71 activity. Images modified from DeColibus et al. 2014.	64
Figure 3.2 IC ₅₀ Inhibitory effects of NLD (green), GPP3 (blue), ALD (orange) and GPP4 (red) on EV71.....	67
Figure 3.3 Inhibition of CVA16 by GPP3. CVA16 samples were titrated via TCID ₅₀ assay in the presence of a range of concentrations of GPP3.	68
Figure 3.4 The inhibitory effects of fatty acids on EV71 (A), PV (B) and BEV2 (C).....	69
Figure 3.5 Toxicity of NLD, GPP3 and ALD to Vero cells.	71
Figure 3.6 Selecting for inhibitor resistant virus.....	74
Figure 3.7 Generation of resistant isolates.....	75
Figure 3.8 (A) Structure of the EV71 protomer in complex with NLD.	78
Figure 3.9 Inhibitor resistant isolates are genetically unstable.....	80

Figure 3.10 One step growth curves of inhibitor-resistant and WT EV71.....	81
Figure 3.11 Inhibitor-resistant mutants are more thermolabile than WT virus.	83
Figure 4.1. Acid induced conformational change in SCARB2 creates a connection between its own hydrophobic tunnel and the EV71 hydrophobic VP1 pocket.....	91
Figure 4.2 Comparative yields of different strains of EV71.	93
Figure 4.3 Comparative yields of EV71 in different cell lines.	94
Figure 4.4. Optimising growth techniques for EV71.	95
Figure 4.5 Growth of EV71. (A)	99
Figure 4.6 Sucrose gradient profiles of ³⁵ S labelled BEV and EV71.....	102
Figure 4.7 Virus titres of different EV71 pellets.....	104
Figure 4.8 Sucrose gradient profiles and titrations of ³⁵ S labelled EV71 after treatment with SDS.	105
Figure 4.9 Sucrose gradient profiles of ³⁵ S labelled EV71 grown in RD cells.	107
Figure 4.10. Analysis and comparison of EV71 purified through Self-forming (40 w/v %) and step (20%-60 w/v %) Nycodenz gradients.	110
Figure 4.11 High buoyancy EV71 is sensitive to NP40 treatment.....	112
Figure 4.12 Effect of chloroquine on high and low buoyancy EV71.....	113
Figure 4.13 The effect of heating on the nycodenz gradient profile of EV71.....	114
Figure 4.14. pH treatment of virus on cells has a fitness cost.	116
Figure 4.15 Sequence alignments of VP1 of Enterovirus A species.....	118
Figure 4.16 Acid induced conformational change in SCARB2 causes an alpha helix to move towards VP1 N104.....	119
Figure 4.17 Analysis of the effect of inhibitors of cell entry.....	121

Figure 4.18 Endosome acidification plays an important role in WT EV71 and acid-resistant EV71.	122
Figure 4.19 Cyclosporine A can prevent EV71 infection but is significantly less effective against the acid-resistant mutant.	123
Figure 4.20 Potential role of cyclophilin A using crystal structure.	125
Figure 5.1 Long term stability of EV71 (A) and CVA16 (B).	135
Figure 0.1 Heat stability curves of WT EV71 and thermostable EV71.....	138
Figure 5.3 Selection of a thermostable EV71 isolate. A T25 was infected with EV71, after 100% cell death.	139
Figure 5.4 Difference in titres between EV71 thermostable mutants before and after heating.....	140
Figure 5.5 Grow kinetics of WT EV71 and thermostable EV71.....	140
Figure 5.6 Location of thermostabilising mutations.	142
Figure 5.7 Effect of fatty acids on heat stability of EV71 isolates with different pocket mutations.	146
Figure 5.8 Effect of a pocket-binding inhibitor on heat stability of EV71 isolates with different pocket mutations.	147
Figure 5.9 Nycodenz gradient profiles	149
Figure 5.10 Crystal structures reveal BEV1 and BEV2 have different sized VP1 pockets.	151
Figure 5.11 Effect of heating on BEV2 after incubation in the presence of short chain fatty acids.	154

Figure 5.12 Antibodies recognise native virus particles but not heated virus particles.....	156
Figure 5.13 Graphs to illustrate ELISA results of EV71.....	158
Figure 5.14 Comparison of location of mutations in (A) inhibitor-resistant/thermolabile EV71 and (B) thermostable.....	160

Table of Tables

Table 1.1 Table of identified HEVA viruses and their symptoms.....	4
Table 1.2 Receptor table.....	21
Table 2.1 Cell lines.....	46
Table 2.2 Concentrations, pre-treatment times and functions of drugs used in this study.....	50
Table 2.3. Primers used in sequencing	57
Table 3.1 Therapeutic window of NLD, GPP3 and ALD against EV71.....	72
Table 3.2 Resistance mutations. Mutations identified in EV71/CVA16 after passage in the presence of NLD, GPP3, ALD or a combination of NLD/GPP3. CVA16 isolates resistant to NLD or ALD were not selected	76
Table 4.1 Recovery of EV71 or BEV2 viruses after sequential steps during purification.....	103
Table 5.1 Pocket factor table.....	145

Chapter 1

Chapter 1 Introduction

Enterovirus 71 (EV71) is a member of the Picornaviridae family and the major causative agent of hand, foot, and mouth disease. This family is made up of non-enveloped viruses that are around 30 nm in diameter and are encoded by a single positive sense RNA segment that is translated as a single poly-protein (Tuthill et al. 2010). Picornaviruses cause a wide range of diseases that affect both human and animal health. Examples include poliovirus (PV) causing poliomyelitis, hepatitis A virus (HAV) causing acute hepatitis and foot-and-mouth disease virus (FMDV) that causes foot and mouth disease in cloven hoofed animals.

1.1 Hand, Foot, and Mouth Disease

The virus species human enterovirus A (HEVA) is composed of several different viruses that can cause a variety of diseases, including, hand, foot, and mouth disease (HFMD), hyperaemia and flaccid paralysis. The details of what symptoms each virus can cause can be found in table 1. Of the diseases caused by the HEVA species, HFMD poses the largest public health problem, with sporadic outbreaks occurring globally and regular seasonal outbreaks occurring in the Asian Pacific region each year (reviewed in McMinn 2012). The disease usually manifests as self-limiting infection of young children, causing small sores to appear on the hands, feet, mouth and buttocks of the individual (Fig 1.1). However in more severe cases it can cause brain stem encephalitis, cardiopulmonary disease and death (McMinn et al. 2001, Zhang et al. 2011). The two most common viruses associated with HFMD are enterovirus 71 (EV71) and Coxsackievirus A16 (CVA16) although CVA16 is

less commonly associated with severe symptoms (McMinn 2003, McMinn et al. 2001, Zhang et al. 2011). In China alone, 7 million cases of HFMD were reported over four years, and of those over 80,000 were classified as severe with EV71 confirmed to be the major causative agent (Xing et al. 2014).



Figure 1.1. Lesions typical of HFMD. Taken from WWW, nhs.uk 2012. Available at: <http://www.nhs.uk/Conditions/Hand-foot-and-mouth-disease/Pages/Introduction.aspx> (Accessed: 09/03/2016)

Virus	Main Symptom	Other symptoms
CVA2	Hyperaemia	HFMD
CVA3	Hyperaemia	HFMD
CVA4	Hyperaemia	HFMD
CVA5	Hyperaemia	HFMD
CVA6	Hyperaemia	HFMD
CVA7	HFMD	Hyperaemia, Neurological
CVA8	Hyperaemia	
CVA10	Hyperaemia	HFMD
CVA12	Hyperaemia	HFMD
CVA14	HFMD	Hyperaemia
CVA16	HFMD	Hyperaemia
EV71	HFMD	Hyperaemia, Neurological
EV76	Flaccid paralysis	
EV89	Flaccid paralysis	
EV90	Flaccid paralysis	
EV91	Flaccid paralysis	
EV92	Flaccid paralysis	

Table 1.1 Table of identified HEVA viruses and their symptoms.

1.2 The Picornavirus life cycle

1.2.1 Genome and capsid structure

The picornavirus family is composed of 29 different genera (WWW picornaviridae 2015. Available at; <http://www.picornaviridae.com/> (Accessed: 09/03/2016)). All of which possess a single stranded positive sense RNA genome that ranges between 7000 and 8500 nucleotides and encodes for a single polyprotein. The genome arrangement between different genera is similar but not identical (Fig 1.2 reviewed in Tuthill et al. 2010). The genome begins with the 5 prime untranslated region (5' UTR) which contains a number of important features, such as the internal ribosome entry site (IRES) and clover leaf that are involved in functions such as replication and translation. It is also covalently linked to a small peptide (VpG) encoded by the viral genome that is essential in replication (reviewed in Tuthill et al. 2010). The genome ends with the 3 prime untranslated region which terminates with a poly-A tract, the 3'UTR has functions in translation and replication (reviewed in Tuthill et al. 2010). The rest of the genome encodes for a single polyprotein, which is co- and post-translationally cleaved into its mature protein components by virally encoded proteases. The first third of the polyprotein (P1) codes for structural proteins (VP0 (VP4/VP2), VP3, VP1) and the remaining two thirds (P2 and P3) consist of non-structural proteins (2A, 2B, 2C and 3A 3B, 3C and 3D) that are involved in viral replication and modification of the cellular environment. Certain picornaviruses (e.g. aphthoviruses and cardioviruses) also encode for another non-structural protein that precedes P1, called the leader protease (L^{pro}). This protein initiates host cell shut off, which is a method of promoting viral gene expression by the

repressions of host gene translation. It performs this by cleaving eukaryotic translation initiation factor 4GI (eIF4GI), which is essential for translation in eukaryotic cells. Other picornaviruses (e.g. enteroviruses) do not possess a leader protein and instead this function is carried out by 2A (e.g. PV). (Reviewed in Tuthill et al. 2010)

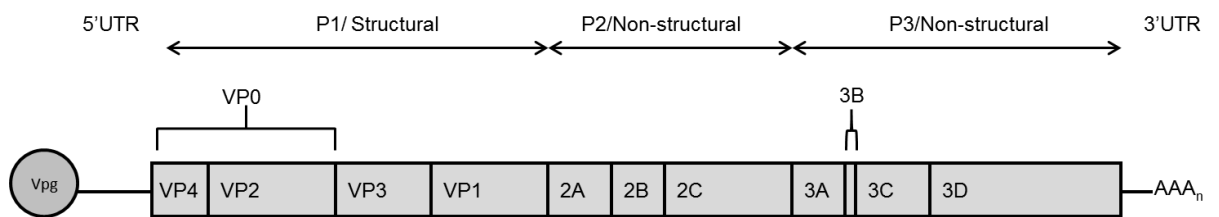


Figure 1.2 Schematic of the enterovirus genome. The single ORF is indicated by a rectangle flanked by 5' and 3' UTRs. A single polyprotein is translated from the ORF which is subsequently cleaved into mature proteins by proteases encoded within the polyprotein.

After translation the structural precursor protein P1, is co- translationally released from the rest of the polyprotein by *cis*-cleavage carried out by 2A^{pro} (Li et al. 2001). In the majority of picornaviruses the N-terminus of P1 is modified by the covalent addition of a myristic acid residue, which is thought to have important roles in assembly and cell entry (Chow et al. 1987). However this does not occur in HAV and viruses from the genera parechovirus and kobuvirus (Tesar et al. 1993; Johansson et al. 2002). Post cleavage, the P1 region of enteroviruses and cardioviruses has been shown to be dependent on heat shock protein (Hsp) 90 and possibly Hsp70, to maintain a processing-competent conformation and as protection from proteasomal degradation (Geller et al. 2007; Macejak & Sarnow 1992; Mutsunguma et al. 2011). These interactions allow P1 to be cleaved (although not

physically separated) into VP0, VP1 and VP3 by 3CD^{pro} to form a protomer (Ansardi et al. 1991; Ypma-Wong et al. 1988).

Cleavage allows protomers to then self-oligomerise into a pentameric subgroup and 12 of these associate to form a capsid (Guttman & Baltimore 1977; Hoey & Martin 1974; Lee et al. 1993). In most picornaviruses if viral RNA is present then pentameric subunits will assemble round it and VP0 will undergo an autocatalytic reaction to form VP2 and VP4 in the mature capsid. This VP0 cleavage does not occur in parechoviruses and kobuviruses (Johansson et al. 2002). If no RNA is present, capsid assembly will still occur, but it will form an empty capsid without VP0 cleavage (Basavappa et al. 1994, Curry et al. 1997). Certain enteroviruses, such as bovine enterovirus (BEV) and PV type 3, naturally produce high ratios of empty particles to full particles, while others such as PV type 1 produce very few naturally empty particles. The reason for production of empty capsids is not currently known, one hypothesis is that they act as a reservoir of capsid proteins (Nugent and Kirkegaard 1995). However work in BEV has shown this to be unlikely as it was deemed energetically unfavourable to force the capsid to dissociate into its components prior to reassembly (Guttman & Baltimore 1977; Marongiu et al. 1981; Li et al. 2012). Another potential purpose of them is that they sequester antibodies from the mature infectious virions to act as a form of immune evasion mechanism (Shingler et al. 2015). Mature capsids will naturally become empty capsids after uncoating, and this can be mimicked by heating. These particles are distinguishable from naturally empty capsids as VP0 cleavage has occurred (Basavappa et al. 1994; Ansardi & Morrow 1995).

It is possible to distinguish between mature and empty capsids by their sedimentation on a sucrose gradient, with the denser mature capsids sedimenting at 160S while empty capsids containing no RNA sediment at 80S. (Chow et al. 1987, Fricks and Hogle 1990)

Picornavirus mature capsids are composed of VP1-3 externally and can be classified as either a T=1 or a pseudo T=3, due to the fact that as mentioned earlier the proteins VP1-3 never actually separate (Reviewed in Tuthill et al. 2010; Wang et al. 2012). VP4 is internal and forms an internal lattice, which is thought to stabilise the capsid. Naturally empty particles do not possess VP4 because VP0 has not undergone cleavage, due to RNA not being present at the time of encapsidation. This causes them to be less structurally stable, readily converting from native (N) type antigenicity to heated (H) type antigenicity (Rombaut and Jore 1997). In PV this has been shown to occur at temperatures above 5 °C (Jim Hogle, personal communication). The three major structural proteins (VP1-3) have a similar basic structure, consisting of eight stranded beta barrels with connecting loops of various lengths, and each has a wedge shape. The composition and shape of these three proteins determine the antigenicity and receptor binding sites (Reviewed in Tuthill et al. 2010). In aphthoviruses and HAV, capsids have a smooth surfaces with the receptor binding site of aphthoviruses being a flexible loop protruding from the surface, the receptor binding site of HAV is unknown (Acharya et al. 1989; Logan et al. 1993; Wang et al. 2015). In cardioviruses the capsid is characterised by a series of shallow depressions spanning the two fold axis, the depressions function as receptor binding sites (Luo et al. 1987; Grant et al. 1994; Hertzler et al. 2000; Toth

et al. 1993). Enterovirus capsids are characterised by a series of much deeper depressions, surrounding the 5-fold axis on VP1, these are referred to as canyons (Rossmann et al 1985). The canyon functions as the major receptor binding site, although other areas of the capsid have also been implicated in receptor binding (Olson et al. 1993; Chen et al. 2012; Colonno et al. 1988). Beneath the canyon is a large hydrophobic space known as the VP1 pocket. In aphthoviruses and cardioviruses this space is filled with large side chains (Acharya et al. 1989; Tuthill et al. 2009). Generally the enterovirus VP1 pocket is filled with various hydrophobic lipids known as pocket factors, this plays an important role in capsid stability and uncoating (Wang et al. 2012; Plevka et al. 2012). Crystal structures have shown that enterovirus pockets can dramatically vary in size, which influences the size of pocket factor that they can accommodate. The predicted fatty acid sizes range from between 10 carbons (e.g. enterovirus 68 (EVD68)) and 18 carbons (e.g. PV) (Liu et al. 2015; Filman et al. 1989). One study using mass spectrometry to determine the pocket factor of bovine enterovirus type 1 (BEV1) revealed that viruses will naturally harbour several different pocket factors (Smyth et al. 2003). This explains observations of crystal structures of different enteroviruses that showed electron densities of the pocket factors can start to fade towards the end, as the structures are on average the fading indicates that the pocket factors vary in size (Smyth et al. 1995). The presence of the pocket factor has been shown to be important for enterovirus capsid stability and the expulsion of this molecule is necessary to facilitate the structural rearrangements necessary for receptor binding and/or uncoating of a number of different enteroviruses (Shepard et al. 1993; Dang et al. 2014).

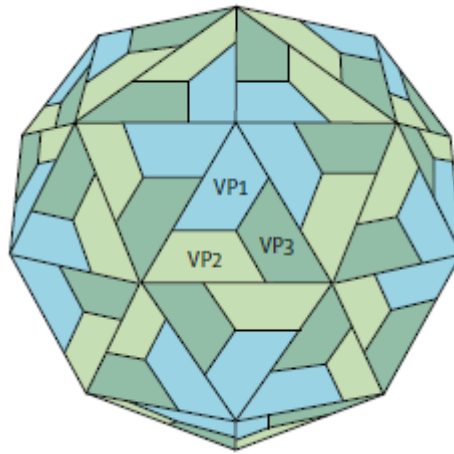


Figure 1.3. Diagram of the icosahedral pseudo-T=3 capsid of EV71. Taken from Solomon et al. 2010.

1.2.2 Receptors and Cell entry of picornaviruses

Binding to a receptor is very important for picornaviruses in terms of its life cycle as it is essential for cell entry and sometimes uncoating. Most picornaviruses studied have been shown to be able to utilise a variety of different receptors and co-receptors. Which receptor it binds can affect what cell type it can enter, which entry pathway it utilises, how it uncoats and pathogenesis (reviewed in Tuthill et al 2010).

The two best characterised entry pathways for the picornaviridae are the clathrin and caveolae dependent pathways, although clathrin and caveolae independent pathways have also been observed.

In the clathrin dependent pathway, the virus binds to a receptor, this initiates the recruitment of clathrin to the surrounding plasma membrane by various adaptor and accessory proteins (Schmid et al. 2006; reviewed in Doherty & McMahon

2009). After recruitment the clathrin polymerises, which forms a curved lattice and induces a curvature of the plasma membrane, this is known as a clathrin coated pit. This then causes deformation of the attached membrane creating a neck, so that it forms a clathrin coated vesicle (reviewed in Doherty and McMahon 2009). After the neck has formed, dynamin which is a large GTPase, forms a helical polymer around the neck of the newly formed vesicle and upon GTP hydrolysis, induces the release of the vesicle from the plasma membrane (Praefcke et al. 2004). The clathrin coated vesicle becomes internalised, and clathrin is released from the vesicle by auxilin and hsc70. The naked vesicle undergoes further trafficking to the early endosome (reviewed in Doherty & McMahon 2009). By this pathway viruses usually enter within a minute of attachment to the receptor. Aphthoviruses (FMDV and Equine Rhinitis A Virus (ERAV)), enteroviruses (Human rhinoviruses (HRV), EV71, swine vesicular disease virus (SVDV)), have all been shown to utilise the clathrin dependent pathway of cell entry using a variety of different receptors between them (reviewed in Tuthill et al. 2010).

Caveolin dependent endocytosis, like clathrin dependent endocytosis, also functions via creating a curvature of the membrane. In this method of endocytosis, receptor binding initiates the recruitment of caveolin 1 to the site of the receptor, which is located in an area rich in sphingolipids and cholesterol (reviewed in Doherty & McMahon 2009; Mulcahy et al. 2014). Oligomerisation of caveolins facilitated by caveolin oligomerisation domains, mediates formation of caveolin rich rafts in the plasma membrane. This causes a curvature in the plasma membrane and forms a pit known as a caveola. The caveolae can be internalised, much like

clathrin coated pits and are released from the plasma membrane by dynamin (reviewed in Doherty & McMahon 2009). Echovirus 1 (EV1) and CVB3 have been shown to enter via the caveolar dependent pathway (Marjomaki et al. 2002, Pelkmans et al 2005).

In addition to the clathrin and caveolin dependent entry pathways other picornaviruses such as PV have been shown to be internalised via a non clathrin, non caveolin pathway (Brandenburg et al. 2007)

1.2.3 Co-receptors

Sometimes viruses need multiple receptors to facilitate cell entry. One example is Coxsackievirus B3 (CVB3) entry into polarized epithelial cells (reviewed in Tuthill et al. 2010). CVB3 has two known receptors; decay accelerating factor (DAF) and Coxsackie and adenovirus receptor (CAR) (Coyne et al 2007). It has been shown that DAF is unable to facilitate cell entry on its own, yet in certain cell lines it is essential for entry (Shafren et al. 1997). In polarized epithelial cells CVB3 requires the presence of both DAF and CAR for cell entry. In these cells CAR is only expressed within tight junctions, an area that is usually inaccessible to the virus. However when the virus binds DAF, it triggers signalling-dependent transport of the receptor-virus complex directly to the tight junctions. This allows the virus to access CAR, and therefore facilitates cell-entry (Coyne & Bergelson 2006).

1.2.4 Viral uncoating

Once the virus has entered the cell, it needs to transport the genomic RNA out of the capsid and into the cytoplasm to undergo translation and replication. This process is known as uncoating. In certain picornaviruses, this has been shown to be triggered by interactions with the receptor (PV), a drop in pH (aphthoviruses, HRV), or both (EV71) (Tuthill et al 2009, Chen et al 2012).

Uncoating of picornaviruses takes place in the endosome. After cell entry the virus is trafficked to the early endosome, which progresses to become a late endosome. During the maturation process the endosomal pH is progressively reduced by the action of an ATP dependent proton pump. Treatment of cells with compounds that prevent either endosomal acidification (e.g. chloroquine) or maturation (e.g. nocodazol) has proven that these functions are essential for infection by some viruses (Baxt 1987; Berryman et al. 2005; Gropelli et al. 2010; Dimmock & Tyrrell 1963; Ashraf et al. 2013).

The following picornaviruses have been shown to be sensitive to disruptions in endosome acidification; aphthoviruses (Gropelli et al. 2010), HRVs (Dimmock & Tyrrell 1963; Ashraf et al. 2013) , EV71 (Lin et al. 2012; Lin et al. 2013) , SVDV (Martín-Acebes et al. 2009; Fry et al. 2003) and HAV (Superti et al. 1987; Feng et al. 2013). Aphthoviruses and HRVs are sensitive to acidic conditions, however this is not the case in EV71, SVDV, HAV or PV. By tracking the conversion of mature capsids into capsid subunits (aphthoviruses) or empty capsids (other picornaviruses) it can be demonstrated that HRVs and aphthoviruses are sensitive towards acidic conditions is because it induces viral uncoating, mimicking what

occurs in the cell during endosome acidification (Tuthill et al 2010). This conversion can be demonstrated by sucrose gradient centrifugation analysis which can separate mature particles and empty particles/capsid subunits which have undergone uncoating and released their RNA. In EV71 conversion of mature to empty capsids can only be triggered by incubation at pHs below six in the presence of either scavenger receptor class B, member 2 (SCARB2, also known as LIMP2) or cyclophilin A (Chen et al. 2012; Qing et al. 2014). While in PV incubation with its receptor CD155 alone is sufficient to induce uncoating (Fricks & Hogle 1990).

Although it is fairly well established what triggers certain uncoating events, the exact mechanisms and the structural rearrangements that occur during uncoating are poorly understood in most non-enveloped viruses (reviewed in Suomalainen & Greber 2013). Most of what is known about picornavirus uncoating has come from comparisons of mature particles, uncoating intermediate particles and empty particles in enteroviruses which are termed 160S, 135S and 80S particles respectively based upon their sedimentation coefficients in sucrose gradients. The RNA has been ejected from empty particles either following heating or receptor binding and as they are derived from mature virions they have undergone VP0 cleavage unlike the natural empty particles discussed in section 1.2.1, where no RNA encapsidation has occurred. From the comparison of crystal structures of PV and EV71/CVA16, 160S, 135S and 80S particles, it is known that during the conversion of 160S to 135S particles and 80S the particles expand, the pocket factor leaves the VP1 pocket and the pocket becomes collapsed so that it can no longer accommodate a pocket factor and openings form at the 5-fold axis, the 2 fold axis

and the base of the canyon (Basavappa et al. 1994; Xiangxi Wang et al. 2012; Ren et al. 2013). During conversion N-myristoylated VP4 and the N-terminus of VP1 become externalised, most likely leaving from either the base of the canyon or the 2 fold axis (Bostina et al. 2011; Bubeck et al. 2005). This allows exit of VP4 and the amphipathic helix on the N-terminus of VP1 (Ren et al. 2013). The VP1 N-terminus is thought to tether the virus to the membrane while VP4 acts as a viroporin, to form a hole in the endosomal membrane (Panjwani et al. 2014). Together they also most likely form a 50 Å long tube between the virus and the membrane that allows RNA egress from the capsid, through the endosomal membrane and into the cytoplasm. This model has been supported by evidence derived by electron tomography analyses (Danthi et al. 2003; Davis et al. 2008; Strauss et al. 2013). It is known that RNA will not spontaneously exit a 135S particle and what triggers release of the RNA and where it exits from the capsid is unknown (Xiangxi Wang et al. 2012; Shingler et al. 2013; Chou et al. 2013). Once the RNA has left the endosome into the cytoplasm it is able to be translated and then replicate.

1.2.5 The EV71 capsid and its involvement in cell entry and uncoating

EV71 has a genome structure and function typical of the picornavirus family Fig 1.2.

The capsid is a standard enterovirus capsid, described in section 1.2.1. In the assembled structure VP2 and VP3 alternate around the threefold axis, which resembles a three-bladed propeller-like structure, while VP1 components cluster around the fivefold axis, which resembles a star shaped protrusion (Fig 1.4) and the VP1 N-termini are situated in close proximity to the twofold axis (Wang et al 2012).

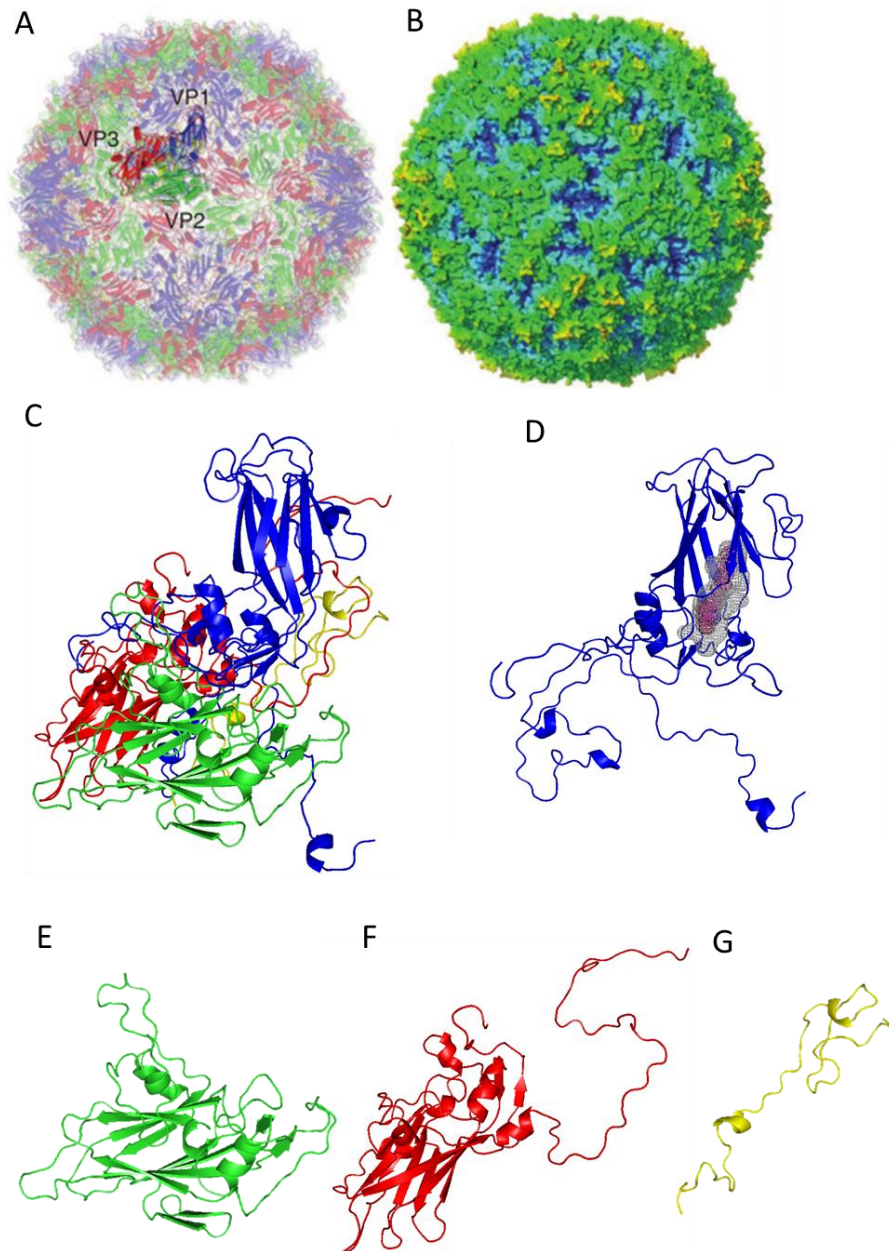


Figure 1.4. Crystal structure of EV71 capsid, radius coloured surface of mature EV71 particle, taken from Wang et al 2012. (A) Cartoon of mature EV71 virion, looking down an icosahedral two-fold axis, VP1, VP2, VP3 and VP4 are drawn in blue, green, red and yellow, respectively. A single icosahedral promoter is highlighted more brightly (taken from Wang et al 2012). (B) Radius coloured surface representation of the EV71 mature particle, the surface is coloured according to distance from the particle centre with blue to yellow (blue being the closest). (C) Cartoon representation of a promoter drawn in PyMol. Individual capsid proteins represented as cartoons using PyMol, VP1 with the hydrophobic

pocket represented as a grey mesh and the pocket factor modelled as a sphingosine in hot pink (D), VP2 (E), VP3 (F) and VP4 (G).

VP1 of EV71 contains several different structures and features that are important for cell entry and uncoating. There is a canyon situated below the fivefold axis and the mesa located on the DE loop, which connects the β D and β E strands of the VP1 β barrel, which are the two receptor binding sites (Yamayoshi et al. 2009; Nishimura et al. 2009). In addition there is a region on the VP1 HI loop, adjacent to the VP1 DE loop, which is an interaction site for the uncoating initiator cyclophilin A. Finally beneath the canyon is a large hydrophobic space known as the VP1 pocket.

Generally this hydrophobic pocket is filled with a lipid known as the pocket factor and in the two crystal structures for EV71 it is predicted to be either sphingosine or lauric acid (Wang et al. 2012; Plevka et al. 2012). The presence of the pocket factor has been shown to be important for enterovirus capsid stability and the expulsion of this molecule has been implicated in receptor binding and or uncoating of a number of different enteroviruses including EV71 (described in more detail in section 1.2.1) (Shepard et al. 1993; Dang et al. 2014).

In many enteroviruses the canyon is the binding site of the major uncoating receptor, which for EV71 is SCARB2. In addition, the mesa on the DE loop is the binding site and the predicted binding site of P-selectin glycoprotein ligand-1 (PSGL1 also known as SELPLG or CD162) and heparan sulphate glycosaminoglycan (HS). There are other proposed receptors which are detailed in table 1.2, but their binding sites are unknown or unconfirmed. SCARB2 and PSGL1 are the only two receptors that have been shown to facilitate cell entry. SCARB2 is able to bind every known isolate of EV71, while PSGL1 is predicted to bind ~20% of EV71 isolates

(Yamayoshi et al. 2012; Nishimura et al. 2013). PSGL1 binding isolates possess residues in the mesa that cause it to have positively-charged amino acid side chains exposed on the virus surface. This coincides with the fact the EV71 has been shown to require a negatively charged sulphated tyrosine at the site of virus interaction within the N-terminal region of PSGL-1 (Nishimura et al. 2013; Nishimura et al. 2010; Nishimura et al. 2009). Both SCARB2 and PSGL1 are able to induce endocytosis using the clathrin and caveolin-mediated endocytosis receptively, and both require endosome acidification to progress a cellular infection (Lin et al. 2012; Lin et al. 2013). This is likely necessary to induce viral uncoating, as both known uncoating initiators of EV71 (SCARB2 and cyclophilin A) require a low pH to induce uncoating, as measured by conversion of S160 to S135 or S80 particles (Chen et al. 2012; Yamayoshi et al. 2013; Dang et al. 2014; Qing et al. 2014).

Cyclophilin A interacts with the HI loop on VP1, which is adjacent to the PSGL1 binding site (DE loop) but its full interaction with the capsid is not known, so it may also interact with other areas (Qing et al. 2014). Interaction with cyclophilin induces structural rearrangements that alter affinity towards certain receptors. Interaction with cyclophilin A has been shown to reduce the capacity of the virus to bind SCARB2, increases its ability to bind HS and does not affect its ability to bind PSGL1 (Qing et al. 2014). It has also been shown to require pH 6 to induce uncoating and is completely ineffective at pHs 5.5 and 6.5 (Qing et al. 2014). However, the exact mechanism of how uncoating is mediated via cyclophilin A is unknown.

The interaction between SCARB2 and the EV71 capsid is better understood and this forms a plausible model for uncoating based on functional data and a docking

model of the two respective crystal structures (Dang et al. 2014). In this model EV71 binds SCARB2, which induces clathrin dependent endocytosis. The endosome undergoes acidification, leading to a reduction in pH which causes SCARB2 to undergo a conformational change. This links the hydrophobic VP1 pocket to its own hydrophobic channel, which is predicted to be a lipid transfer tunnel, thus creating a hydrophobic channel between the two (Fig 1.5) (Dang et al. 2014). Using co-Immunoprecipitation it was shown that at low pH SCARB2 was able to dislodge ^3H sphingosine from the virus capsid, sphingosine being the predicted pocket factor (Dang et al. 2014; Wang et al. 2012). It was predicted that the pocket factor leaves the pocket through the hydrophobic tunnel in SCARB2. Loss of the pocket factor reduces capsid stability and allows the capsid to undergo the conformational changes necessary to uncoat (Dang et al. 2014). SCARB2 induced uncoating has been shown to occur at pHs between 4.8 and 5.6 but is most efficient at pH 5.6. (Chen et al. 2012; Dang et al. 2014) (Fig 1.5).

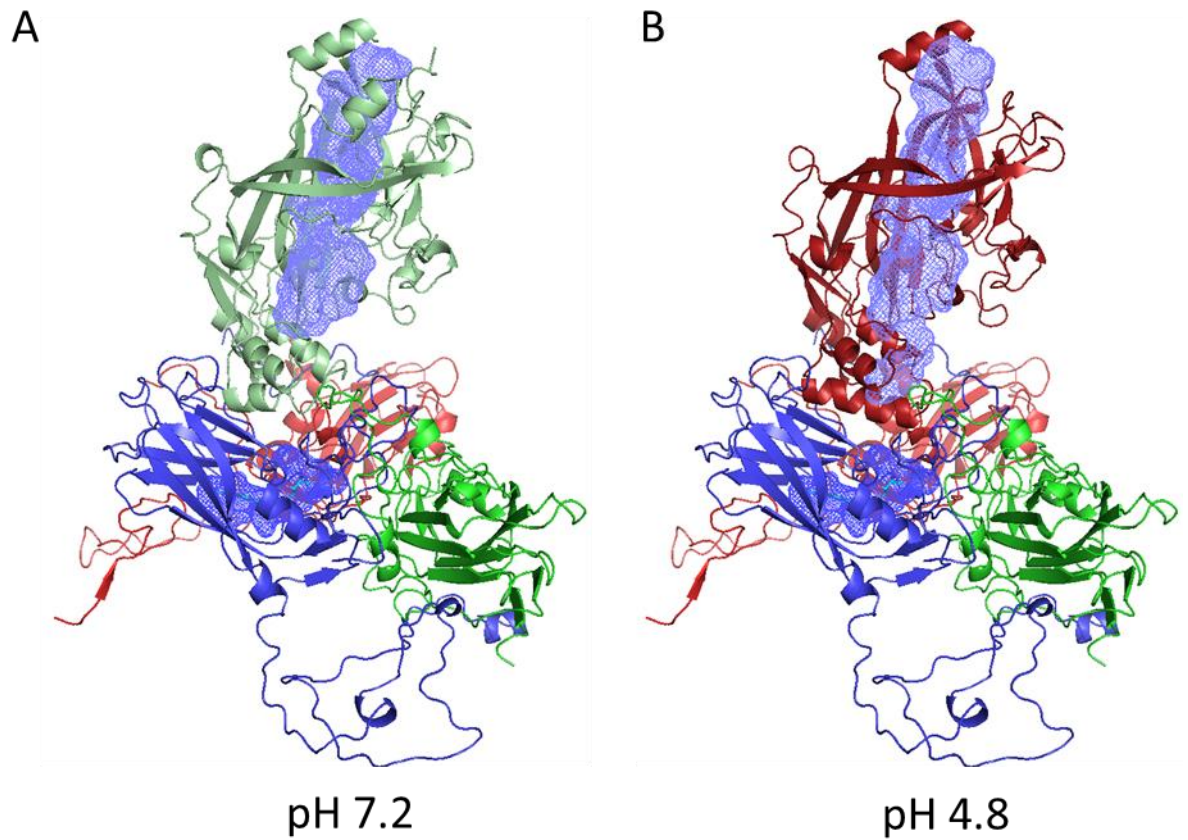


Figure 1.5. Acid induced conformational change in SCARB2 creates a connection between its own hydrophobic tunnel and the EV71 hydrophobic VP1 pocket. PyMol cartoon representation of docking model SCARB2 in its neutral conformation (A mint green) and acid induced conformation (B brick red) with an EV71 protomer composed of VP1 (Blue), VP2 (Green), VP3 (Red), hydrophobic spaces are represented by blue mesh, pocket factor is represented by cyan sticks in the VP1 pocket. Produced in PyMol using the Protein Data Bank (www.rcsb.org/pdb) from Dang et al. 2014.

Receptor	Cell Line(s)	Uncoating	Interaction sites	Reference
SCARB2/Lysosome membrane protein 2 (LIMP-2)	Vero, RD	✓		Yamayoshi et al. 2009
P-selectin glycoprotein ligand-1 (PSGL1)/SELPLG/CD162	Jurkat	X		Nishimura et al. 2009
Heparan Sulphate	RD, CHO	X		Tan et al. 2013
Annexin II	RD	X	VP1 40-180	Yang et al. 2011
Sialic acid (SA)	DLD-1 intestinal cells	X		Yang et al. 2009
DC-SIGN	immature DCs	X		Lin et al. 2009
Vimentin	RD, HeLa, Vero	X		Du et al. 2014
Nucleolin	RD, NIH 3T3	X		Su et al. 2015

Table 1.2 Receptor table. Cell surface molecules that can bind to the capsid and assist either cell entry or uncoating. ✓ confirms it is involved in that process, while X denotes it is not. Sites of the virus capsid interacts are mentioned when known.

1.3 Capsid-binding inhibitors

As mentioned in section 1.2.1, enteroviruses have a structure known as the VP1 pocket, which for most enteroviruses contains a hydrophobic lipid known as the “pocket factor”. This molecule stabilises the capsid and is expelled during receptor binding. This destabilises the capsid and allows it to undergo structural rearrangements that are associated with either receptor binding and/or uncoating (Dang et al. 2014). Certain molecules are able to displace the pocket factor, due to a higher binding affinity, and prevent infection by preventing the viruses from binding to its receptor and/or uncoating (Pevear et al. 1999).

The original pocket binding compounds discovered were the WIN compounds; these were effective against a small subset of rhinoviruses and had IC_{50} values of $\sim 0.06 \mu\text{M}$ (Smith et al. 1986). Since the discovery of WIN compounds, many new pocket binding compounds have been either discovered or developed, with increased potency and different host ranges. Two such compounds that show promise for clinical use are Pleconaril and Vapendavir (BTA798) which have both undergone phase II clinical trials; these are to be used to treat asthmatic patients with chronic rhinovirus infections (Rotbart et al. 1998; Feil et al. 2012).

These pocket binding compounds, along with many others have been tested against a large range of enteroviruses. In the case of EV71 however it was shown that many of these broad range acting pocket binding compounds had either no effect or relatively high EC_{50}/IC_{50} values. Vapendavir and another promising pocket binding compound Pirodavir have been shown to have a relatively modest inhibitory capacity when compared to other enteroviruses with EC_{50} values of $0.7 \mu\text{M}$ and 0.5

μM respectively in EV71, while *in vitro* studies for Pleconaril showed this to have no anti-EV71 activity (Shia et al. 2002; Thibaut et al. 2012; Wildenbeest et al. 2012; Tijmsa et al. 2014). Due to the lack of EV71 capsid binding-inhibitors with therapeutic level $\text{IC}_{50}/\text{EC}_{50}$ values, initiatives were taken to develop new compounds with specific activity against EV71 (Shia et al. 2002; Ke & Lin 2006; De Colibus et al. 2014; Chern et al. 2004). In the initial studies, structure activity relationships were employed using the skeletons of Pleconaril and other WIN compounds. This allowed the design and creation of a novel class of imidazolidinones (3-(4-pyridyl)-2-imidazolidinone) with a significant viral activity towards EV71 (Shia et al. 2002; Chern et al. 2004). Following this, homology modelling and molecular dynamics simulation techniques were used to predict the structure of VP1, so that the compounds could be further refined using structure based design; this resulted in an improved IC_{50} value, the most powerful of which was termed GPP3 (Ke & Lin 2006). When the crystal structure of EV71 became available (Xiangxi Wang et al. 2012; Plevka et al. 2012), it allowed further refinement, by studying the interactions of a variety of compounds with varying anti-EV71 activity with the EV71 capsid (De Colibus et al. 2014).

From this it was shown that there was an optimal size for the compounds, ones that were too small will not be able to bind as deep in the pocket, thus reducing the number of hydrogen bonds formed and reducing its affinity. If too large it is possible that it is unable to fit in the pocket. For example a correctly positioned aromatic moiety in the compound that forms links within a structure known as the “hydrophobic trap” was shown to be important for binding and if the two do not

link, binding efficiency is reduced (Figure 1.6) (DeColibus et al. 2014). In addition, the molecule also requires linkers to bind at the pore, near residues A112 and I113 and Pleconaril is unable to reach this region, which explains its inability to inhibit EV71 (Tijmsma et al. 2014; De Colibus et al. 2014; Plevka et al. 2013).

De Colibus et al 2014 developed two novel compound (termed NLD and ALD) using the skeleton of GPP3, the previous most effective EV71 pocket-binding inhibitor and modified it to improve its binding capacity. This was achieved characterising the structure of EV71 in combination with four GPP compounds (GPP2, GPP3, GPP4 and GPP12). Then based on these interactions, *In silico* scanning was performed to identify areas on the capsid which could act as additional binding sites for these inhibitors, and the mouth of the VP1 pocket was identified as one such area. To improve the binding to this area, an amide or an amine were added to the C-terminus of GPP3 on the pyridine ring, thus creating NLD and ALD. Both these molecules are predicted to have a higher binding efficiency than GPP3, by creating extra binding site to the mouth of the VP1 pocket (DeColibus et al. 2014).

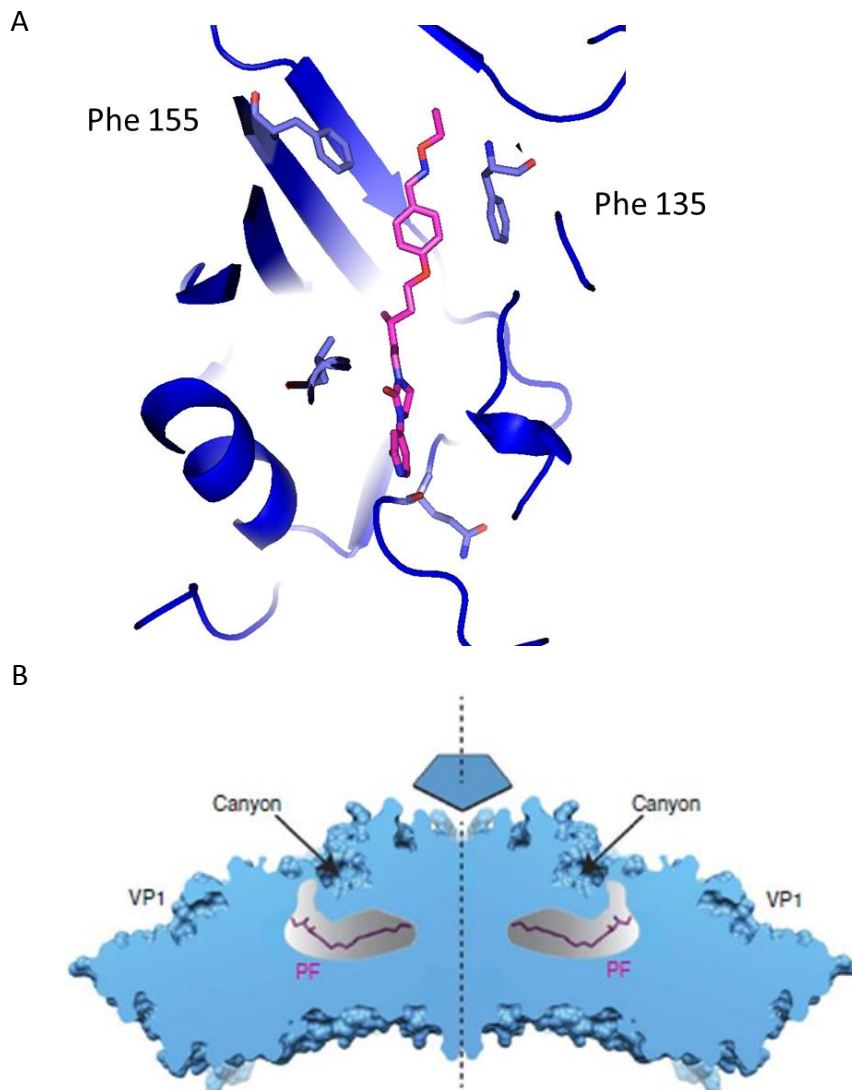


Figure 1.6 The enterovirus pocket. (A) PyMol diagram depicting the hydrophobic trap; pocket binding inhibitor NLD in combination with EV71 VP1 pocket and phenylalanine residues 155 and 135 trapping NLD in its place. Produced using PyMol (B) The organization of the EV71 inhibitor-binding pocket, lying below the canyon floor, shown occupied by a natural pocket factor (PF). An icosahedral five-fold axis is marked. VP1 subunits are shown as a cyan surface. A segment around the five-fold axis is cut away to reveal two pockets. (Taken from De Colibus et al. 2014).

1.3.1 Resistance against pocket binding compounds

A potential drawback in the development of pocket-binding compounds as useful therapeutics is the rapid evolution of resistance. RNA viruses such as enteroviruses characteristically have very high rates of mutation with between 1 and 7 mutations occurring during every round of replication per genome (Rodriguez et al. 2001).

Also, the selection of resistance against pocket-binding compounds has been demonstrated with several enteroviruses including EV71, HRV14, PV 1,2,3 and CVB3 (Shih et al. 2004; Heinz et al. 1989; Chang et al. 2012; Groarke & Pevear 1999a; Salvati et al. 2004; Mosser et al. 1994). From studying resistant isolates, of namely HRV14 and PV3, two different resistance mechanisms have been shown to evolve towards these compounds. These are termed expulsion and compensation mutations, both are associated with reduced capsid stability.

Expulsion mutations occur in the VP1 pocket and either shrink or fill the pocket to prevent the compound from occupying the space (Mosser et al. 1994). These mutations also likely prevent the natural pocket factor from binding, which may explain their thermolability. Compensation mutations occur in other areas of the virus capsid, and act to reduce the stability so that it becomes more flexible. This therefore allows the capsid to still undergo the conformational changes necessary to either bind to the receptor or uncoat, even in the presence of these stabilising inhibitors (Mosser et al. 1994). It is easy to distinguish between these two different mutations as in a compensation mutation the compound is still able to protect the virus from thermal inactivation, while with expulsion mutations the compound is unable to prevent thermal inactivation.

Katpally et al. 2007 show that these mutations do not affect the fitness of the virus *in vitro*, however reversion to WT genotype has been shown to occur within 10 passages in the absence of inhibitors (Liu et al. 2012). Also, in both PV and CVB3, resistant mutants have been shown to be asymptomatic and associated with a reduced viral load in *in vivo* models, similar results have been observed in Pleconaril-resistant HRV isolated from patients (Kouiavskaia et al. 2011; Groarke & Pevear 1999b; Pevear et al. 2005).

1.4 Vaccines

A variety of different vaccine strategies exist, the two most common being attenuation and inactivation. In attenuated vaccines a live organism with reduced virulence is used, while inactivated vaccines use a version of the pathogen that cannot replicate due to chemical or physical treatment. Both strategies have provided extremely successful vaccines. However, it is becoming evident that there are issues with both these types of vaccines in terms of safety and cost, which have generated a drive towards development of recombinant vaccines which are pathogen free, as they are safer and have the potential to be cheaper.

1.4.1 Attenuated vaccines

Attenuated vaccines consist of replicating organisms with reduced virulence but are still antigenically similar enough to induce an appropriate immune response. There are a variety of different ways these can be created. Sometimes a naturally

avirulent strain with cross neutralising capacity towards the more virulent strain can be used, an example of which is the smallpox vaccine. Here the closely-related vaccinia virus was used as a vaccine. In most cases though, the pathogen is made to be less virulent and there are two ways by which this can be achieved. One method is to passage the virulent strain in an environment that is different from its natural host such as in eggs or cell culture using animal cells and/or at lower temperatures. The Oral Polio Vaccine (OPV) was developed in this way. After repeated passage, the accumulation of mutations allows adaptations to the new environment, and the mutations are often associated with reduced virulence for the original host. Another more recent method of attenuating vaccines is the use of reverse genetics, an example of which is the introduction of mutations into the 5' UTR which has been shown to be able to further attenuate PV (Macadam et al. 2006).

Efforts to design an EV71 attenuated vaccine have focused on the reverse genetics approach. In these attempts the attenuating mutations seen in OPV were modelled into EV71 using molecular genetics (Arita et al. 2005). The efficacy of this virus as a vaccine was tested using rhesus macaque monkeys and immunisation with this modified virus was shown to induce neutralising antibodies and to protect them from a lethal challenge with wild type virus (Arita et al. 2008). However, the vaccine itself produced mild neurological symptoms such as tremors when inoculated via the intravenous route, showing that the vaccine has not been attenuated enough to be used safely (Arita et al. 2008).

Complications of residual virulence are a major issue for attenuated vaccines along with reversion to a virulent phenotype; however both occurrences are infrequent in

the field (reviewed in Kew et al. 2005). Problems with attenuated vaccines are more prominent with small positive strand RNA viruses as they have small genomes and are very prone to mutations. For example, the OPV is a largely successful and effective vaccine (Paul 2009; John 2009), however it can mutate to a more virulent strain and cause vaccine-derived paralytic poliomyelitis (VDPP). This occurs ~ 1 in every 6.7 million doses of vaccine administered (reviewed in Guo et al. 2015). In addition, if the vaccine is administered to patients with B cell immunodeficiency, there is $\sim 16\%$ chance that the vaccine will not be cleared by the individual, and they will become a life time excretor of VDPP. This occurs ~ 1 in 27 million doses of vaccine administered and is especially dangerous in communities with low vaccine coverage, as unvaccinated people in the community can be exposed to virulent VDPP (Halsey et al. 2004, Reviewed in Kew et al. 2005). The existence of these life time excretors means that VDPP is still present in the environment in countries that are free of the disease. This has been demonstrated by testing the sewage of many western countries (Esteves-Jaramillo et al 2014, Kuryk et al 2014, Centres for Disease Control and Prevention (CDC 2008).

This poses major problems in terms of eradication, as if vaccine coverage dwindles there is a real chance that PV cases will begin to emerge again, as has happened in Syria (Gulland 2014).

1.4.2 Inactivated vaccine

Inactivated vaccines are produced by either physically or chemically treating pathogens in a way that renders them non-infectious while maintaining their

antigenicity. This is usually achieved by treating with formaldehyde. Successful inactivated vaccines have been produced for a number of human and non-human diseases, such as influenza virus, HAV, PV and FMDV (Clarke et al. 2001, Clarke 2001, Martín-Acebes et al. 2011).

It is likely that a formaldehyde inactivated EV71 vaccine will be available soon.

There are currently three companies working on their own vaccine and they are all in currently in phase III trials (Li et al 2014). The vaccine has been shown to induce cross-neutralising antibodies to all genotypes in adults and children (Chou et al. 2013; Mao et al. 2013) and can produce long term immunity in rhesus macaque models (Li et al. 2014).

Inactivated vaccines are much safer than attenuated vaccines as they cannot replicate and therefore there is no chance of infection. However as large quantities of live virus need to be grown there is always a chance of escape from the production facility. An outbreak of FMDV in the UK in 2007 was linked to an inactivated FMDV vaccine production plant (WWW,bbcnews 2007, Available; <http://news.bbc.co.uk/1/hi/uk/6930684.stm>, Accessed; 09/03/2016). In addition to this GSK also accidentally released large amounts of live PV in Belgium from a vaccine manufacturing plant (WWW,globalresearch 2015, Available; <http://www.globalresearch.ca/pharmaceutical-giant-glaxosmithkline-accidentally-released-45-liters-of-concentrated-live-polio-virus-in-the-environment/5405801>, Accessed: 09/03/2016).

1.4.3 Pathogen free vaccines: subunit and virus-like particle (VLP) vaccines

Another type of vaccine is a “pathogen free” vaccine; generated by expression of pathogen proteins in a recombinant system such as yeast, baculovirus or another viral vector such as Adenovirus or Lentivirus. These can be just an epitope vaccine that uses a single small antigenic feature, a whole virus protein, a combination of pathogen proteins or the entire capsid region assembled into a virus like particle (VLP). These have an advantage over traditional vaccines as they are much safer, because there is no chance of infection or outbreak.

The most widely used virus-free vaccine is the hepatitis B (HBV) vaccine; this is a subunit vaccine, in which one of the envelope proteins, hepatitis B surface antigen (HBsAg), is expressed in *Saccharomyces cerevisiae*. This strategy has been very successful for HBV, as HBsAg can self-assemble into VLPs. However most single proteins do not self-assemble into VLPs, which means they do not have as rigid and regular shape. Because of this they will form a less effective immune response, compared to how effective they would be in the context of a VLP and are therefore unsuitable to be used as a subunit vaccine.

With EV71 there have been several attempts to generate vaccines using entire capsid proteins or just small epitopes. One strategy used *E.coli* to express a recombinant VP1 protein, this proved successful at provoking an immune response in mice, however only 30% of the mice survived a lethal challenge (Zhang et al. 2014). Other strategies have used the yeast *Pichia pastoris* to produce VP1 which protected up to 90% of mice when used at its highest dose. However, the neutralising titre was not tested (Wang et al. 2012).

As mentioned previously, proteins produced in this manner are not usually successful as vaccines, as the conformation and therefore the antigenicity is often not maintained as they do not form VLPs. If the protein is expressed in a VLP vector then this can help maintain the structure, other attempts have focused on this approach. In one such study a recombinant baculovirus VP1 EV71 vaccine that expressed EV71 VP1 as a fusion protein with baculovirus surface protein (gp64) was shown to express EV71 VP1 in insect cells. The particles maintained structural and antigenic conformity of VP1 when analysed by immunofluorescence and western blot (Meng et al. 2011). Furthermore the protein was able to protect neonatal mice against a lethal challenge and elicit neutralising antibody titres of 1:64 compared to 1:128 in formaldehyde inactivated vaccines (Meng et al. 2011; Premanand et al. 2012). It also induced antibodies that could neutralise all sub-genotypes of the virus. Studies with another VP1 baculovirus vaccine showed that it was able to stimulate both humoral and cellular immunities (Kolpe et al. 2012).

Other EV71 subunit vaccines have focused on using small epitopes, using various presentation vectors such as the HBVcore. The different epitopes expressed were VP1 epitopes SP70 (amino acids 163–177) and SP55 (amino acids 208–222), the VP2 EF loop (amino acids 141-155) and VP4 N-terminus (amino acids 1-20), all were expressed in HBVcore (Foo et al. 2007a; Foo et al. 2007b; Xu et al. 2014; Zhao et al. 2013). All four epitopes have been shown to produce neutralising antibodies and are able to protect neonatal suckling mice from a lethal challenge. In the suckling mouse model adult mice, that show no clinical symptoms of EV71 infection, are immunised and their neo natal offspring, that are susceptible to EV71, are

challenged to assess if antibodies present in the mother's milk are able to protect the suckling mice (Ye et al. 2014; Xu et al. 2014; Zhao et al. 2013).

Although these types of vaccines can elicit protection in mice, they are often not as efficient as an inactivated whole virus vaccine and they generate a lower titre of neutralising antibodies (Chou et al. 2012). This is most likely because there are not as many immunogenic epitopes to stimulate an immune response, as it lacks the other proteins, the folds and the conformation of the protein is less well maintained.

To overcome this problem the entire virus capsid must be used and, assembled into a VLP.

Examples of commercial vaccines that use this strategy are the human papillomavirus (HPV) vaccines Gardasil and Cervarix. These use *S.cerevisiae* and insect cell expression systems respectively to produce the HPV major structural protein L1 that is able to self-assemble into VLPs (Garland et al. 2007, Paavonen et al. 2007, Lehtinen et al. 2012, Mulder et al. 2012). Other ongoing studies have created a number of VLP vaccines, examples being influenza and severe acute respiratory syndrome (SARS) (López-Macías et al. 2011, Lokugamage et al. 2008). VLPs for influenza have proven effective at immunising ferrets for a number of different strains and a VLP vaccine for H1N1 2009 Mexico is currently in phase II trials (López-Macías et al. 2011).

There have also been attempts to create picornavirus VLPs, for FMDV, PV, EV71 and CVB3 (Porta et al. 2013; Rombaut & Jore 1997; Ku et al. 2013; Liu et al. 2011; Zhang

et al. 2012). These essentially create the empty capsids described in section 1.2.2, but produced in a recombinant system. In these systems the P1 structural protein coding region and either 3C^{pro} or 3CD^{pro} are expressed together. The protease cleaves P1 into VP0, VP1 and VP3 which then self-assemble into an empty capsid VLP as described in section 1.2.1.

Both baculovirus and *S.cervisiae* have been tested as systems to produce EV71 VLPs. EV71 VLPs produced by a baculovirus system were identical in size and shape to naturally occurring empty particles and the antibodies produced through immunisation have been shown to inhibit virus replication both pre and post attachment (Ku et al. 2013). VLPs from both systems were able to induce an immune response and offered protection to suckling neonatal mice with efficiencies of 89% and 100% respectively, when the highest concentration of vaccine was used (Hu et al. 2003; Chung et al. 2006; Chung et al. 2008; Chung et al. 2010; Li et al. 2013). Cryo-EM images of EV71 and CVA16 particles produced in the baculovirus system highly resemble the natural empty particles and the majority of the neutralising epitopes are well preserved (Gong et al. 2014).

Overall this looks like a more promising strategy than the subunit vaccine strategy as full capsid VLPs are able to produce higher native neutralising titres than the single recombinant proteins, the small immunogenic epitopes, heat inactivated EV71 and heated VLPs. However they still produce lower levels compared to the formaldehyde inactivated virus vaccines (Chung et al. 2008; Chou et al. 2012; Lin et al. 2011; Zhao et al. 2015).

It is possible that the inactivated vaccine produces a higher level of neutralising antibodies because of an adjuvant effect of RNA, which is lacking in the VLPs. However it is more likely that this higher level of neutralising antibody is due to greater antigenic stability of the inactivated vaccine. As both untreated VLPs and formaldehyde inactivated vaccines can elicit higher titres of neutralising antibodies than heated virus or heated VLPs it is likely that the non-heated (native) conformation is important for producing high antibody levels. This is supported by evidence in other picornaviruses such as PV where the heated conformation has previously been shown to convert to an alternative form of antigenicity (Rombaut & Jore 1997).

As PV empty capsids are less stable than mature virions and therefore more likely to convert to an alternative antigenicity, it is likely that the reduced stability of the empty capsids results in lower levels of neutralising antibodies (Porta et al. 2013, Rombaut & Jore 1997). PV empty capsids have been shown to convert to an alternative antigenicity at temperatures above 5 °C (Jim Hogle, personal communication). This antigenic shift and reduction in neutralising titre would likely be exacerbated further if used as a commercial vaccine, where it becomes more difficult to maintain a cold chain.

Although this instability is inconvenient, there is work that shows that it is possible to improve the stability of the empty particles. PV empty capsids grown in *S. cerevisiae* expression systems were shown to be more stable and maintain native antigenicity when they were grown and incubated in the presence of the pocket-binding inhibitor Pirodavir (Rombaut & Jore 1997). Introduction of stabilising

mutations into FMDV and PV have been shown to improve the stability of empty capsids (Porta et al 2013, unpublished data). Other work with EV71 has shown that different buffers can prevent the expansion of empty particles, although it is not clear if they are able to maintain N-antigenicity (Lin et al. 2014).

Incubation in stabilising compounds or introduction of stabilising mutations are two approaches that could be used to improve the stability of EV71 VLPs.

1.5 Project objectives

- Test efficacies of pocket binding inhibitors *in vitro*
- Generate resistant isolates towards pocket binding compounds
- Establish mechanism of action and resistance of pocket bind compound NLD
- Assess heat stability of EV71
- Determine methods to improve the heat stability
- Explore mechanism of pH induced uncoating

Chapter 2

Chapter 2 Materials and methods

2.1 General Buffers, media and reagents

2.1.1 Luria-Bertoni (LB) Broth

10 g NaCl

10 g Tryptone

5 g Yeast extract

1 L dH₂O

Add 15 g of Bacto agar to make LB agar

2.1.2 10xTBE (Tris-borate-EDTA) buffer pH 8.3

100 g Tris base

55 g Boric acid

9.3 g Na₄EDTA

1 L dH₂O

Dilute 100 ml to 1 L in dH₂O to make x1

50 mM EDTA (pH8.0)

2.1.3 6x DNA loading buffer

0.03 % bromophenol blue

0.03 % xylene cyanol FF

30 % glycerol

10 mM Tris-HCl (pH 7.5)

2.1.4 10x Sodium dodecyl sulphate - Polyacrylamide gel electrophoresis (SDS-PAGE) running buffer

10 g SDS

30.3 g Tris-HCl

144.1 g glycine

1L dH₂O

2.1.5 SDS-PAGE stacking gel

0.2 mM Tris-HCl (pH 6.8)

5 % 29:1 Acrylamide:bisacrylamide

10 % SDS

10 % Ammonium persulphate

2.1.6 15 % SDS-PAGE resolving gel

0.4 M Tris-HCl (pH 8.8)

15 % 29:1 Acrylamide:bisacrylamide

10 % SDS

10 % Ammonium persulphate

1 % NNNN-tetramethyl-ethane-1,2-diamine (TEMED)

1 % TEMED

Dilute 100ml to 1L in dH₂O to make x1

2.1.7 Coomassie blue protein stain

2.5 g Coomassie Brilliant blue

450 ml methanol

100 ml acetic acid

400 ml dH₂O

Mix and add dH₂O to make 1L

2.1.8 Cell growth medium (Suspension/microcarrier)

Eagle's Minimum Essentials Medium (EMEM)

10 % Foetal Bovine serum (FBS)

100 units/ ml penicillin

0.05 mg/ ml streptomycin

2.1.9 Coomassie de-stain solution

450 ml methanol

100 ml acetic acid

400 ml dH₂O to make 1L

2.1.10 Tris EDTA (TE) buffer

10 mM Tris-HCl (pH7.5)

1 mM EDTA

2.1.11 Cell growth medium (Flask)

Dulbecco's Modified Eagle's Medium (DMEM)

10 % Foetal bovine serum (FBS)

100 units/ ml penicillin

0.05 mg/ ml streptomycin

1 % L-glutamine

2.1.12 Radio labelling medium

Roswell Park Memorial Institute medium (RPMI) 1640 media containing 1 µl per ml of ³⁵S labelled cysteine and methionine supplied by perkin elmer.

2.1.13 Radio-immuno precipitation assay (RIPA) buffer

50 mM Tris HCl (pH 8.0)

150 mM NaCl

1 % Nonidet P40

0.5 % Sodium deoxycholate

0.1 % SDS

2.1.14 Enhanced chemiluminescence (ECL)

Solution 1

2.5 mM luminal

400 µM p-coumaric acid

100 mM Tris-HCl (pH 8.5)

Solution 2

0.018 % H₂O₂

100 mM Tris-HCl (pH 8.5)

2.1.15 10 x Transfer buffer

30.3 g Tris-Base

144.1 g Glycine

5 g SDS

Make up to 1L dH₂O

To make 1 x buffer, dilute 100 ml in 200 ml methanol and 700 ml dH₂O

2.1.16 *Phosphate-buffered saline (PBS) TWEEN*

10 PBS tablets

0.5 % TWEEN-20

1 L dH₂O

Mix solution 1 and 2 in a 1:1 ratio prior to use.

2.1.17 RNA loading buffer

95 % formamide

0.025 % SDS

0.025 % bromophenol blue

0.0025 % xylene cyanol FF

0.0025 % ethidium bromide

0.05 mM EDTA

2.1.18 Crystal violet stain

40 ml 1% crystal violet

300 ml dH₂O

80 ml 95% ethanol

2.1.19 Blocking buffer

1 % Skimmed milk powder

200 ml PBS TWEEN

2.1.20 Gel dry down buffer

250 ml isopropanol

100 ml acetic acid

50 ml glycerol

600 ml dd H₂O

2.1.21 Virus re-suspension buffer

0.25 M NaCl

0.25 M HEPES

In dd H₂O

2.1.22 pH 5.6 buffer

42 ml 0.1M citric acid

58 ml 0.2M Sodium phosphate dibasic

2.1.23 Carbonate Coating buffer

Na₂CO₃ 1.590g

NaHCO₃ 2.930g

in 'ultrapure' water to 1 litre.

Check pH 9.6.

2.1.24 ELISA Dilution Buffer

Add 0.5g Bovine Serum Albumin to 100ml PBS w/o Ca Mg containing 0.1% TWEEN 20.

2.1.25 ELISA Wash Buffer

Salt PBS containing 2.0% dried milk and 0.5% Tween 20 - prepare on day of assay and discard any unused buffer after use.

2.1.26 ELISA Assay diluent

PBS containing 2.0% dried milk

2.1.27 Antibodies

mAb 979 (Mouse monoclonal anti VP-2), AbCam

Goat anti-mouse IgG peroxidase conjugate, Sigma Aldrich

A9 mAb , The Chinese Academy of Science, Beijing

A6 mAb, The Chinese Academy of Science, Beijing

2.1.28 Lipids

Lauric acid (Sigma)

Myristic acid (Sigma)

Palmitic acid (Sigma)

Sphingosine (Cambridge Bioscience)

Arachidic acid (Sigma)

Stored at 10 mM in 100% ethanol, at temperature specified by the manufacturer.

2.2 Cell culture

2.2.1 Cell lines used

Cell line	Isolated from	Split	Notes
Vero Cells	Kidney epithelial cells of an African green monkey	1in10	Adherent cell line that does not secrete type 1 interferons when infected by viruses
Rhabdomyosarcoma (RD) Cells	Connective tissue cancer cell line	1 in 4	Adherent cell line. Is very sensitive to cold temperatures.
Baby hamster kidney cells (BHKs)	Kidney fibroblasts of a hamster	1 in 10	Adherent cell line
Jurkat cells	T lymphocyte cells	1 in 4	Suspension cell line
HeLa cells	Cervical cancer cells of a human (Henrietta Lacks)	1 in 10	Adherent cell line
HeLa Suspension cells	Cervical cancer cells of a human (Henrietta Lacks)	1 in 10	Suspension cell line

Table 2.1 Cell lines

2.2.2 Maintenance of cell culture Flasks

Maintenance of Vero, BHK and HeLa cells was managed in DMEM (Sigma Aldrich) supplemented with 10 % foetal bovine serum (FBS), 100 units/ ml penicillin, 0.1mg/ ml streptomycin in T175 flasks. Cells were observed using a light microscope. Cell passages were performed every 2-4 days when they became 80-90% confluent. Old medium was removed from the flask and cells were washed with 1 x PBS before addition of 2 x trypsin. When cells detached from the flasks an equal volume of medium containing FBS was added. Then 90% of the cell suspension was discarded and 20ml medium was added to the remainder. Flasks were then placed in a horizontal position in a humidified incubator (37°C; 5 % CO²). The same flask was used for a maximum of 5 times.

2.2.3 Microcarrier cultures

Cultures were initiated by inoculating a 100 ml siliconised spinner flask with 1×10^6 cells and 0.2g of microcarriers in 1/3 the final volume, this was then spun for three hours with the cells being allowed to settle for one minute every half hour. After three hours the culture was made to a final volume of 100 ml to make cell density at 1×10^5 cell ml⁻¹ and microcarrier density of 2 g/l. Inoculating at 1/3 volume final volume and allowing to settle every half hour was found to be very important to achieve maximum cell attachment to microcarriers. Cell number was counted everyday using 0.1 M citric acid crystal violet stain until they reached 1×10^8 cells ml⁻¹. To perform cell counts, 1 ml of the culture was removed, microcarriers were allowed to settle and 700 µl of medium was replaced with 0.1M citric acid crystal violet stain. This was left for one hour before being used for cell counts. When cells

reached a density of 1×10^8 cells ml^{-1} , medium was removed and microcarriers were washed with 2 X PBS. They were incubated with virus in a siliconised tube for 30 minutes on a rocking platform before being returned to a spinner flask and being made to final volume of 100 ml with serum free medium.

2.2.4 Revival of frozen cells

A vial of cells from liquid nitrogen or -80°C was removed and thawed in a water bath at 37°C . The content was then pipetted into a T70 flask and made to a final volume of 15 ml with medium. This was then placed in a horizontal position in a humidified incubator (37°C ; 5 % CO_2). The next day the medium was changed and cells were passaged into a T175 flask when confluent.

2.2.5 Preparation of preserved cell stocks

Cells were collected from flasks as mentioned previously. These were then transferred into 50 ml falcon tubes. This was then centrifuged at 800 rpm for 10 minutes to pellet cells. Medium was removed and cell were re-suspended in 3 ml of freezing mixture (10 % DMSO, 90 % FBS), which was aliquoted into three tubes. Cells were then transferred to a -80°C freezer.

2.2.6 Virus infection T175

Cells were grown to near confluency in T175 flasks before infection. Old medium was removed from the flasks and cells were washed with 1 x PBS before addition of trypsin. Virus was then made to an MOI of 1 $\text{TCID}_{50}'\text{s}/\text{cell}$ in 4 ml of serum free medium. The cells were then incubated at room temperature on an oscillating platform for 20 minutes before 10 ml of serum free medium was added and the

flasks placed in a horizontal position in a humidified incubator (37 °C; 5 % CO₂), until 100 % cell death was observed.

2.2.7 Tissue culture infective dose 50 (TCID₅₀) assay

96 cell well plates were seeded with Vero cells at 1×10^4 cells per well in 100 µl of complete medium. They were then left overnight. The next day serial dilutions of samples were made ranging between 10^{-2} to 10^{-9} in serum free media. The first 10 wells of each row was incubated with 100 µl of the diluted samples and the last two were incubated 100 µl of serum free media alone as controls. These were then incubated for seven days. On the seventh day they were inactivated under UV for 30 minutes to kill all virus, then the media was removed into virkon and each well was washed twice with PBS. Each well was then stained with 30µl of crystal violet. Final titre was calculated using the Reed & Muench method, this works by calculating the dilution at which 50% of cells are infected (Reed and Muench 1938).

2.2.8 Inhibition of pocket binding inhibitors IC₅₀ curves

TCID₅₀ assays were carried out, in the presence of either 50 µM of fatty acids lauric acid, myristic acid and palmitic acid or increasing concentrations of either NLD, GPP3 or ALD at 1% DMSO and GPP4 at 4% DMSO.

2.2.9 Drug inhibition curves knocking down host cell pathways

Vero cells were seeded into a 24-well plate at 10^5 cells suspended in 500 µl of 10 % FBS-DMEM per well and incubated at 37 °C overnight. Media was removed from the wells and the cells were pre-treated with different concentrations of drug (in serum-free DMEM) (Table 2.1) at 37 °C. Cells were then infected on ice (MOI = 1 TCID₅₀'s/cell) for 30 minutes. Unbound drug and virus were removed, and cells

were washed with PBS, before adding 500 µl of drug in serum-free DMEM to the wells. The plates were incubated overnight at 37 °C, cells lysed by freeze-thawing, followed by TCID₅₀ assay to determine the viral titre.

Compound	Concentrations	Incubation time prior to virus infection	Effect
Ammonium chloride	12.5, 25, 100 mM	2 h	Inhibitor of endosome acidification
Chlorpromazine	10, 20, 30 µM	2 h	Inhibitor of clathrin-dependent endocytosis
Chloroquine	25, 50, 100 µM	2 h	Neutralises acidic endocytic vesicles
Cyclosporine A	0.16, 0.8, 4, 20 µM	4 h	Inhibitor of cyclophilin A
Genistein	6, 12, 25, 50 µM	2 h	Tyrosine kinase inhibitor

Table 2.2 Concentrations, pre-treatment times and functions of drugs used in this study

2.2.10 Time courses

Monolayers of Vero cells were infected with virus at an MOI of 1 TCID₅₀'s/cell and then cells were harvested at every time point by scraping the monolayer out and re-suspending it in the lysate. Lysate was then freeze-thawed three times, before titration by TCID₅₀ assay.

2.2.11 Drug selection

1 ml of viral lysate was used to infect a T25 flask of confluent Vero cells before being topped up to 5 ml with either 0.1 nM NLD, 0.9 nM GPP3 or 80 nM ALD. Cells were left till 100% cell death had occurred and 1 ml of supernatant was taken and used to infect another flask. Titrations were carried out by TCID₅₀ assay between each passage.

2.2.12 pH selection

1 ml of crude virus lysate was incubated in a pH 5.6 buffer for one hour at 4 °C. 5 ml of solution was taken and incubated in a T175 flask of confluent Vero cells for 20 minutes on a rocking platform at room temperature, before it was topped up with 20 ml of refrigerated DMEM. The flask was then incubated at 37 °C until 100% cell death was observed. Process was repeated until for five passages. Titrations were carried out by TCID₅₀ assay between each passage.

2.2.13 Heat selection

For the first passage enough virus to infect a T25 flask at an MOI of 10 TCID₅₀'s/cell, post heating was used, it was first concentrated by ultracentrifugation, then resuspended in volume of 700 µl of serum free medium. A 10 µl sample was taken for titration and the rest was heated to 50 °C for 30 minutes in a thermo cycler.

Another 10 µl of the heated virus was taken for titration and the rest was used to infect a T25 flask of Vero cells. The flask was left until 100 % cell death was observed, and then harvested. Cell debris was removed and freeze thawed three times in RIPA buffer, before being added to the rest of the supernatant. This supernatant was then concentrated by ultracentrifugation at 50,000 RPM for one hour and the resulting pellet was re-suspended in 700 µl of serum-free media. The re-suspended pellet was then heated to 50 °C and used to infect another T25 flask of Vero cells. This process was repeated until passage eight, where there less than a 10% drop in logarithmic titre was observed before for four consecutive passages

2.2.14 Heat stability curves

Up to 70 µl of crude virus lysate added to PCR tube and different pocket factors or PBS was added. Samples were then heated to different temperatures for 30 minutes using a thermo cycler, after 30 minutes samples were chilled to 4 °C and then titrated by TCID₅₀.

2.2.15 Radio labelling

Virus was used to infect a monolayer of cells and then left for either one hour (BEV) or six hours (EV71), at which point medium was removed and cells were washed with PBS. Media was replaces with 10 ml (T175) or 1 ml (6 well plate well) of RIMP 1640 media supplemented with 10 µCi per ml of ³⁵S labelled cystine and methionine (perkin elmer).

2.3 Gel Electrophoresis methods

2.3.1 Agarose gel electrophoresis

Gel electrophoresis were performed using 1 % agarose gels containing SYBR Safe at 0.3 µg/ml. Samples were loaded onto gels with 1x DNA loading buffer.

Electrophoresis for separation of DNA was carried out at 80V (constant) for 30-60 minutes in 1 X TBE buffer. Agarose gels were viewed and imaged using a Syngene GeneDoc imaging system.

2.3.2 RNA gels

RNA samples were mixed with 2 x RNA loading dye and incubated at 95 °C for 10 minutes. RNA samples were then loaded along with RiboRuler™ low range RNA ladder and electrophoresis was performed at 80 V (Constant) for 40 minutes. Gels were viewed and imaged using a Syngene GeneDoc imaging system.

2.3.3 SDS-PAGE

Analysis of protein samples by SDS-PAGE. All analyses were performed on 15 % tris-glycine resolving gels with 5% stacking gel. The Mini-PROTEAN r 3 electrophoresis system (BioRad) was used for electrophoretic analysis. Samples were mixed in a 50/50 ratio of sample and 2x loading buffer and heated at 95 °C for 10 minutes, they were then loaded into each well and run at 200 V (constant) for one hour. SDS-PAGE gel analysis was carried out with precision plus protein molecular weight ladder. Resolving gels were then submerged in Coomassie Brilliant Blue stain for + 2 hours on an oscillating platform (10 rpm) at room temperature. Gels were then transferred to de-staining solution under the same conditions until blue bands were

evident on a clear back ground. The destain solution was replaced whenever it turned a strong blue.

2.3.4 Western blotting

Polyvinylidene difluoride (PVDF) were cut according to the size of the SDS-page gel, first they were put in 100% methanol for 10 seconds then they were soaked in dH₂O for 10 minutes and then in 1 x transfer buffer for 10 minutes. Sponges and blotting paper were also soaked in 1 x transfer buffer for 10 minutes. The SDS-PAGE gel and other components were assembled in a Bio Rad cassette and an ice pack was put in the tanks. Transfer was then carried out either for 1 hour at 100 V or overnight at 30 V. At this point the membranes could be dried and stored for a later date, if membranes were to be used that day then they progressed directly to the blocking stage. If membranes had been dried they were reconstituted in methanol for 10 seconds and washed in PBS for 10 minutes. The membranes were then washed in PBS for 10 minutes before transferring into blocking buffer for 1 hour. They were then transferred into primary antibody diluted in blocking buffer 1/5000 and incubated for 1 hour. Membranes were then washed 3 x 10 minutes in PBS-Tween. They were then probed with an anti-mouse peroxidase conjugated secondary antibody diluted in blocking buffer 1//2000 for 1 hour. Membranes were then washed again in PBS-Tween 3 x 10 minutes. The excess buffer was drained off and they were incubated in ECL for 1 minute at room temperature followed by exposing to X-ray film (Hyperfilm ECL, Amersham Biosciences).

2.3.5 Gel dry down

After completion of electrophoresis of the SDS-page gel, gels were incubated in gel dry down buffer for 30 minutes, then incubated for 15 minutes in Amplify GE health care (Amplify can be reused). Upon completion of incubation, the gel was placed upon a 3 mm CHR Whatmann paper, and cling film was placed on top of the gel, and an additional piece of 3 mm CHR Whatmann paper was placed on top of the cling film. The gel was then placed in BioRad gel dryer, the plastic sheet of the gel dryer was placed over the top and the vacuum was turned on, ensuring that the plastic had formed a seal. Settings were then set as follows; slowest rate of heat increase (Setting three), final heat 80 °C and for a total of 2 hours. Once the gel had been dried down, it was exposed to film in a cassette at -80 °C, for 12 to 144 hours.

2.4 Cloning

2.4.1 Transformation of competent cells

Transformation of plasmid DNA into *E.coli* gold cell was performed using heat shock method. 50 µl of competent cells were mixed with 20-40 ng of plasmid DNA and 2 µl of beta mercaptoethanol and incubated on ice for 30 minutes. Cells were heat shocked at 42 °C for 45 seconds and then incubated on ice for 5 to 10 minutes. They were then added to 3 ml of antibody free LB and incubated at 37 °C for ~ 1 hour. 50 µl and 100 µl samples were then plated out onto LB/amp plates and incubated overnight; different amounts were plated to assess the effectiveness of the transformation. The following day three colonies were picked from each plate and grown on a shaking platform overnight at 37 °C in 5 ml of LB broth. The next day

glycerol stocks were prepared, by mixing equal volumes of 80 % glycerol and cell suspension. These were then stored at -70 °C. These stocks were then used to initiate cultures for plasmid extraction by mini or maxi prep (QIAGEN).

2.4.2 RNA Extraction

Viral RNA extractions were carried out from crude lysates of infected cells, using QIAGEN universal RNA extraction kit following the manufactures instructions.

2.4.3 RNA Transcriptions

Transcription was carried out using a RiboMAX™ Large Scale RNA Production T7 System following the manufactures instructions.

2.4.4 Reverse transcriptions

Reveres transcriptions were carried out using Qiagen reverse transcription kit using the manufactures instructions.

2.4.5 PCR

PCR was carried out using Qiagen fast cycle PCR, following the manufactures instructions. Using primers in table 2.2.

2.4.6 TOPO cloning

TOPO cloning was carried out using the Life Technologies TOPO cloning kit, following the manufactures instructions.

2.4.7 Sequencing

Samples for sequencing were sent to Beckman Coulter using their speciation's using the primers in table 2.3.

Primer Name	Sequence
EV71-667-F	CTATTTGTTGGCTTTGTACC
EV71-1386F	CCCTCCTTACAAACAAACACAACC
EV71-1954F	GAATTGTGCGCCGTGTTTAGAGCC
EV71-2408F	CCAGTCACATTTTACAGACAGCCTC
EV71-2806F	GTCGAGCTATTCATTACATGCG
EV71-3451F	TAGTGTCGTCTACCACCGCCC
EV71-3989F	TAGCCCTGATCGGGTGTCATGG
EV71-4591F	GTCACAGTAATGGATGACCTGTGTC
EV71-5264F	CAGTTGTGGCAGTCGTTTCACTGG
EV71-5992F	GGCCAACTCGCACTAAGCTCG
EV71-6656F	TCTCAGCCCAGTGTGGTTCAGGGCGC
EV71-747R	ACCGCTGAGTAGACACTTGTGA
EV71-1576R	GGTTCAGGGCAGAGTCGAAAGG
EV71-2132R	CCACCAGGAGGTGTATAAGCTATA
EV71-2622R	CTCATCACTAGTATTTGACGATGCCCC
EV71-3111R	CGCTCCATATTCAAGATCTTTCTCC
EV71-3519R	GTACACTCCTGTTTGACAATTGCAACG
EV71-4098R	TTTCTTTAACCAAGATGCACTCTGC

Table 2.3. Primers used in sequencing

2.5 Purification

2.5.1 Purification of Virus through a sucrose gradient (A)

Once 100 % cell death was observed, the supernatant was removed and centrifuged at 10,000 RPM for 30 minutes. The supernatant was then poured off and stored at 4 °C if to be saved for future use. The pellet was re-suspended in an appropriate amount of RIPA buffer and freeze-thawed 3 x before adding the supernatant to the main supernatant. This would then be made up to 50 % saturated ammonium sulphate or a 10 % polyethylene -glycol solution and stirred at 4 °C for 90 minutes. This was then centrifuged at 10,000 RPM for 1 hour; the suspension supernatant would be poured off and saved for titration. The pellets were re-suspended in an appropriate amount of PBS. These would then be centrifuged at 29,000 RPM for 3 hours through a 30 % sucrose cushion after which the supernatants were poured off and saved for titration. The pellets were re-suspended overnight on a rocking platform at 4 °C. The re-suspended pellets were made 1% SDS and loaded onto a 36 ml 15-45 % sucrose gradient in PBS and centrifuged for 3 hours at 29,000 RPM/ 151,000 RCF at 20 °C. 2 ml fractions were collected from the bottom of the centrifuge.

2.5.2 Purification of Virus through a sucrose gradient B

Virus was grown in culture flasks and labelled with ³⁵S labelled cystine and methionine, the supernatant was then clarified by centrifugation at 10,000 g for 30 minutes. The resultant pellet was then freeze-thawed three times in 1% NP40 to release trapped virus particles, this was then clarified and added to the supernatant. This was then subjected to ultracentrifugation at 32K rpm for one

hour through a 2 ml 30% sucrose cushion. The resulting pellet was then subjected to ultracentrifugation through 15-45% sucrose gradient for 50 minutes at 296,000 x g, this was then fractionated and the resulting fractions were added to scintillation fluid and counted.

2.5.3 Nycodenz

Virus was grown in culture flasks and labelled with ^{35}S labelled cystine and methionine, the supernatant was then clarified by centrifugation at 10,000 g for 30 minutes. The resultant pellet was then freeze-thawed three times in RIPA or 1% NP40 buffer to release trapped virus particles, this was then clarified and added to the supernatant. This was then subjected to ultracentrifugation at 32K rpm for one hour through a 2 ml 30% sucrose cushion. This was re-suspended overnight in virus re-suspension buffer and then subjected to ultra-centrifugation either through a 40% self-forming Nycodenz gradient, or a 20%,30%,40%,50%,-60% layers step gradient. This was then separated into 300 μl fractions.

2.5.4 ^3H Palmitic acid

Virus was grown in culture flasks and labelled with ^{35}S labelled cystine and methionine, the supernatant was then clarified by centrifugation at 10,000 g for 30 minutes. The resultant pellet was then freeze-thawed three times in RIPA or 1% NP40 buffer to release trapped virus particles, this was then clarified and added to the supernatant. This was then subjected to ultracentrifugation at 32K rpm for one hour through a 2 ml 30% sucrose cushion. It was then incubated in ^3H palmitic acid overnight and then split into two equal volumes, 2 nM NLD was added to one tube and the other was left untreated. After two minutes of NLD treatment the two

fractions were subjected to ultracentrifugation through a self-forming nycodenz gradient.

2.5.5 Scintillation counting

10 to 200 µl of sample was added to 2 ml of perkin elmer scintillation fluid in a scintillation fluid tube, samples were then counted using a scintillation counter.

Counting for one minute per tube.

2.6 Immunoprecipitation

50 µl of crude virus lysates were incubated with 10 µl of sepharose G beads (GE Healthcare) and 5 µl of either D6 or A9 antibody and then topped up to 500 µl with PBS. This was left spinning on a rotating platform overnight at 4 °C. The following day the beads were subjected to centrifugation at 10,000 RPM to pellet the beads, the supernatant was removed and the beads were re-suspended in PBS. The process was repeated three times, then the beads were re-suspended in 50 µl of LB buffer, and were then heated to 100 °C for 10 minutes. The samples pelleted for 5 minutes at 13,000 RPM, and the sample was then analysed by SDS-PAGE.

2.7 ELISA

Purified SCARB2 or PSGL1 were diluted to 0.1 µg in Carbonate Coating buffer and 50 µl was incubated individual wells on a 96 well plate. The plate was incubated overnight at 2-8 °C in a box with a humidified atmosphere. The next day each well was washed 4 x with wash buffer, leaving the plate containing the last wash at

room temperature for at least 30 minutes. 50 µl of sample was added to each well. The plate was then sealed and incubated for two hours at 37 °C and then washed 3 x with ELISA wash buffer. Then 50 µl of either mAb D6 or A9 diluted 1 in 100 in ELISA assay diluent and added to each well. The plate was then sealed and incubated for 1 hour and then washed with ELISA wash buffer three times. 50 µl of peroxidase conjugated anti-mouse diluted in ELISA assay diluent at 1/400 was added to each well. After 30 minutes 1M H₂SO₄ was added to each well and the optical density at 492 was read as soon as possible.

2.8 PyMol

Structural figure were prepared using PyMol

Chapter 3

Chapter 3 EV71 Compounds – In vitro characterisation and selection of resistant isolates

There are currently no compounds available for clinical use against EV71, although *in vitro* studies have shown that several different approaches could potentially lead to effective EV71 therapeutics (Reviewed in Kok, 2015; Kuo & Shih, 2013; Shang, Xu, & Yin, 2013). One such strategy is the use of small inhibitory compounds that bind the enterovirus VP1 pocket (discussed in section 1.3). In an untreated enterovirus population the VP1 pocket is filled with a hydrophobic lipid known as the pocket factor. The pocket factor is expelled from the pocket upon receptor binding; this initiates viral uncoating and genome release and is associated with capsid instability (Ren et al. 2013; Dang et al. 2014). The presence of compounds that bind to the VP1 pocket with a higher affinity are therefore able to prevent receptor binding/uncoating and infection of the cell (Rotbart 2002). In the case of BEV1 the use of certain fatty acids, shown to be natural pocket factors by mass spectrometry have also been shown to have an inhibitory effect (Ismail-Cassim et al. 1990; Smyth et al. 2003).

Since the discovery of the first of these pocket binding compounds (refer to Introduction 1.3), other pocket binding compounds have been found for a wide variety of enterovirus including; HRV, CVB3 and PV (Mckinlay et al. 1992; Groarke & Pevear 1999a; Liu et al. 2012). With certain compounds, such as the HRV pocket binding compound Pleconaril in phase III trials (Feil et al. 2012). Although they are shown to be effective inhibitors, resistance has been shown to evolve rapidly towards them (Groake and Pevear 1999; Liu et al. 2012).

In addition to the many other pocket binding compounds, 3-(4-pyridyl)-2-imidazolidinone derivatives have been shown to be the most effective pocket binding compounds against EV71 which were termed the GPP compounds, the most inhibitory of which was GPP3 (Chern et al. 2004; Ke & Lin 2006). Since the generation of these compounds the crystal structure of EV71 has been solved (Wang et al. 2012; Plevka et al. 2012), and the interactions between four GPP compounds (GPP2, GPP3, GPP4 and GPP12) and the EV71 capsid were modelled (DeColibus et al. 2014) (Figure 3.1).

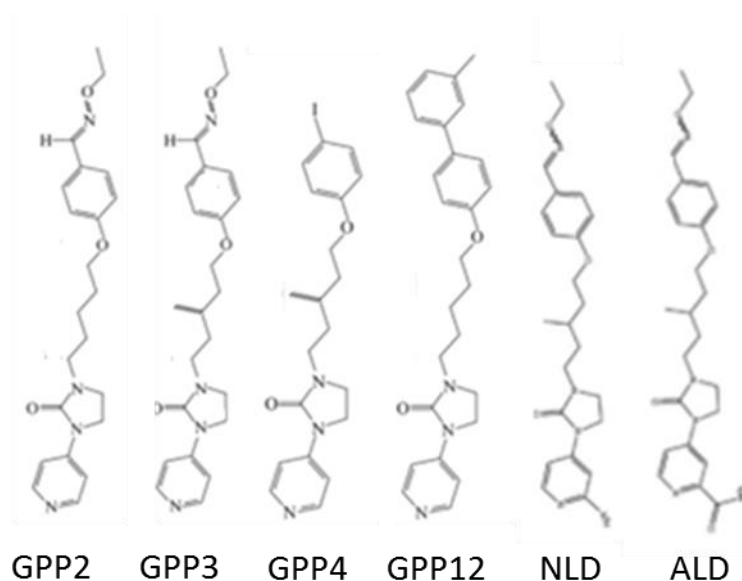


Figure 3.1 Structures of different 3-(4-pyridyl)-2-imidazolidinone derivatives with anti-EV71 activity. Images modified from DeColibus et al. 2014.

In addition to this, *in silico* docking was used to predict the energy of interaction between the compounds and VP1. This was performed by computing the docking poses of the compounds in the VP1 pocket using quantum mechanics-polarised ligand docking (QMPLD). Compounds that were predicted to have a higher energy of interaction had previously been shown to have lower IC₅₀ value (DeColibus et al. 2014). Based on these observations, *in silico* scanning was performed to identify areas

on the capsid which could act as additional binding sites for these inhibitors, and the mouth of the VP1 pocket was identified as one such area. To improve the binding to this area, an amide or an amine were added to the C-terminus of GPP3 on the pyridine ring, thus creating NLD and ALD. Both these molecules are predicted to have a higher binding efficiency by QMPLD than GPP3, by creating an extra binding site to the mouth of the VP1 pocket (DeColibus et al. 2014).

In this chapter, the effect of NLD and ALD on EV71 grown in Vero cells is characterised and compared to two compounds previously identified (GPP3 and GPP4) and potential pocket factors (lauric acid, myristic acid and palmitic acid). Isolates of virus that were found to be resistant to these compounds are also identified and characterised.

3.1 Characterisation of viral inhibition and cellular cytotoxicity

The effectiveness of NLD and ALD as inhibitors towards EV71 and other enteroviruses was assessed and compared to previously characterised inhibitors GPP3 and GPP4, as well as to fatty acids/natural pocket factor candidates, lauric acid, myristic acid and palmitic acid. This was carried out by titrating EV71 via TCID₅₀ assays (Refer to section 2.2.7, 2.2.8), in a range of different concentrations of each inhibitor for seven days.

Prior to this the minimum amount of DMSO able to dissolve 1000 nM of each compound was assessed. This was carried out by adding a range of DMSO concentrations from 0.5 v/v % to 5 v/v % DMSO to each compound and observing at what concentration it dissolved each compound. This was 1 v/v % for NLD, ALD and GPP3 and 5 v/v % for GPP4. These DMSO concentrations were kept constant in each TCID₅₀ assay and DMSO only control wells were included in each assay. All fatty acids were dissolved in ethanol to make a 10 mM stock and remained soluble at concentrations of 50 µM when ethanol was diluted down to 0.05 v/v % ethanol.

The TCID₅₀ values were represented as a sigmoidal curve, modelled using a nonlinear regression (curve fit) to fit the data (Figure 3.2). This showed that NLD was the most effective inhibitor, with an IC₅₀ value of 0.025 nM and the ability to reduce titres below 5% at 0.05 nM. GPP3 was the next most effective inhibitor with an IC₅₀ of 0.39 nM, then ALD which had an IC₅₀ value of 8.54 nM although a more complex relation was seen in the curve and it did not fit the curve perfectly, which will reduce the precision of the IC₅₀ values. Control wells were exposed to the equivalent amount of DMSO (1%) to ensure that this was not causing any cytopathic effect or an effect on viral titre. Also GPP4 was shown to have no inhibitory effect up to concentrations of 1 µM (Figure 3.2) (De Colibus et al. 2014).

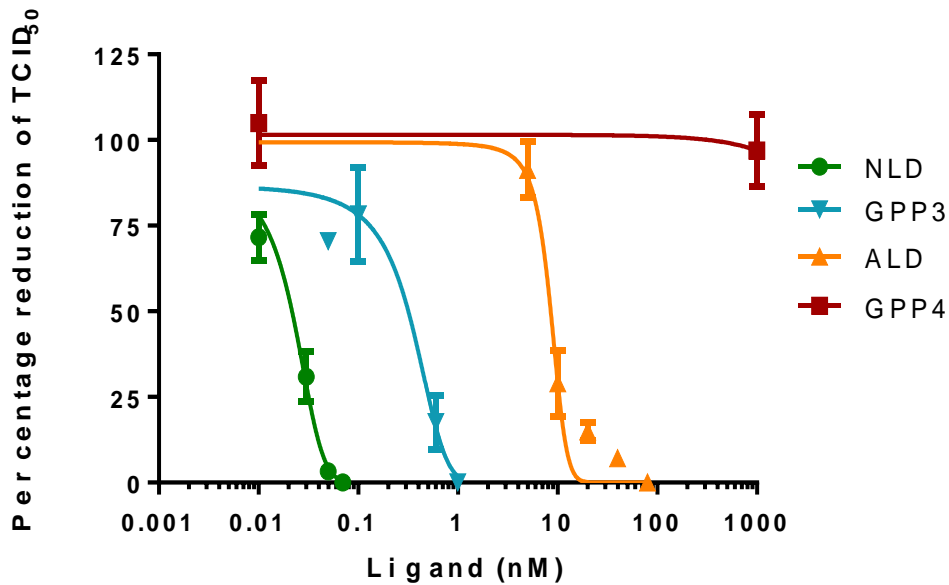


Figure 3.2 IC_{50} Inhibitory effects of NLD (green), GPP3 (blue), ALD (orange) and GPP4 (red) on EV71. EV71 samples were titrated in triplicate via $TCID_{50}$ assays in the presence of a range of concentrations of NLD, GPP3 and ALD. Error is represented by standard error. Non-linear regression was used to determine the IC_{50} value. The IC_{50} is the point at which the $TCID_{50}$ value is reduced by 50%. For clarity the curves are represented on a logarithmic scale.

The effectiveness of NLD and GPP3 was also analysed for other enteroviruses. CVA16 (closest relative of EV71) was also shown to be sensitive to GPP3, which was shown to have an IC_{50} values of 12 nM (Figure 3.3 work carried out by Lauren Elliott an undergraduate under my supervision). PV was also shown to be sensitive to NLD and was completely inhibited by it at concentrations over 100 nM (work carried out by Oluwapelumi Adeyemi unpublished data), while NLD at a concentration of 100 nM had no inhibitory effect on BEV2 (Data not shown). The inhibitory effect of fatty acids was also tested for EV71, PV and BEV2, but incubation in the presence of fatty acids did not cause a reduction in titre (Figure 3.4). The observation with BEV2 is in contrast to published data for BEV1 which showed lauric acid and myristic acid to have a strong

inhibitory effect and palmitic acid to have a weak inhibitory effect (Ismail-Cassim et al. 1990). This could be due to the fact that the two BEV serotypes have different sized pockets. Higher concentrations were not used due to the cytotoxic effect.

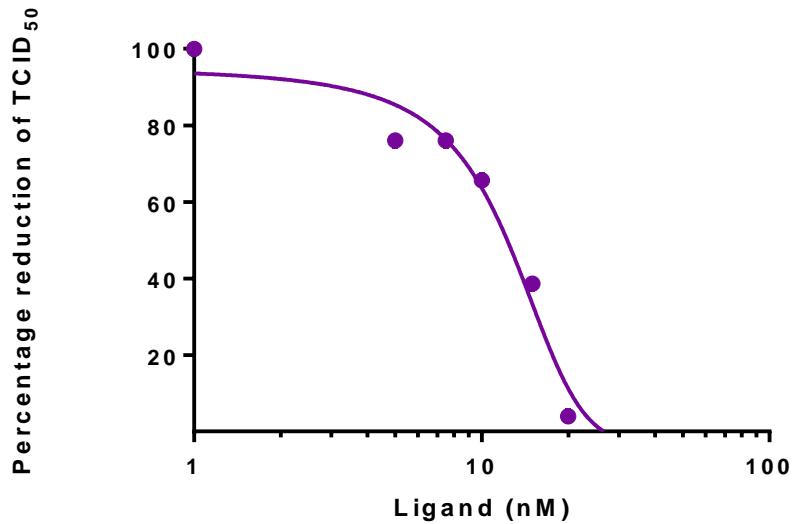


Figure 3.3 Inhibition of CVA16 by GPP3. CVA16 samples were titrated via TCID₅₀ assay in the presence of a range of concentrations of GPP3. Non-linear regression was used to determine the IC₅₀ value. The IC₅₀ is 14 nM the point at which the TCID₅₀ value is reduced by 50%. For clarity the curves are represented on a logarithmic scale. N=1 (Work was conducted by Lauren Elliott an undergraduate student under my supervision).

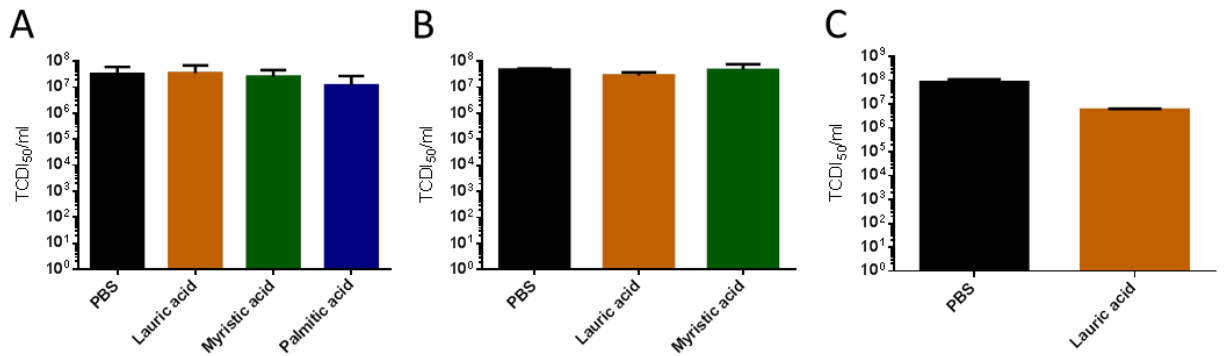


Figure 3.4 The inhibitory effects of fatty acids on EV71 (A), PV (B) and BEV2 (C). The inhibitory effects of lauric acid, myristic acid and palmitic acid on EV71 (A), PV (B) and BEV(C) were tested by TCID₅₀ assays in the presence of 50 μM fatty acids. Media containing PBS was used as a control. (A) Log₁₀ (TCID₅₀/ml) values obtained from EV71 titrated in media containing 50 μM fatty acids (lauric acid, myristic acid or palmitic acid). (B) Log₁₀ (TCID₅₀/ml) values obtained from PV titrated in media containing 50 μM fatty acids (lauric acid, myristic acid). Each point represents the average of three measurements. Error bars, s.e.m. For PBS, lauric acid and myristic acid, each point represents the average of three measurements. For palmitic acid, the average of two measurements is shown. (C) Log₁₀ (TCID₅₀/ml) values obtained from BEV2 titrated in media containing 50 μM lauric acid. Error bars, s.e.m. All compounds are supplied at 0.05 % ethanol (A and B were conducted by Amy Radcliffe a Mbiol student under my supervision).

These results show that low concentrations of NLD, GPP3 and ALD could potentially be used to treat EV71 infections. However, the cytotoxicity of these compounds needed to be assessed so that the therapeutic window could be calculated, i.e. the amount of inhibitor that can be used before it becomes toxic to cells still needed to be assessed. Vero cells were incubated in the presence of media containing a range of concentrations of NLD, GPP3, ALD or DMSO for seven days, after which the cellular cytotoxicity was evaluated by MTT assay (Figure 3.5). From these results we can see that the CC_{50} values for the three inhibitors respectively are 270 nM, 250 nM and 1000 nM. The CC_{50} value is the value at which the compounds cause a 50% reduction in the OD reading judged by MTT assay. DMSO did not have a cytotoxic effect at the concentration of 1% that was used for NLD, GPP3 or ALD. This gives a therapeutic window of 1×10^4 for NLD, 6.8×10^2 for GPP3 and $> 1.3 \times 10^3$ for ALD (Table 3.1). Both NLD and ALD therefore have a larger therapeutic window than the previous best EV71 inhibitor GPP3.

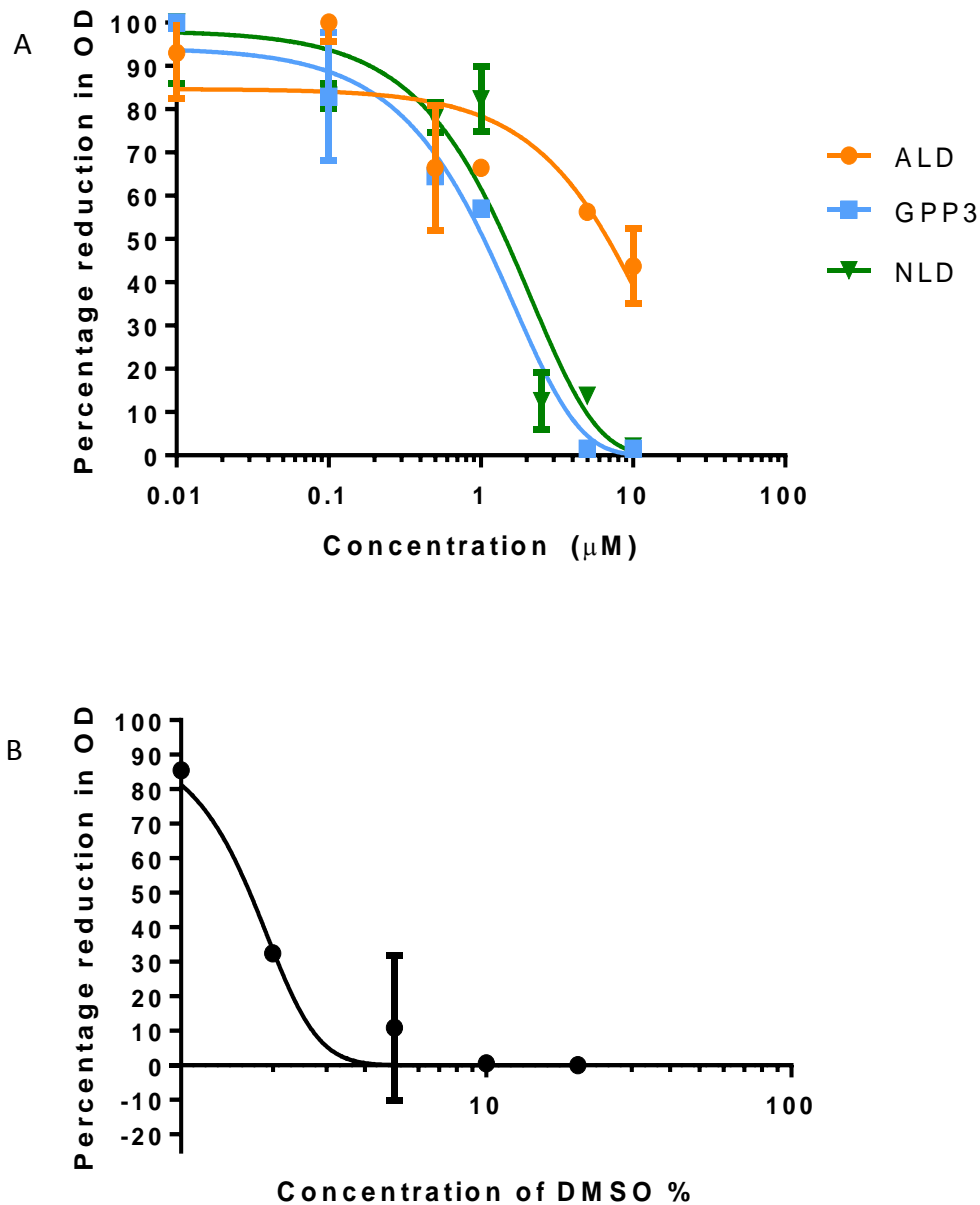


Figure 3.5 Toxicity of NLD, GPP3 and ALD to Vero cells. Vero cells were incubated with a range of concentrations of **NLD (green filled triangle)**, **GPP3 (blue filled square)**, **ALD (orange filled circle)**. (A) or DMSO (B) for seven days. MTT assays were then performed and the CC_{50} was derived from the OD (692 nm) by non-linear regression. Each point represents an average of three measurements and error was measured using standard error.

	NLD	GPP3	ALD
CC₅₀	250 nM	270 nM	>1000 nM
(Cell toxicity)			
IC₅₀	0.025 nM	0.39 nM	8.7 nM
(EV71 inhibition)			
Therapeutic window	1×10^4	6.8×10^2	$> 1.3 \times 10^3$
(CC₅₀ : IC₅₀)			

Table 3.1 Therapeutic window of NLD, GPP3 and ALD against EV71. This table displays the CC₅₀ (from Figure 3.5) and IC₅₀ (from Figure 3.2). The CC₅₀ value has been divided by the IC₅₀ value to give the therapeutic window for each compound.

3.2 Selection of resistant mutants

As stated previously (section 1.3), enteroviruses are known to evolve resistance rapidly towards pocket binding inhibitors, therefore it is likely that resistance can arise to NLD, GPP3 and ALD.

To investigate this, EV71 or CVA16 were grown in the presence of these pocket binding compounds at a concentration able to reduce the TCID₅₀ value by over 99.9% (Figure 3.7). Concentrations of 0.1 nM NLD, 0.9 nM GPP3, 70 nM ALD or a combination of 0.1 nM NLD/ 0.9 nM GPP3 were used as the selection pressure for EV71 and concentrations of 20 nM GPP3 was used for CVA16. Virus was grown under of one of these selection pressures until 100% cell death was achieved, samples were then titrated and passaged in the presence of the same concentration of inhibitor, until 100% cell death was achieved again. This was repeated for eight passages (Figure 3.7). Titres were seen to rise after just one or two passages and continued to rise until either passage six or eight at which point the titres were equivalent to WT virus in the absence of any compounds (EV71 ~ 1×10^7 TCID₅₀/ml and CVA16 ~ 1×10^5 TCID₅₀/ml) (Figure 3.7).

Each isolate was then sequenced to determine the mutations which may have arisen to generate resistance. Isolates were sequenced from purified PCR products that had been sub-cloned into a vector (See methods sections 2.4.5, 2.4.6), this was to ensure that the mutations seen in combination were present in individual isolates. 18 of the sequenced sub-clones possessed the same two VP1 amino acid changes, I113M and L123V. These were observed in the GPP3 resistant isolates (4/4), the ALD resistant isolate (1/1), one of the NLD resistant isolates (1/13), and all the isolates taken from

EV71 that was resistant to a combination of NLD and GPP3 (12/12). In the NLD resistant EV71 a mixed population was observed; in addition to the I113M and V123L (1/13), single mutations of 113 of VP1 (I to M 8/13 or I to L 4/13) were also observed. Virus passaged in a combination of NLD/GPP3 over 30 passages maintained the same two I113M and L123V mutations (1/1) (Table 3.2). All CVA16 mutants selected by GPP3 had a L113F mutation in VP1 (10/10) (Table 3.2). Comparison with the NCBI gene bank database revealed that none of the 5830 EV71 or 248 CVA16 sequences deposited contained any combination of these three mutations. No mutations were seen in any other structural protein.

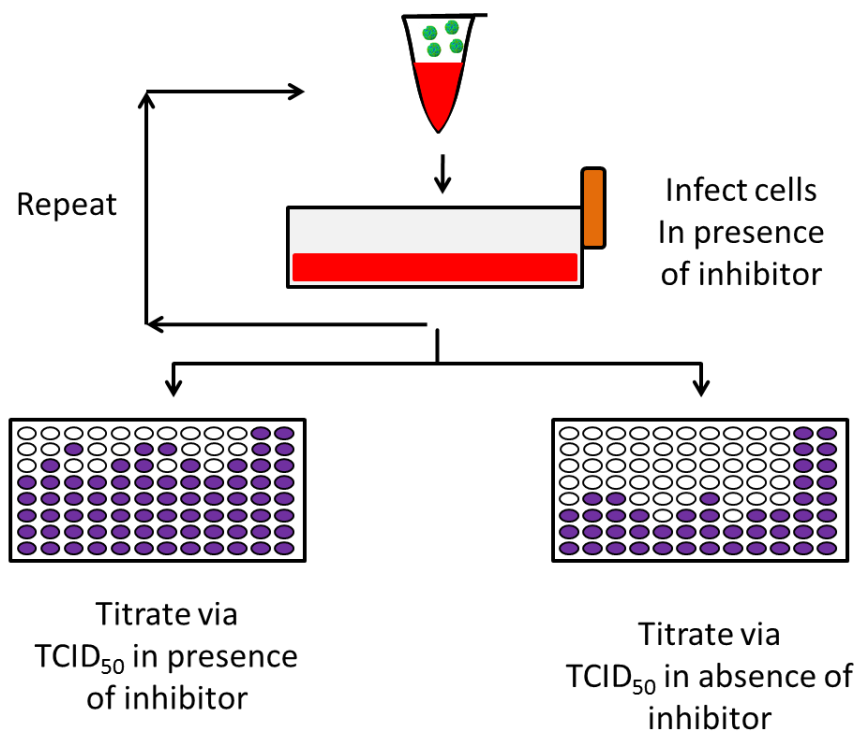


Figure 3.6 Selecting for inhibitor resistant virus. Virus was used to infect a T25 flask of confluent Vero cells in the presence of different inhibitors that had previously been shown to reduce virus titre by 99.9%. After each passage the virus was titrated in either the presence or absence of the inhibitor, and then used to infect another T25 flask. This process was repeated for eight passages.

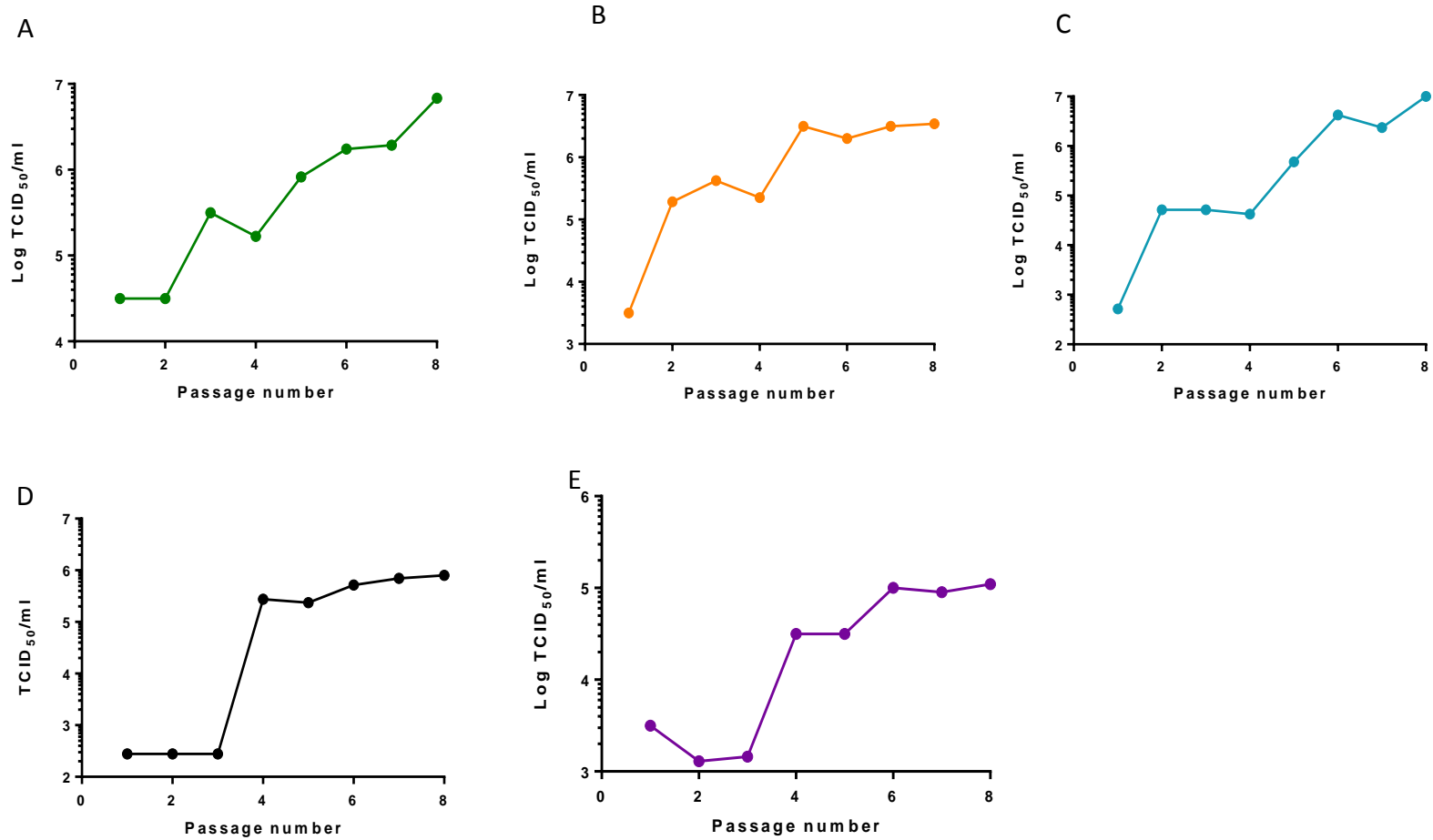


Figure 3.7 Generation of resistant isolates. WT EV71 was passaged in the presence of either (A) 0.1 nM NLD, (B) 0.9 nM GPP3, (C) 80 nM ALD or, (D) a combination of 0.1 nM NLD and 0.9 nM GPP3, (E) WT CVA16 was passaged in the presence of 20 nM GPP3. Each isolate was passaged a total of 8 times and after each passage a sample was titrated in the presence of the selecting concentration of compound.

Virus/Compound	Mutation(s)	Number sequenced
EV71/NLD	I113M (62%), I113L (31%), I113M/V123I (7%)	n=13
EV71/GPP3	I113M/V123I	n=4
EV71/ALD	I113M/V123I	n=1
EV71/NLD + GPP3	I113M/V123I	n=12
CVA16/GPP3	L113F	n=10

Table 3.2 Resistance mutations. Mutations identified in EV71/CVA16 after passage in the presence of NLD, GPP3, ALD or a combination of NLD/GPP3. CVA16 isolates resistant to NLD or ALD were not selected.

To better understand the effects these mutations are having on the structure, computational modelling using Rosetta was carried out by Luigi De Colibus (Oxford University). Figure 3.8 illustrates the crystal structure of EV71 in complex with NLD and shows the interactions between NLD and the VP1 pocket. This demonstrates that NLD is able to bind the capsid in several places, including residue I113 where resistance mutations occurred. Predictive modelling of mutation I113M suggested that the methionine side chain comes out to fill the pocket, possibly causing a steric clash with NLD. While predictions of the effect of mutation V123L suggested that the leucine residue causes the pocket to shrink, leaving less space for the compound to occupy. In CVA16 the L113F mutation was predicted to have the same effect as I113M in EV71, with phenylalanine causing a steric clash with GPP3. To

further assess how the mutations could be affecting stability, the change in free energy of folding ($\Delta\Delta G$ -folding) between WT and the mutant viruses was assessed and compared. This works on the principle that proteins with the lowest free-energy states are more stable. This was carried out by Luigi De Colibus at Oxford University using Rosetta. This software computes atom-atom interactions, and is able to predict the hydrophobic effects, electrostatic desolvation cost associated with burial of polar atoms and an explicit hydrogen-bonding potential to predict a $\Delta\Delta G$ -folding value. Here structures of WT EV71 in complex with NLD and WT CVA16 in complex with GPP3 (De Colibus. et al 2014, De Colibus. et al 2015) were used. Differences in $\Delta\Delta G$ -folding were calculated by Rosetta by relaxing the VP1 subunit structure with coordinate constraints, and applying monomer $\Delta\Delta G$ -folding calculation without sampling alternative backbone conformations (Fowler et al. 2010, Kellogg et al. 2011, Tyka et al. 2011).

This predicted that differences between $\Delta\Delta G$ -folding between the WT and EV71 I113M mutant was +0.73 kcal/mol, WT and V123I -0.98 kcal/mol whereas the combination of both mutations gave $\Delta\Delta G$ -folding of $\sim +1.1$ kcal/mol, this suggests that the mutant virus capsid may be less stable than WT (Fowler et al. 2010; Kellogg et al. 2011; Tyka et al. 2011 carried out by Luigi DeColibus Oxford University). However, the $\Delta\Delta G$ -folding for CVA16 mutant was -1.7 Kcal/mol, suggesting that this mutant may be more stable than WT.

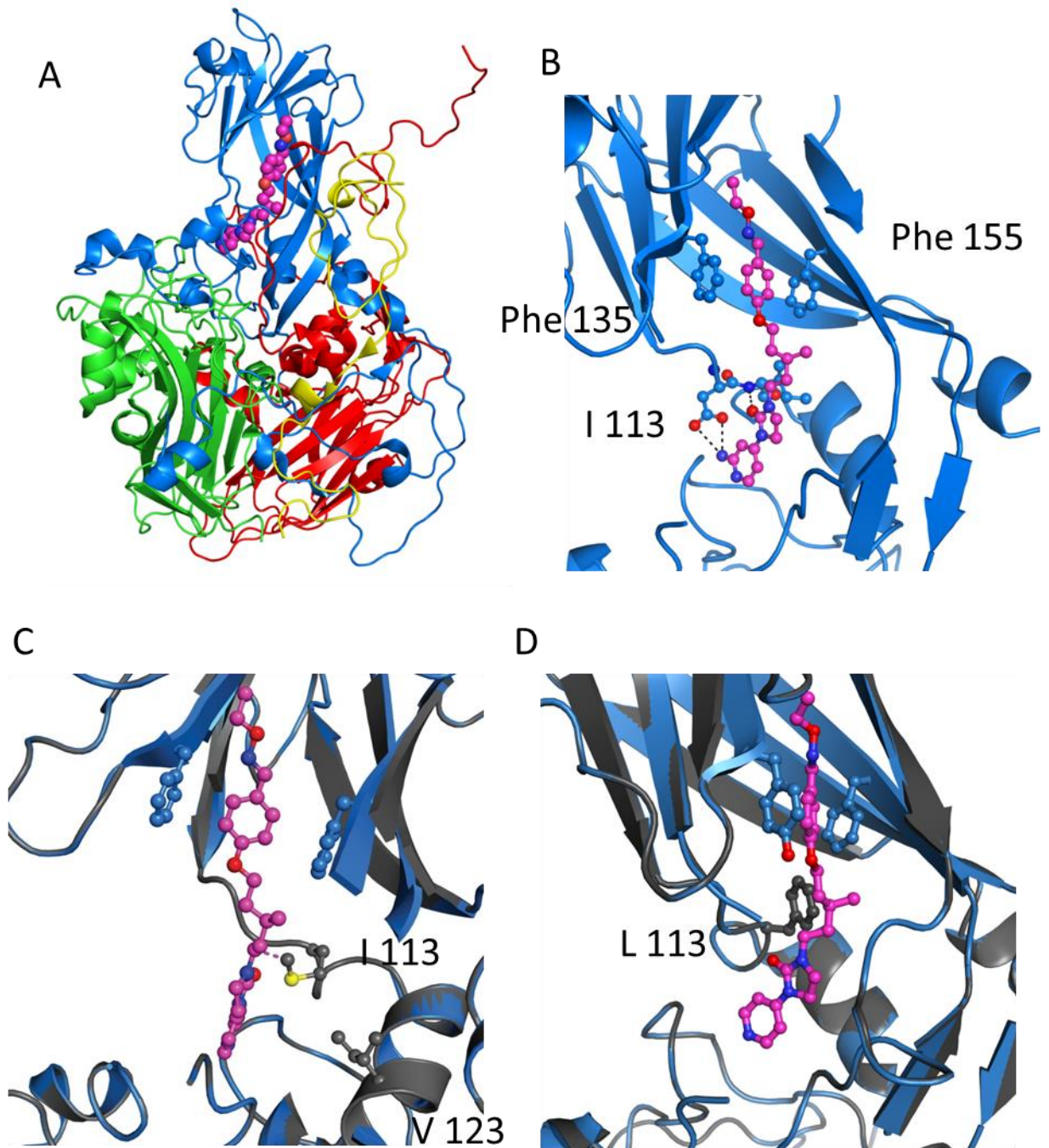


Figure 3.8 (A) Structure of the EV71 protomer in complex with NLD. Icosahedral protomeric unit of EV71 (PDBID:4CEY), viewed from the inside of the capsid. VP1, blue, VP2, green, VP3 red, VP4 yellow, NLD magenta. Protein shown in cartoon representation, NLD as spheres. (Figure produced by Luigi De Colibus)(B)EV71 (PDBID 4CEY) showing a close up of the VP1 (blue) pocket with NLD (magenta) in place. The side-chains of Phe135, Phe155, Asp112 and Ile113 are shown as ball-and-sticks. Hydrogen bonds are shown as dashed lines (Figure produced by Luigi De Colibus). (C) Predicted structure of pocket binding inhibitor resistant mutant in complex with NLD. EV71 (PDBID 4CEY) in blue, with the model generated by

Rossetta shown in grey. The two mutated side chains I113M and V123L are shown as grey balls-and-sticks (Figure produced by Luigi De Colibus). (D) Predicted structure of CVA16 GPP3 resistant mutant in complex with GPP3. CVA16 in complex with GPP3 (unpublished). I113F is shown (blue and grey balls-and-sticks). (Figure produced by Luigi De Colibus).

3.3 Fitness cost of inhibitor resistant mutations

As mutations that deviate from WT often incur a fitness cost, the genetic stability of the inhibitor-resistant EV71 isolate selected using both NLD and GPP3 (I113M, V123L) was tested by repeated passage in the absence of inhibitors (Figure 3.9). After each passage, virus was titrated in the presence or absence of inhibitor. This showed that while the titre remained unaffected in the absence of inhibitor, in the presence of the inhibitor the titre dropped dramatically after just one passage. This continued for the next two passages, after which the titre became equivalent to the WT when in the presence of the inhibitors (Figure 3.9). Sequencing confirmed that the virus had reverted to a WT genotype (n=1), indicating a strong selection pressure for reversion. However, as the experiment was performed with a “pool” of virus it is not possible to determine if this is back mutation or if it is amplification of residual WT virus.

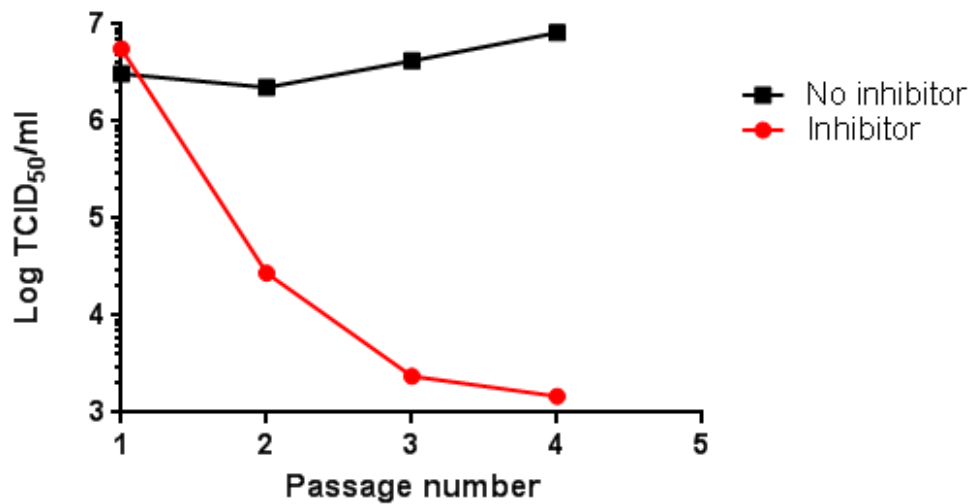


Figure 3.9 Inhibitor resistant isolates are genetically unstable. An inhibitor-resistant isolate that was selected with a combination of 0.1 nM NLD and 0.9 nM GPP3 was passaged four times in the absence of any inhibitor. It was then titrated in the presence (red circles) and absence of inhibitor (black squares) using TCID₅₀ assay. n = 1.

To determine the reason for the reduced fitness of the inhibitor-resistant virus, the growth kinetics of the both WT EV71 and the inhibitor-resistant isolate were compared. To do this a one-step growth curve was performed; samples from both isolates were taken every three hours for 18 hours and then titrated via TCID₅₀. This revealed no difference between the growth kinetics of the two variants (Figure 3.10).

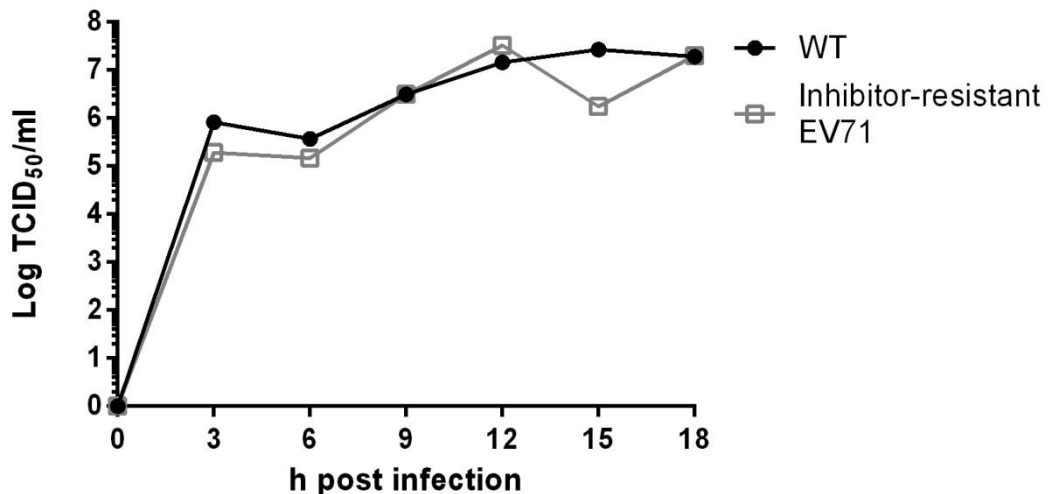


Figure 3.10 One step growth curves of inhibitor-resistant and WT EV71. WT (black filled circle) and inhibitor-resistant EV71 selected in the presence of 0.1 nM NLD and 0.9 nM GPP3 (grey open square) were used to infect six wells each of a 96 well plate at an MOI of 10 TCID₅₀'s/cell. Every three hours the supernatant and cells of a well from each isolate were removed, and freeze-thawed to lyse the cells. These samples were then titrated by TCID₅₀ assay. *n* = 1.

As the growth kinetics did not appear to be the fitness cost, the thermostability was then assessed. The thermal stabilities of WT EV71 and inhibitor-resistant mutant virus selected in the presence of NLD/GPP3 were evaluated in the absence and presence of 0.1 nM NLD / 0.9 nM GPP3 or 2 nM NLD. To do this all isolates were exposed to a range of temperatures using a thermocycler for 30 minute periods and each sample was then titrated (Figure 3.11A). This showed that WT heated in the presence of NLD was able to tolerate temperatures 6 °C higher before inactivation began to occur and 3.5 °C higher before total inactivation occurred compared to the inhibitor-resistant virus. In contrast to WT virus, inhibitor-resistant virus could not be rescued from heat inactivation by the presence of 2 nM NLD or by a combination of 0.1 nM NLD and 0.9 nM GPP3. The inhibitor-resistant virus was also

shown to be more thermolabile than the WT, with initial inactivation occurring at $\sim 3^{\circ}\text{C}$ lower and the complete inactivation temperature occurring 4°C lower. This suggests that the I113M/V123L mutation prevented the compounds from binding within the VP1 pocket and results in increased thermolability. Also each stability curve appeared to have a step, indicating that there is population of viruses with different heat stabilities. Similar results were obtained with inhibitor-resistant CVA16 where heat inactivation was shown to occur at 54°C in the WT and at 51°C in the GPP3 resistant L113F mutant, although there was a less obvious step here (Figure 3.11B). These results are consistent with observations in PV and HRVs in which pocket-binding compounds were able to increase thermostability while inhibitor resistant isolates with mutations located in their pockets were shown to be more thermolabile (Katpally et al. 2007; Mosser et al. 1994; Shepard et al. 1993).

In addition to a reduced stability at higher temperatures, the resistant isolates were also noted to be less stable during long term storage at $\sim 4^{\circ}\text{C}$ in the fridge and after storage at -20°C and -80°C , when no cryoprotectant was used. Inhibitor-resistant isolates start to become non-viable after 3 weeks storage at $\sim 4^{\circ}\text{C}$ or after one freeze thaw after being stored at -20°C or -80°C . In contrast, WT virus titre remains constant after months of storage at 4°C and after multiple freeze thaw cycles.

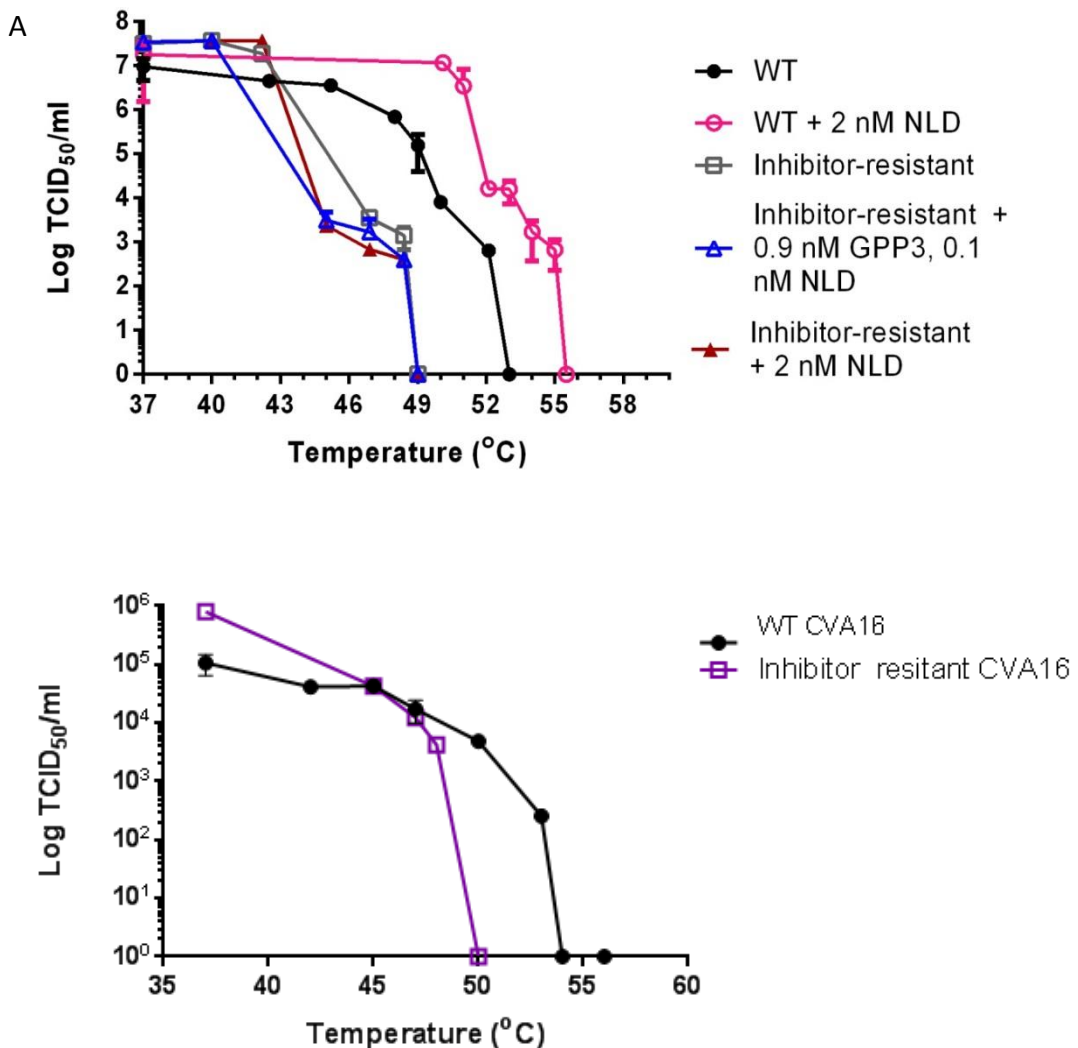


Figure 3.11 Inhibitor-resistant mutants are more thermolabile than WT virus. (a) Thermolability curves of EV71 WT (black filled circle) and inhibitor-resistant EV71 (grey open square), WT EV71 in the presence of 2 nM NLD (hot pink open circle), inhibitor-resistant EV71 in the presence of 0.9 nM GPP3 and 0.1 nM NLD (blue open triangle) and 2 nM NLD (red filled triangle) (b) Thermolability curves of WT CVA16 (black filled circle) and inhibitor-resistant CVA16 (purple open square). All samples were heated at a range of temperatures for 30 minutes using a thermocycler, prior to titration by TCID₅₀ assay. Samples containing NLD were first diluted to a level at which the inhibitor has no effect before titration. Titrations were carried out in triplicate and error was measured using standard error.

3.4 Chapter summary

In this chapter it has been shown that two novel EV71 inhibitors, NLD and ALD, are active against EV71, while short chain fatty acids that bind to the same site as these compounds are ineffective at inhibiting infections in cell culture. NLD was shown to be more than 10 fold more potent against EV71 than the previous best inhibitor, GPP3 (De Colibus, et al. 2014). It was also shown that when EV71 or CVA16 are grown in the presence of these compounds, they rapidly acquired resistance, however this appears to come with a fitness cost as the viruses reverted back to a WT phenotype and genotype after very few passages in the absence of selection. Similar mutations associated with resistance were seen in EV71 for each of the compounds used. For GPP3, ALD or a combination of NLD and GPP3 two mutations in VP1, I113M and V123L, were seen in every isolate sequenced. However, EV71 passaged in the presence of NLD alone resulted in a population containing three different mutations; two single mutations in VP1, I113M or I113L, and the same double mutation described above (I113M, V123L). CVA16 passaged in the presence of GPP3 gained a single L113F mutation, which is analogous to the I113M mutation seen in EV71. The mutations selected are likely to prevent the compounds from binding, as the thermostability of the resistant isolates was not increased in the presence of NLD. Similar results have been reported for WIN51711-resistant PV3 and WIN52035-2-resistant HRV14, with mutations identified in the VP1 pocket (Mosser et al. 1994; Shepard et al. 1993).

Using the crystal structures of EV71 in complex with NLD (De Colibus et al. 2014) and CVA16 in complex with GPP3, (unpublished data) modelling was used to predict

the effect of resistance mutations. From this analysis, the bulkier side chains of the I113M and L113F mutations were predicted to point directly into the pocket, reducing the space available for inhibitor binding and likely causing a steric clash with the compounds, while the V123L mutation was predicted to reduce the space further. It is important to note that I113 is one of the residues involved in compound binding, as shown in Figure 3.7 B (De Colibus, et al. 2014). Also a change to M or F could be achieved by a single point mutation for both EV71 and CVA16 and it is interesting that the same selection pressure has resulted in different mutations in the two viruses. Furthermore, $\Delta\Delta G_{\text{folding}}$ calculations predicted that there is little difference in the stability of the viruses carrying the resistance mutations (in the absence of pocket factor) which suggests that the thermolability of the mutant virus potentially arises instead from the reduced affinity of the pocket factor. Studies with other enteroviruses have documented many different mutations associated with resistance to a variety of pocket-binding compounds (Appendix table 1); for example all PV types are susceptible to the antiviral capsid inhibitor V-073 and growing PV in the presence of V-073 results in the selection of variants with reduced susceptibility to the drug (Liu et al., 2012). The majority of the mutant viruses exhibited a VP1 I194F/M substitution (equivalent position 192 in type 3). Generally, drug-resistant viruses have acquired mutations which interfered with the correct placement of the inhibitors in the binding pocket. However, this also has a deleterious effect on the binding of the natural pocket factor, which is known to be a virion stabiliser, and results in greater thermolability of the drug resistant viruses compared to the WT, however there have been no observable

difference in growth kinetics (Heinz, et al. 1989; Groarke & Pevear 1999b; Mosser et al. 1994; Salvati et al. 2004; F. Liu et al. 2012; Lacroix et al. 2014).

Infections with pocket inhibitor-resistant CVB3 and PV were asymptomatic or associated with reduced virulence in murine models (Groarke & Pevear 1999b; Kouivaskaia et al. 2011). Similarly, Pleconaril-resistant HRV B isolated from patients was shown to be asymptomatic and be associated with a greatly reduced viral load (Pevear et al. 2005b). In addition, the PV Sabin strains, which are avirulent, are also thermolabile and other thermolabile EV71 mutants have previously been shown to have reduced pathogenesis in Cynomolgus monkeys (Arita et al. 2005). Further work will be necessary in order to evaluate if inhibitor-resistant EV71 and CVA16 mutants behave in a similar fashion.

To summarise, the effect of different inhibitory compounds in EV71 and CVA16 has been accessed and characterised as well as resistance towards these compounds. For further work on the subject it would be interesting to look at virulence of the mutant viruses in mice and also to see if the same mutations arise. The effect of fatty acids on virus stability is further explored in section 5.1.4

Chapter 4

Chapter 4 Growth, cell entry and uncoating of EV71

In this chapter the growth and life cycle of EV71 is described, to allow a better understanding of the life cycle as a whole and to improve yield of virus for purification.

In addition to this, purification of virus is studied in an attempt to analyse different types of particles that occur at different points in the virus life cycle; these being mature (160S), uncoating intermediate (135S) and empty particles (80S) (discussed in section 1.2.4). The mature particles are the infectious particle that would typically infect a cell, the uncoating intermediates are particles that have undergone structural rearrangements to allow uncoating, and empty particles are virus capsids containing no RNA. This can occur naturally, or they can be generated by forcing mature particles to uncoat by heating or treatment with receptor (discussed in more detail in section 1.2.4).

The possibility of EV71 producing enveloped virus particles is also explored, as there is currently evidence that two other picornaviruses (HAV and PV) are able to produce enveloped virus particles, as well as the standard non-enveloped virus particles (Feng et al. 2013; Chen et al. 2015).

Further to the role of different particles involved in the EV71 life cycle, specific aspects of EV71 cell entry and uncoating are also studied here. EV71 has two known receptors that are able to facilitate cell entry, SCARB2 and PSGL1 (discussed in more detail in section 1.2.5). The function of these entry receptors has been demonstrated by loss of function studies. Knock down of SCARB2 in RD cells and

PSGL1 in Jurkat cells, renders the cells non-susceptible to EV71 infection (Yamayoshi et al. 2009; Nishimura et al. 2009). In addition, expression of SCARB2 or PSGL1 in cells that are generally non-susceptible to EV71 renders them susceptible to infection (Yamayoshi et al. 2009; Nishimura et al. 2009). Both receptors have been shown to facilitate endocytosis, although they use different pathways, with SCARB2 utilising the clathrin-dependant pathway and PSGL1 utilising the caveolar pathway. This has been demonstrated by blocking these pathways with inhibitors or by knocking down various components of each pathway with siRNA (Yamayoshi et al. 2009; Nishimura et al. 2009). In addition to inducing endocytosis, SCARB2 has also been implicated in viral uncoating, along with the proline isomerase cyclophilin A. Each of these host factors induces uncoating in a pH-dependant manner (Figure 4.1). SCARB2 functions most efficiently at pH 5.6 and docking models of the EV71 crystal structure and the SCARB2 crystal structure in its low pH and neutral pH conformations show that at low pH SCARB2 undergoes a conformation shift that could allow additional interactions with the EV71 capsid (Chen et al. 2012; Dang et al. 2014). Cyclophilin A was shown to function best at pH 6, and is completely inactive at pH 5.5 and 6.5. There is no structural data of EV71 and cyclophilin A in combination available so exactly where it binds is unknown, however residues S243, P246 on VP1 have been implicated in cyclophilin A interaction (Figure 4.1) (Qing et al. 2014) (described in more detail in the 1.2.5). In addition, endosome acidification has been shown to be essential for infection through both SCARB2 and PSGL1 mediated cell entry (Lin et al. 2012; Lin et al. 2013).

To study the mechanisms of uncoating, an evolution experiment was conducted to analyse the effect of low pH on virus fitness. The resultant mutant's susceptibility towards different inhibitors was compared to the WT and the mutation was mapped onto the crystal structure. In addition, the timings of key events in relation to the life cycle, such as cell entry, uncoating, protein production and host cell shut off were also analysed.

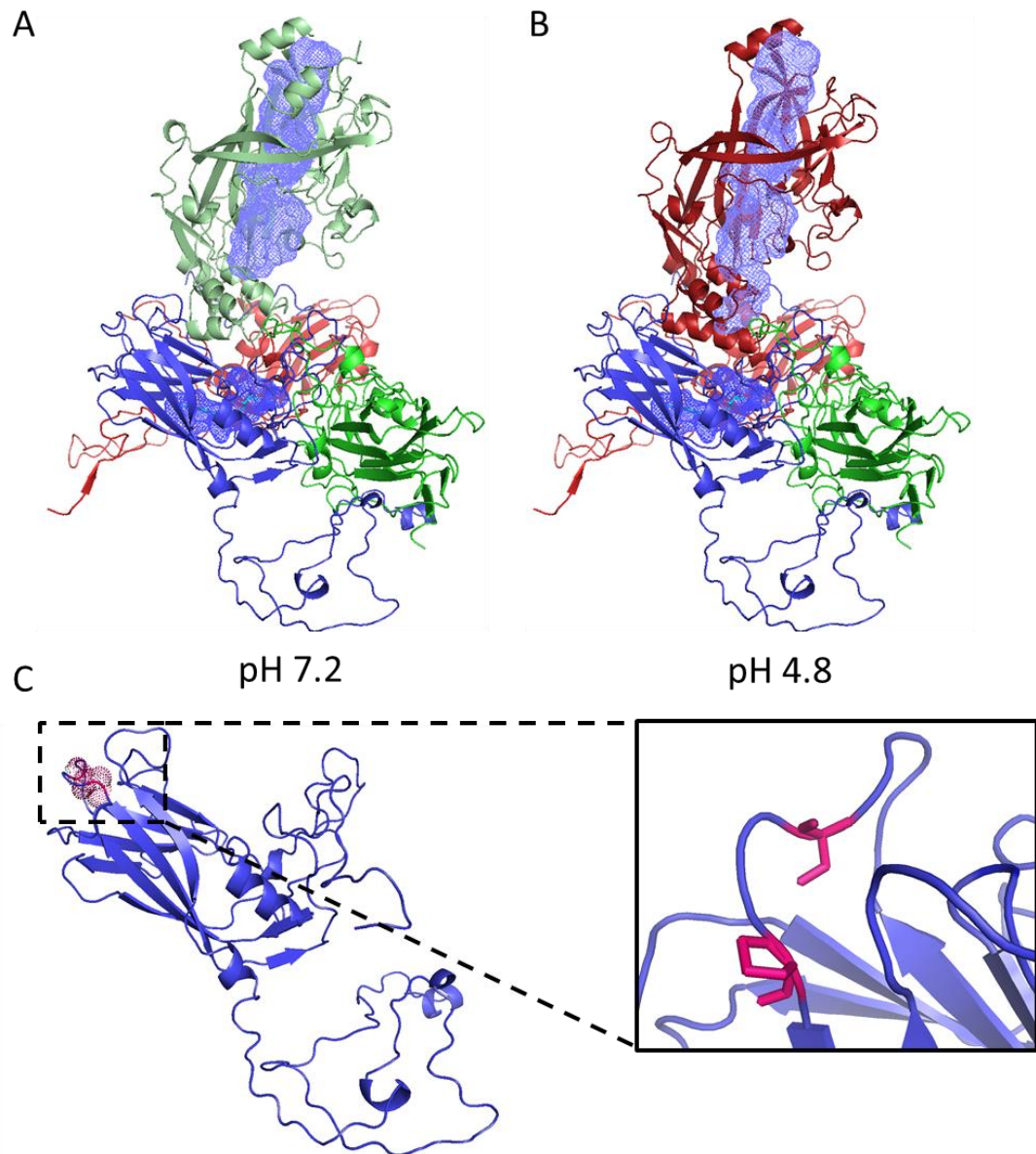


Figure 4.1. Acid induced conformational change in SCARB2 creates a connection between its own hydrophobic tunnel and the EV71 hydrophobic VP1 pocket. PyMol representation of docking model SCARB2 in its neutral conformation (A mint green) and acid induced conformation (B brick red) with an EV71 protomer composed of VP1 (Blue), VP2 (Green), VP3 (Red), hydrophobic spaces are represented by blue mesh, pocket factor is represented by cyan sticks in the VP1 pocket. Produced in PyMol using the Protein Data Bank (www.rcsb.org/pdb) from Dang et al. 2014. C VP1 is represented by in blue, residues that have previously been reported by Qing et al 2014 to be involved in cyclophilin A (S243, P246) interactions are represented in hot pink. Produced in PyMol using the PDB from Dang et al. 2014

4.1 Cells and purification

4.1.1 Optimisation of viral growth

The literature details a number of different methods of growing EV71 (Lin et al. 2012; Plevka 2012; Nishimura et al. 2009). To ensure that the maximum yield of virus could be achieved a number of different virus strains, cell lines and growth conditions were explored.

The virus strains tested were ED1, a clinical isolate (Supplied by Prof Peter Simmonds), a genotype B2 isolate MS742387 (Supplied by SingVac), and BrCr a genotype A isolate and prototype EV71 strain (Supplied by Prof Frank van Kupperveld). This initial work was carried out by infecting Vero cells grown in a T175 flask. It was determined that MS742387 gave the highest yields and all further work was conducted with this strain (Figure 4.2).

Next, the yield of EV71 grown in Vero cells, Rhabdomyosarcoma (RD) cells, HeLa cells, suspension HeLa cells, and Jurkat cells was evaluated; Vero, RD, HeLa and Jurkat cells have previously been shown to support growth of EV71 (Lin et al. 2012; Plevka, Perera & Rossmann 2012; Nishimura et al. 2009). Vero and RD cells have been shown to allow entry through the receptor SCARB2, although SCARB2 was shown to be non-essential for entry in Vero cells (Lin et al. 2012). Jurkat cells allow entry via the PSGL1 receptor and the entry mechanism of EV71 in HeLa cells has not been studied. To assess which cell line can produce the highest yield, monolayers of cells were grown in T175 flasks, except for the Jurkat cells and suspension HeLa cells, which are non-adherent cell lines. These were grown in suspension. After

100% cell death had been achieved, samples were titrated via TCID₅₀ assay in Vero cells (Figure 4.3).

Vero and RD cells produced the highest yields of virus, with titres of between 1×10^7 to 1×10^8 TCID₅₀ per/ml (Figure 4.3). However, it had previously been reported that HeLa cells were also able to yield titres close to this, but here only a titre of 3.5×10^5 TCID₅₀ per/ml was achieved (Figure 4.3) (Plevka et al. 2012). An attempt was made to adapt the virus to grow to higher yields in HeLa cells. However, after 5 passages the titre did not increase (data not shown). As Vero cells produced the highest yields and grew faster than RD cells, work was subsequently continued in Vero cells.

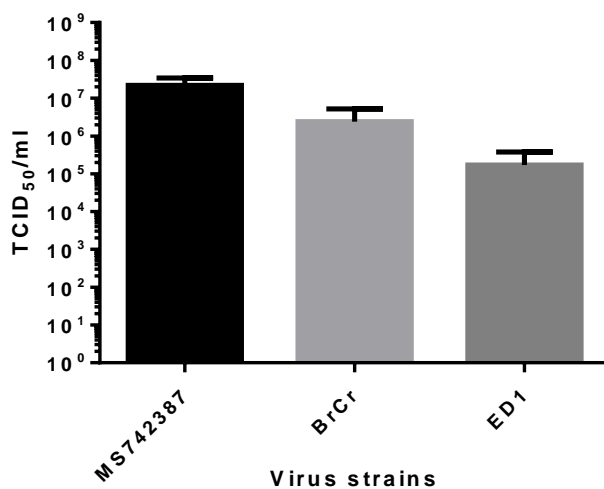


Figure 4.2 Comparative yields of different strains of EV71. EV71 strains MS74387, BrCr and ED1 were used to infect Vero cell monolayers at MOI 1 TCID₅₀'s/cell TCID₅₀'s/cell. They were incubated at 37 °C until 100% cell death had been achieved and harvests were titrated by TCID₅₀ assay. Each bar represents an average of three measurements and error was measured using s.e.m.

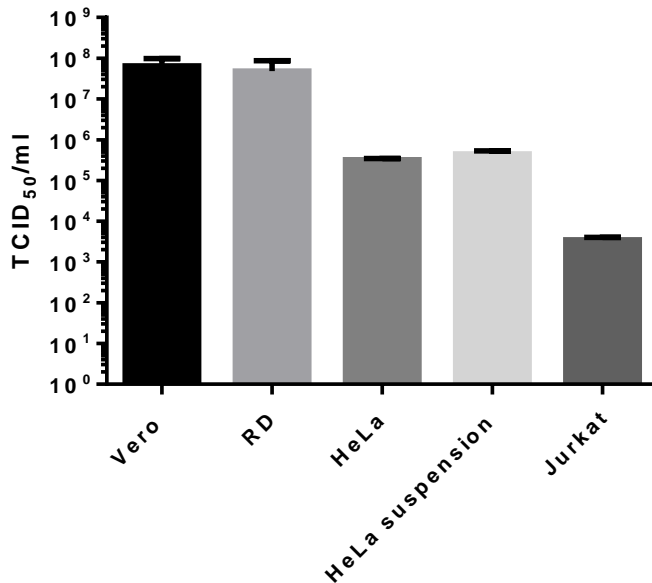


Figure 4.3 Comparative yields of EV71 in different cell lines. Monolayers of Vero cells, RD cells and HeLa cells and suspension cultures of HeLa cells and Jurkat cells, were infected with EV71 strain MS74387 at an MOI 10 TCID₅₀'s/cell. When 100% cell death had been achieved, samples were titrated by TCID₅₀ assay. Each bar represents an average of three measurements and error was measured using s.e.m.

A number of different methods of cell culture were employed in attempts to improve virus yields. These were; flasks, roller bottles and microcarrier beads. All have been shown to be successful for growth of EV71 (Chou et al. 2012; Liu et al. 2007). In standard flasks the adherent cells stick to the bottom and are incubated with media. With roller bottles the entire bottle is coated with cells and media is slowly rolled over the inner surface, which reduces the volume of media required. With microcarrier beads adherent cells are attached to the beads so that the cells can be grown in suspension, which enables a greater number of cells per ml. Greater number of cells could help obtain higher virus yields and reduce the resources needed for bulk virus growth. The latter two methods are generally used

for large scale preparation, with microcarriers being used on an industrial scale.

Figure 4.4 summarises the results from these experiments. It was evident that there was relatively little difference between the titre per ml that could be achieved between each technique. However, flasks were the least labour-intensive so this was the method chosen for bulk growing virus.

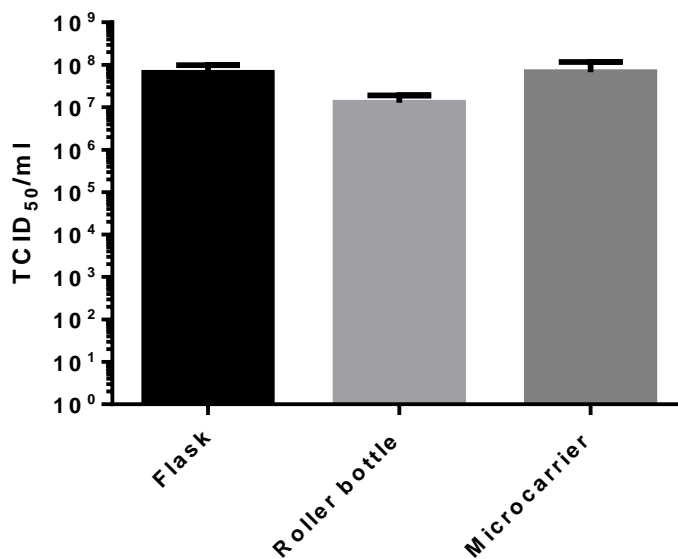


Figure 4.4. Optimising growth techniques for EV71. Vero cells were grown in either flasks, roller bottles or on microcarrier beads in suspension. Once cells were confluent, they were infected at MOI 10 TCID₅₀'s/cell and left until 100% cell death was achieved and then titrated by TCID₅₀ assay. Each bar represents an average of three measurements and error was measured using s.e.m.

4.1.2 Replication kinetics of WT EV71 in Vero cells

Next the viral replication kinetics were studied. This is useful in understanding the virus life cycle, as it can identify when certain events occur, such as cell entry, uncoating and viral replication. In PV it is known that a full replication cycle from

receptor binding to cell lysis takes around nine hours, and cell entry, uncoating and replication occurs within the first 30 minutes of infection (Brandenburg et al. 2007).

Initially EV71 growth kinetics were studied to establish the time required to undergo a full life cycle. This was done by performing a one-step growth curve experiment in which Vero cell monolayers were infected with virus at an MOI of 1 TCID₅₀'s/cell and a sample for titration was taken each hour. These were taken by scraping cells from the wells and freeze-thawing three times to release intracellular virus, total virus was then titrated via TCID₅₀ assay. This revealed that there is a drop in titre at three to four hours post infection. At seven hours post-infection titres began to increase, and continued to until they peaked at 20 hours (Figure 4.5 A). The drop in titre at 2-3 hours post infection indicates that uncoating has occurred as uncoated virions are not infectious and the increase in titre at seven hours post infection is indicative that mature infectious virions have been produced (Lu et al 2011). This indicates that virus uncoating continues until three hours after infection and infectious virus is produced between seven and 20 hour post-infection, at which point replication ends due to cell lysis. This is consistent with the findings of Lu et al 2011.

Further analysis to determine the time of uncoating were carried out using time of addition studies with the uncoating inhibitor NLD previously discussed in Chapter 3. NLD is able to bind the virus capsid and stabilise it to prevent conformational changes necessary for uncoating, and infection of cells (De Colibus et al. 2014; Dang et al. 2014, discussed in more detail in section 1.3 and chapter 3). In this experiment monolayers of Vero cells were infected with EV71 and from zero to

seven hours post-infection NLD was added to a new well and left for 24 hours before cells were harvested. Virus was then titrated via TCID₅₀ assay and the percentage loss in titre was calculated for each time point by comparing it to an infected monolayer that had not been treated with NLD. This allows the time of uncoating to be estimated, as a reduction in titre will only occur when NLD has been added prior to virus uncoating. This experiment revealed that NLD had complete activity against EV71 until five hours post infection (Figure 4.5B). Six hours post infection the inhibitory effect of NLD was greatly reduced. Results in PV have shown that NLD only has maximum activity up to one hour post infection (unpublished data Oluwapelumi Adeyemi). This indicates that uncoating does not complete until after five hours post infection (Figure 4.5B). Taken together with the infectivity data (Figure 4.5B), it indicates that uncoating occurs for a prolonged period of time, between three and five hours post-infection.

To attain a better understanding of when post entry events such as translation and replication occurred, protein production was analysed using ³⁵S labelling. Cells were infected with virus at an MOI of 1 TCID₅₀'s/cell using RPMI cysteine and methionine free media and ³⁵S labelled cysteine and methionine was added to a different well every hour for 24 hours. Cells from all wells were harvested after 24 hours, meaning that each subsequent well had been incubated in the presence of ³⁵S labelled cysteine and methionine for an hour less than the previous well. As the ³⁵S labelled cysteine and methionine, will be incorporated into all proteins that are synthesised after its addition, it is possible to detect when the proteins were synthesised. The cell samples were taken and analysed by SDS PAGE (Figure 4.5C). From these

analyses it is evident that viral protein production continues until very late in the infection, with viral banding patterns still visible up until 22 hours after infection, just prior to lysis. To better understand the portion of the labelled protein that forms mature virions, samples were subjected to immunoprecipitation using an antibody that has previously been shown to recognise mature EV71 virus particles (Wang et al. 2012). Samples were then analysed using an SDS PAGE gel (Figure 4.5C). This shows that the majority of mature particles are produced between three and nine hours post-infection, and by 12 hours post-infection significantly fewer mature particles are formed. The labelling data and the infectivity data are contradictory and are n=1 experiments, so both would need to be repeated further before any conclusions could be made.

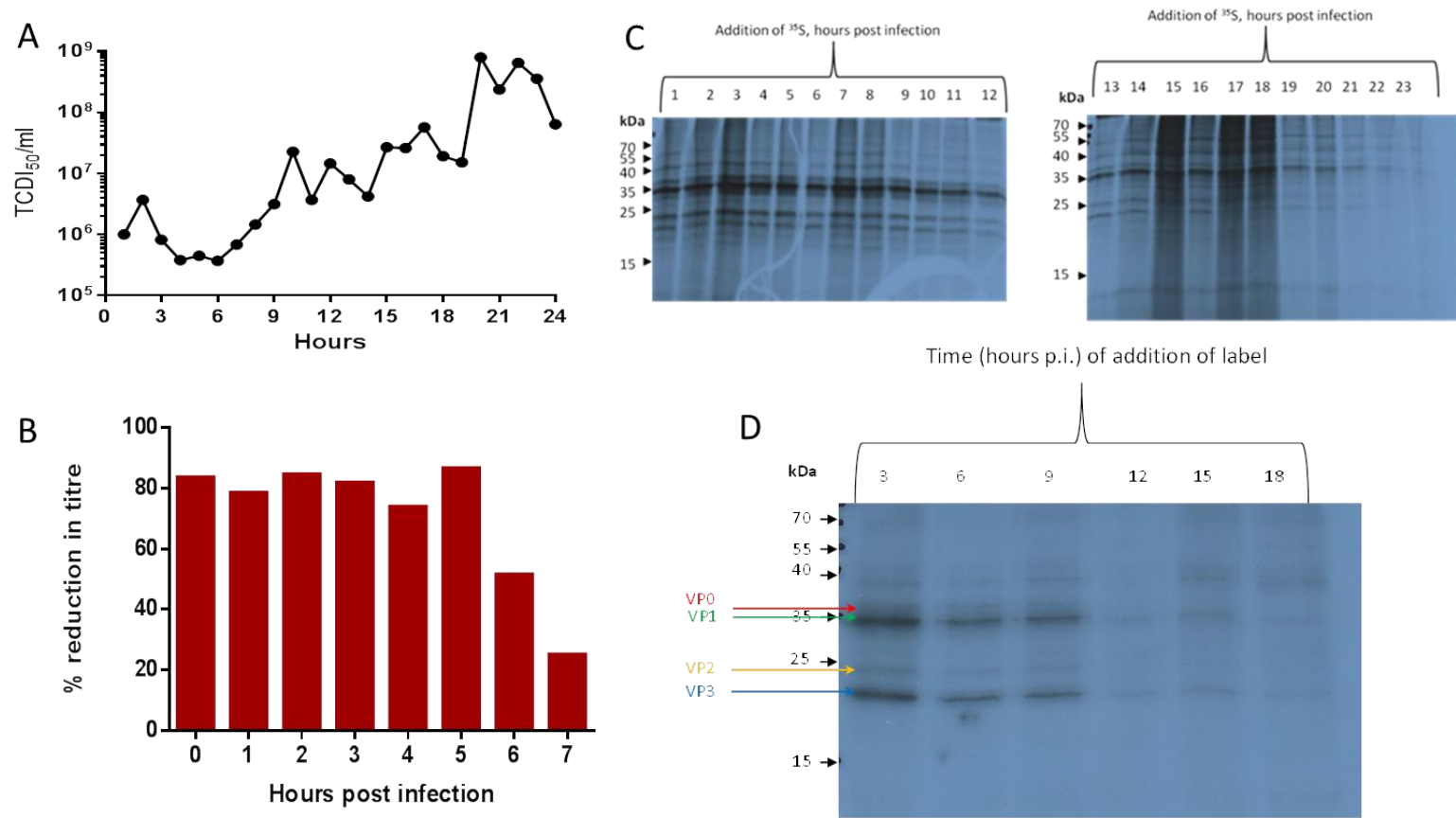


Figure 4.5 Growth of EV71. (A) Vero cells were grown in six well plates and infected with EV71 at an MOI 10 TCID₅₀'s/cell. Every hour whole cell samples were taken. The viral titre of each sample was measured by TCID₅₀ assay. n = 1. (B) Cells were infected with EV71 at MOI 1 TCID₅₀'s/cell and NLD was then added to a different well of cells every hour. After 24 hours, samples were titrated by TCID₅₀ assay. n = 1 (Performed by Amy Radcliffe). (C) Vero cells were grown in six well plates and every hour ³⁵S labelled cysteine and methionine was added to a new well and left for

the duration of the infection. After 24 hours the samples were harvested and analysed by SDS PAGE gel. n = 1. (D) Vero cells were grown in 6 well plates and every hour ³⁵S labelled cysteine and methionine was added to a new well, after 24 hours the samples were harvested, samples were then immunoprecipitated with mature capsid recognising antibody mAb A6 and analysed by SDS PAGE gel. n = 1. The sizes are accessed by using a BioRad precession plus protein marker.

4.1.3 Viral purification and empty capsid production

To better understand the EV71 life cycle, the different particles that occur at different stages in the life cycle were analysed. These particles can be distinguished by density and buoyant density. Initially particles were separated by sucrose density gradient centrifugation, as is commonly performed for other enteroviruses. To ensure that the purification techniques employed were working, ³⁵S labelled EV71 and BEV2 (as a control) were grown side by side and purified at the same time using the purification technique in the Materials and Methods section 2.5.1. Particles were then separated on sucrose gradients and fractions analysed by either scintillation counting or SDS PAGE.

When the BEV2 gradient was analysed by scintillation counting there were two peaks, one towards the bottom of the gradient, which is where full particles are expected to sediment, and one around the middle of the gradient, where empty particles were expected to sediment. A large amount of labelled material was also observed towards the top of the gradient (Figure 4.6A). This profile is consistent with sucrose gradients profiles of BEV and other enteroviruses (Ismail-Cassim et al. 1990). However, for EV71 there was only detectable material towards the top of the gradient, which was speculated to be viral subunits, cellular debris or both

(Figure 4.6B). It was suspected that no EV71 particles were detectable because the level of virus was too low for detection. Consequently the scale of EV71 production was increased so that there was 10 times more virus than in the BEV experiment; however, there were still no detectable peaks (Figure 4.6C). The total virus present after each purification step was then measured using TCID₅₀ assay to assess if virus was lost at any stage. This showed that over 1 log (1×10^9 TCID₅₀/ml) of infectious virus was lost after the precipitation stage and then a further 2 logs (1×10^8 TCID₅₀/ml) was lost after the sucrose cushion stage while less than one log of BEV was lost in total (Table 4.1).

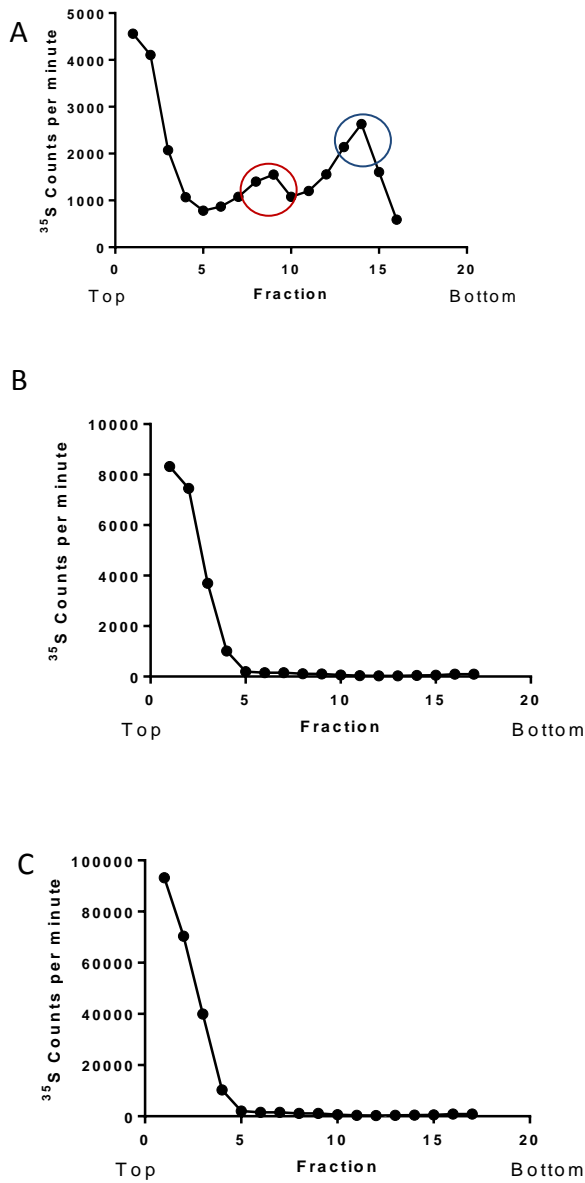


Figure 4.6 Sucrose gradient profiles of ³⁵S labelled BEV and EV71 BEV grown in a well of a six well plate (A) EV71 grown in one T175 flask (B) or 20 T175 flasks (C). Mature particles (circled blue 14) and empty particles (circled red fraction 9) were separated by centrifugation through a continuous 15-45 (w/v) % sucrose gradient. 300 µl fractions were taken and analysed by scintillation counting.

	Total number of infectious units EV71 (TCID₅₀)	Total number of infectious units BEV (PFU)
<i>Supernatant</i>	8.88 x 10 ⁻¹⁰	6.31 x 10 ⁸
<i>Pellet after precipitation</i>	2.28 x 10 ⁹	4.48 x 10 ⁸
<i>Pellet after sucrose cushion</i>	1.90 x 10 ⁶	1.74 x 10 ⁸

Table 4.1 Recovery of EV71 or BEV2 viruses after sequential steps during purification. EV71 was grown in 20 T175 flasks of Vero cells and BEV was grown in one T175 of BHK21 cells.

The appearances of the pellets at each stage were then compared. The EV71 pellet after the precipitation step was seen to be layered. A white layer appeared at the bottom of the tube and a yellow pellet on the side. In contrast only a white pellet was formed in the BEV samples. When the white pellet and the yellow pellet were titrated separately the majority of the infectious virus was present in the yellow pellet (Figure 4.7). Furthermore, the yellow material formed if EV71 cell lysate was stored in the fridge overnight. The yellow material was also observed in Vero cells infected with BEV and uninfected Vero cells that were lysed by freeze thawing.

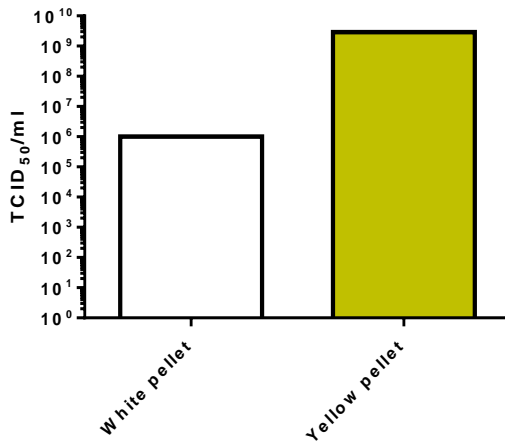


Figure 4.7 Virus titres of different EV71 pellets. 10 flasks of Vero cells were infected with EV71 at MOI 10 TCID₅₀'s/cell. The virus harvest was clarified and the cell debris was freeze-thawed three times in a small volume and the supernatant added to the first. The pooled supernatant was then precipitated in 50% saturated ammonium sulphate overnight at 4 °C. This was then centrifuged at 10,000 RPM for one hour. The supernatant was then decanted, leaving two separate pellets, a white pellet at the bottom of the tube and a yellow pellet up the side of the tube. Both pellets were resuspended in 1 ml of PBS and titrated by TCID₅₀ assay.

It was then attempted to separate the virus from the yellow material with detergents and then analysing the virus after centrifugation through a 15-45 w/v % sucrose gradient. However, this was not successful as it did not separate the virus from this material, as virus was still present at the top of the gradient. It was then decided to omit the precipitation stage and progress directly to the sucrose cushion stage. However, a yellow insoluble pellet was formed after ultracentrifugation that could not be solubilised, even with 10 w/v % SDS, in which the suspension was very cloudy. When this suspension was separated on a sucrose gradient the yellow insoluble matter pelleted but a white cloudy substance remained at the top of the gradient (Figure 4.8 A). The highest virus titres were found in the high count fractions towards the top of the gradient (Figure 4.8 B). This implies that the majority of virus associates with the cloudy substance.

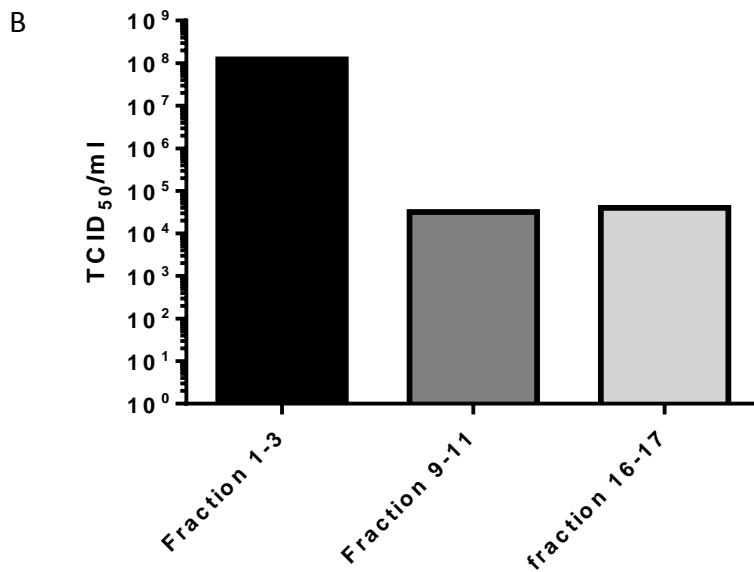
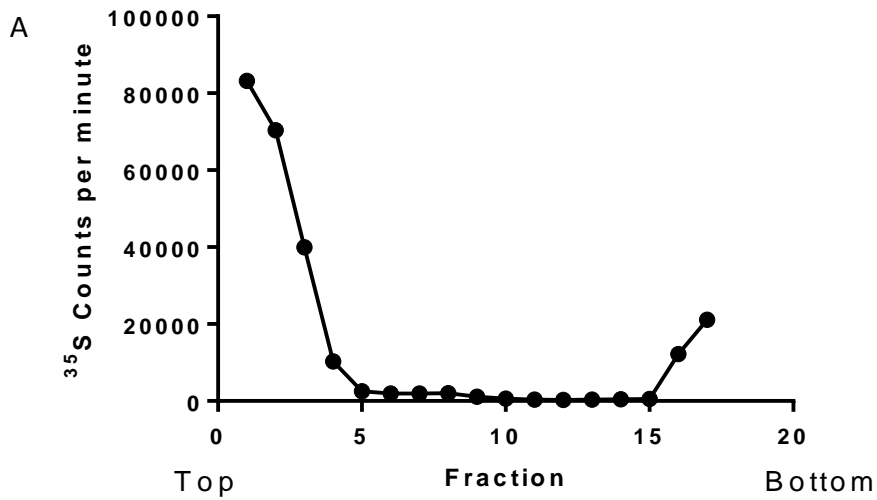


Figure 4.8 Sucrose gradient profiles and titrations of ³⁵S labelled EV71 after treatment with SDS. (A) Virus was separated by centrifugation through a 15-45 w/v % sucrose cushion. 300 µl fractions were taken and analysed by scintillation counting. (B) Titration of an EV71 sucrose gradient. Different fractions were pooled together and then titrated by TCID₅₀ assay.

It was hypothesised that this yellow/cloudy substance was specific to Vero cells and so RD cells were used to grow the virus. Virus grew in RD cells to a similar level to Vero cells (Figure 4.2), and the pellet formed was less yellow, but still insoluble after purification through a sucrose cushion. When analysed by sucrose density gradient centrifugation after purification through a sucrose cushion, the majority of the counts were still seen at the top of the gradient, but a small peak was consistently seen just below the material at the top (Methods section 2.5.2) (Figure 4.9 A). Next, virus supernatant was treated with 50 μ M DNase (AlphiChem) or 1% w/v SDS for 3.5 hours prior to the sucrose cushion as performed in Kattur Venkatachalam et al. 2014. Both treatments resulted in a post-sucrose cushion pellet that could be solubilised. After sucrose density gradient centrifugation the DNase treated sample produced a slightly larger peak compared to the small one seen in Figure 4.9 A, although the majority of counts were still seen at the top of the gradient. However, after SDS treatment the number of counts at the top of the tube was reduced, but there were still no faster sedimenting peaks (Figure 4.9 A). The small peak with DNase treatment was reproducible (Figure 4.9 B) and when examined by SDS PAGE gel a viral capsid band profile was visible (Figure 4.9 C). The large amount of material seen at the top of the EV71 gradient also had bands at positions compatible with viral capsid proteins. This indicates that the virus is associated with the cloudy material, indicating that the particles could potentially be envelope

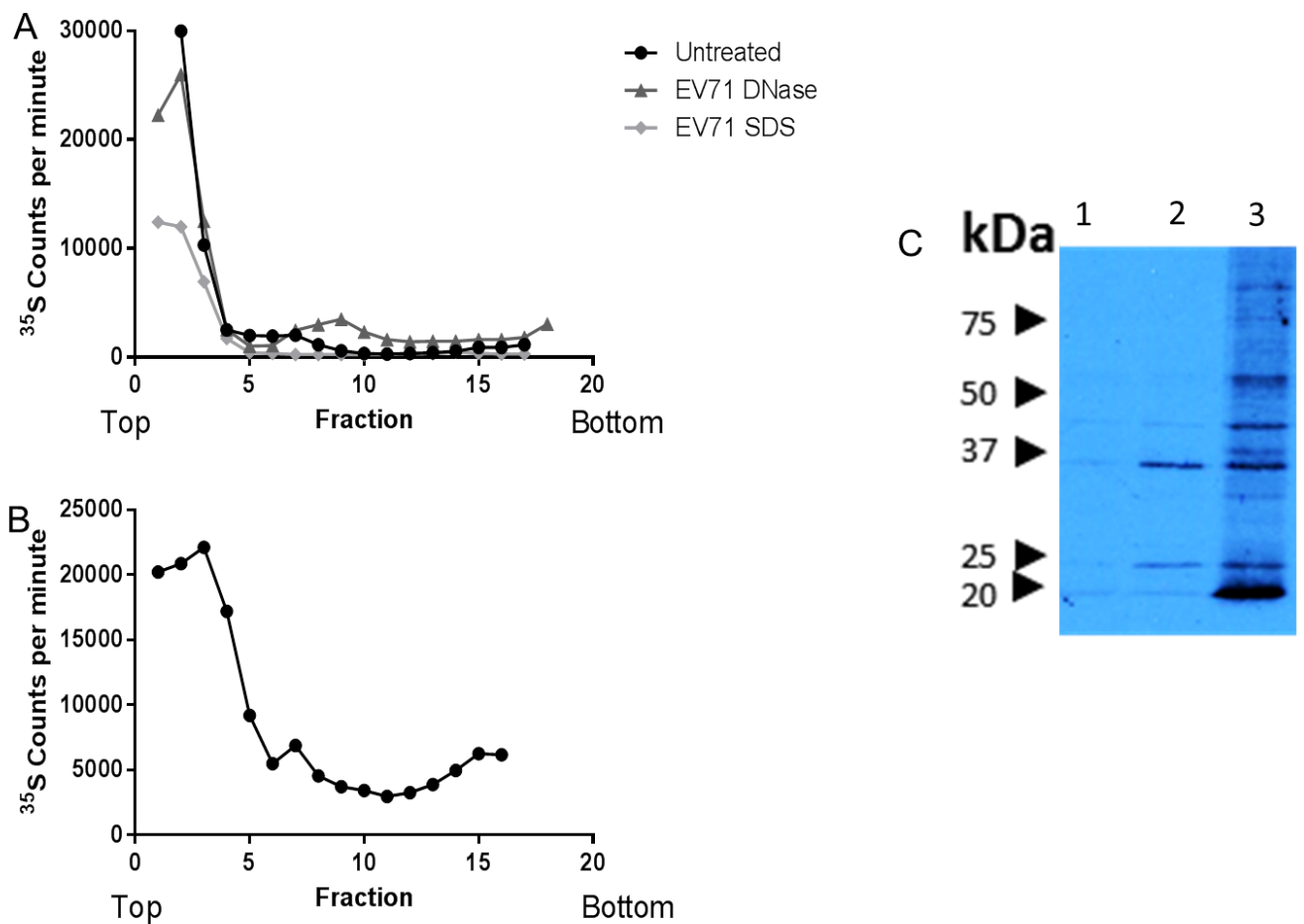


Figure 4.9 Sucrose gradient profiles of ³⁵S labelled EV71 grown in RD cells. (A) Samples untreated, treated with SDS or DNase prior the sucrose gradient were run alongside each other. (B) Repeat of EV71 gradient treated with DNase. All particle were separated by centrifugation through a 15-45 w/v % sucrose gradient. 300 µl fractions were taken and analysed by scintillation counting. (C) SDS PAGE gel Sample 1, 2 and 3 correspond to A, 1 is the peak from the DNase treated sample (fraction 10) and 2 is top of the gradient (fraction 2), sample 3 is from the top of the gradient that was treated with SDS (Fraction 2). Expected band sizes; VP1 36 kDa, VP2 25 kDa, VP3 23 kDa

To further analyse the virus another purification method was employed using Nycodenz gradients (Methods 2.5.3). This separates particles based upon buoyant density rather than rate of sedimentation. Both 20-60 w/v % step gradients and 40 w/v % self-forming gradients were used. Bands visible by eye were formed in both gradients, and these correlated with the ^{35}S peaks observed by scintillation counting (Figure 4.10). In the step gradients, peaks were seen towards the centre of the gradient, but for the self-forming gradients there was one peak near the top of the gradient and another towards the bottom of the gradient. However if the cell pellet was freeze-thawed with RIPA buffer, instead of 1 v/v % NP40 then the higher (less dense) peak was greatly diminished (Figure 4.10).

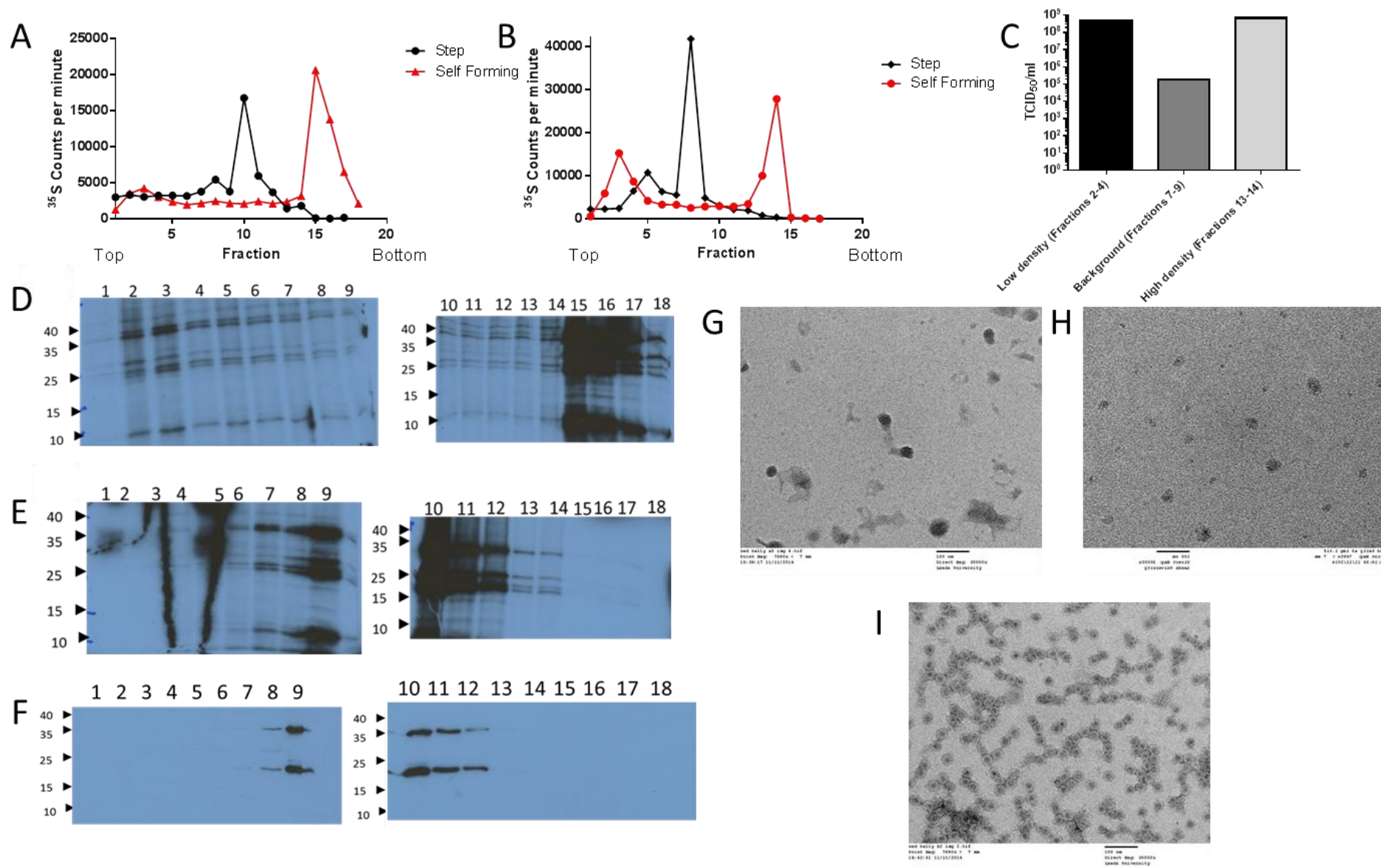


Figure 4.10. Analysis and comparison of EV71 purified through Self-forming (40 w/v %) and step (20%-60 w/v %) Nycodenz gradients. EV71 was used to infect a flask of RD cells, after 100% cell death the cells were lysed with RIPA buffer (A) or 1 v/v% NP40 (B), clarified and subjected to ultracentrifugation through a 30 w/v % sucrose cushion and then subjected to ultracentrifugation for 22 hours (A), or 20 hours (B) at 55,000 RPM in a SW55 rotor through a 40 w/v % self-forming nycodenz gradient, or a 20-60 w/v % step gradient. Gradients were then fractionated and analysed by scintillation counting the ³⁵S counts per minute (A-B). The self-forming gradient from graph B was further analysed by TCID₅₀, to assess the titres of the different fractions (C). Samples from graph B were further analysed by SDS PAGE autoradiography, (Self forming D, Step E). (F) Western Blot analysis of the step gradient from graph B using an anti VP1 mAb was performed. Fractions from the self-forming gradient in graph B were then further analysed by TEM, Low density (fractions 2-4), (A), background no peak (fractions 7-9) (B) and high density peaks (fraction 13-14).

Analysis of the gradient fractions by SDS PAGE followed by autoradiography or western blotting with an EV71 VP1 antibody revealed these peak fractions to contain the highest proportion of EV71 viral capsid proteins, it is also evident that the self-forming gradient can produce cleaner peak fractions (Figure 4.10 D,E). Titration of the fractions from the self-forming gradient revealed there to be significantly higher amounts of infectious virus in the peak fractions compared to the non-peak fractions, and the low density had higher titres per count/banding intensity than the high density fraction titre (Figure 4.10 C). The viral banding pattern and infection data indicates that infectious EV71 particles are present in both peaks. When samples were viewed using EM, viral particles were observed in the lower fraction (Figure 4.10 G-I). In the higher density fraction particles were observed that resembled the enveloped HAV particles observed in Feng et al 2013 (Figure 4.10). In non-peak fractions no clear regular structures were observed.

To further investigate whether this low density EV71 fraction is enveloped virus, an aliquot of the low density ^{35}S labelled EV71 (Fractions 2-4) was split across two tubes, one was incubated with 1% NP40 overnight, and an equal portion left untreated overnight. These samples were ultracentrifuged in parallel on 40% self-forming nycodenz gradients. The gradients were then fractionated and analysed by scintillation counting. From this experiment it was seen that treatment with 1% NP40 reduced the radioactivity in the low density peak with a corresponding increase in the high density peak (Figure 4.11).

The data also suggests that enveloped particles are more infectious than the non-enveloped particles as they have a higher specific infectivity based on radioactive counts (figure 4.10). This mirrors the observations of Chen et al. 2015, where enveloped PV particles were shown to produce a higher plaque forming unit (PFU) per virion than naked PV. Although it is not certain these are the same type of particles as in Chen et al. 2015 the particles were often bigger with diameters over 500 nM compared to a maximum diameter of 50 nM observed here.

Next the entry mechanisms of the high and low density forms were explored, as the difference in specific infectivity of the two particles may be a reflection of differences in cell entry. Observations by Chen et al. 2015, showed that enveloped PV utilises an additional receptor to non-enveloped PV and Feng et al. 2013 observed that non-enveloped HAV is insensitive to chloroquine, a compound that can prevent endosome acidification. Endosome acidification has been shown to be essential for infection by EV71 and chloroquine can prevent infection *in vitro* (Lin et al. 2012; Lin et al. 2013). The susceptibility of low density (enveloped) or high

density (non-enveloped) virus to chloroquine was investigated. Here cells were pre-treated with chloroquine, to prevent endosome acidification and after two hours were infected with either low density (enveloped) or high density (non-enveloped) EV71. Cells were then incubated until 100% cell death had occurred, when samples were titrated by TCID₅₀ assay (Figure 4.12, performed by a PhD student Özlem Cesur). This showed that low density (enveloped) EV71 is susceptible to chloroquine while high density (non-enveloped) virus was not. This suggests a different entry/uncoating mechanism between the two particles, although more repeats are necessary as it currently n = 1.

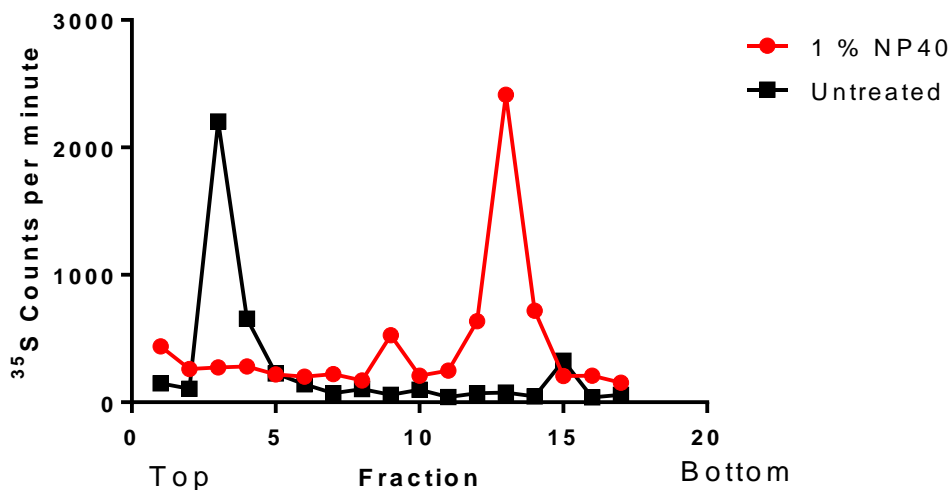


Figure 4.11 High buoyancy EV71 is sensitive to NP40 treatment. ³⁵S labelled low density EV71 that had previously been purified through a self-forming nycodenz gradient was either treated with 1% NP40 over night or left untreated. They were then ultracentrifuged through further self-forming nycodenz gradients in parallel. Gradients were then fractionated and analysed by scintillation counting.

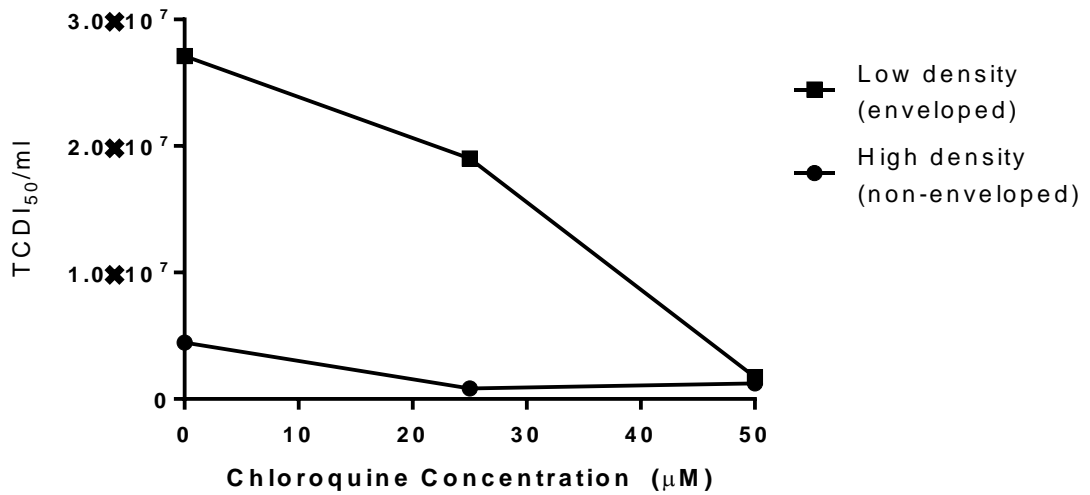


Figure 4.12 Effect of chloroquine on high and low buoyancy EV71. High density and low density particles were used to infect cells pre-treated with increasing concentrations of chloroquine and then titrated by TCID₅₀ after 100% cell death had occurred. (Performed by Özlem Cesur). n = 1.

As enveloped and non-enveloped particles appear to separate on nycodenz gradients they were also used to distinguish between empty and mature virions. Empty particles can occur naturally ('natural empties' as discussed in section 1.2.4) but they can also be produced by heating virions. These types of particles sediment similarly on sucrose gradients, but they have different protein profiles as natural empty particles have not undergone VPO cleavage (discussed in section 1.2.4). Virus was heated at 60 °C to convert to 'artificial' empty particles and separated by nycodenz density gradient centrifugation. After centrifugation the sample was fractionated and analysed by scintillation counting this revealed that a different sedimentation pattern to the untreated virus (Figure 4.13). This indicates that it is possible to distinguish between the two particles via Nycodenz gradients.

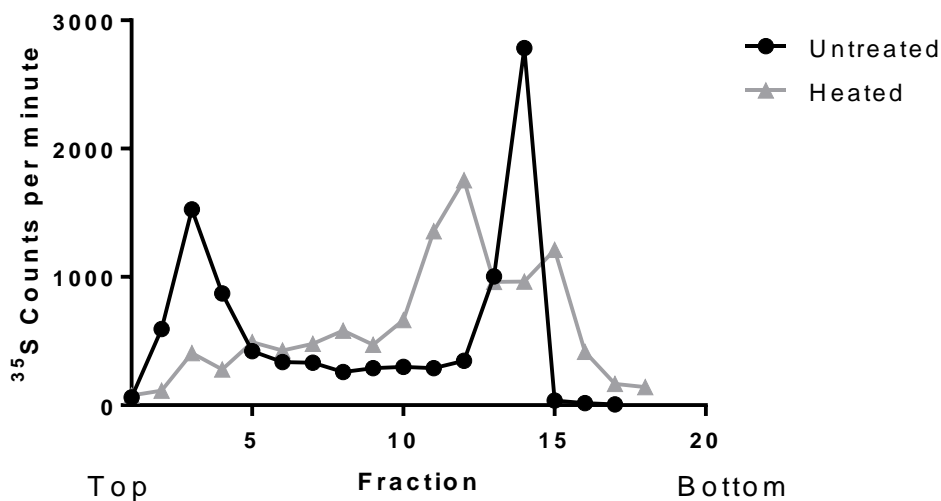


Figure 4.13 The effect of heating on the nycodenz gradient profile of EV71. Heated (60 °C for 30 minutes) or unheated EV71 was separated on self-forming Nycodenz gradients.

4.2 A mutant with an altered uncoating phenotype

To further study the effect of pH on EV71 uncoating the effect of low pH on cell entry and uncoating of the virus was assessed. Virus was incubated in pH 5.6 buffer for one hour at 4 °C. 5 ml of the solution was added directly to Vero cells and incubated on them for 30 minutes at room temperature, before being topped up with 20 ml of serum free DMEM. At this point cells were incubated at 37 °C until 100% cell death had occurred. This treatment reduced the virus titre by 1×10^3 TCID₅₀ per/ml (i.e. three orders of magnitude) (Figure 4.14). However, when media was neutralised with 1 M Tris before infection or if the incubation was at pH 7.2 there was no reduction in virus titre compared to incubating in pH 5.6 buffer (Figure 4.14B). When the virus was passaged under low pH conditions resistance developed after one passage and the resulting virus has been termed the acid-resistant virus (Figure 4.14C).

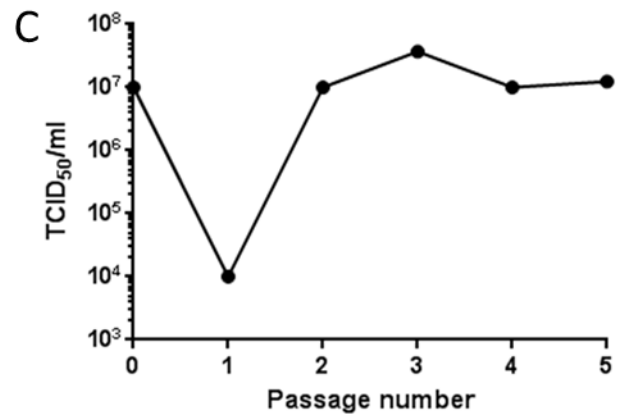
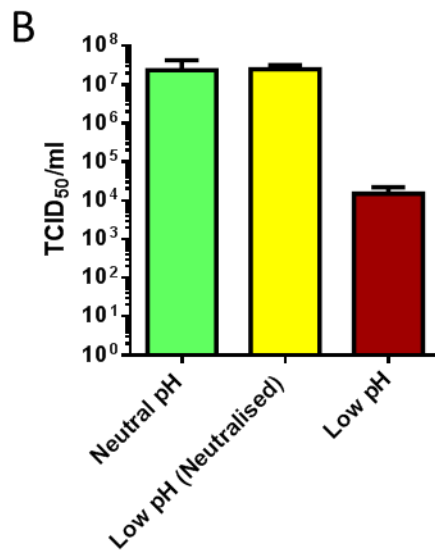
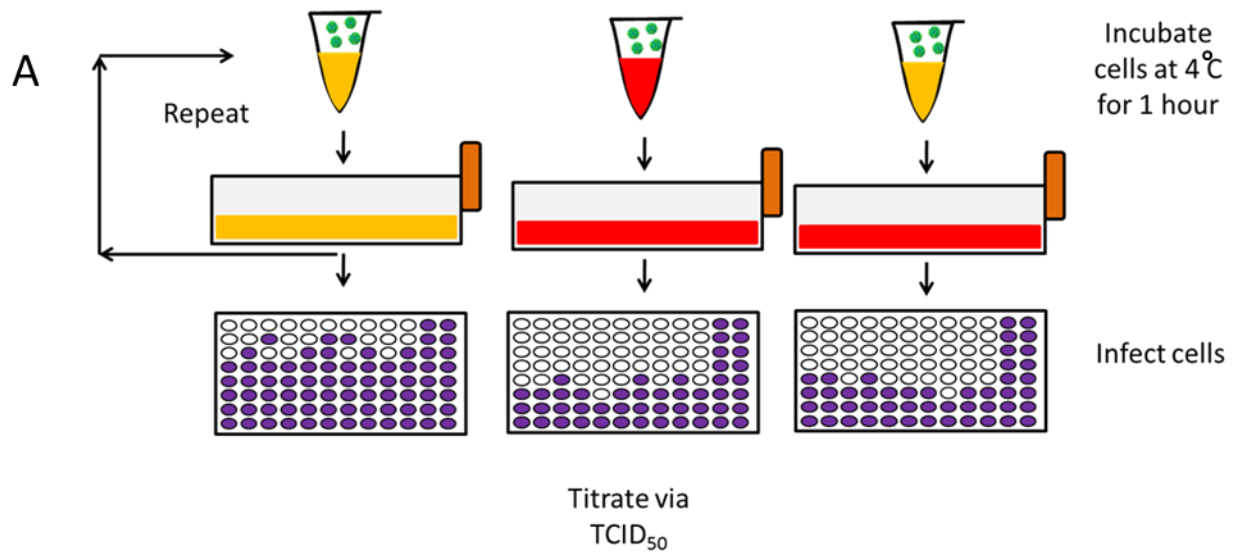


Figure 4.14. pH treatment of virus on cells has a fitness cost. Virus was incubated in either PBS pH 7.2 (green) or a pH 5.6 buffer (red) for one hour, then used to infect Vero cells at an MOI of 1 TCID₅₀'s/cell. Virus incubated in pH 5.6 buffer was also neutralised with a 1 M Tris prior to infection of cells (yellow) (A). (B) After 100% cell death, lysates were then titrated via TCID₅₀ assay. Each bar represents an average of three measurements and error was measured using standard error. (C) Evolution of an acid-resistant virus. EV71 was incubated in a pH 5.6 buffer for one hour at 4 °C and then 5 ml of this solution was used to infect cells for 20 minutes at room temperature before adding 20 ml of DMEM. Cells were then incubated at 37 °C until 100% cell death. The process was repeated, for 5 passages. Virus was titrated via TCID₅₀ assay after each passage.

Sequencing of the capsid coding region of the acid-resistant virus, revealed a single point mutation between every isolate observed (VP1 N104S n=6/6) and a duplication of three codons in VP2 (n = 1/5). Sequence alignments show that N104 is conserved among all EV71 genotypes and is close to N102 which is a highly conserved residue among all EV71/CVA16 genotypes and among all enterovirus A species that utilize SCARB2 as their major receptor, but it is not conserved among viruses that have not been shown to utilize SCARB2 (Yamayoshi et al. 2012). Similar observations were made in Dang et al. 2014 (Figure 4.15). This indicates that it could be an important residue for SCARB2 mediated cell entry.

Mapping N104 in a docking model of the crystal structures of EV71 and SCARB2 reveals that it is located in loop of VP1, which is predicted to be a SCARB2 binding site (Dang et al. 2014) (Figure 4.16). Comparing the docking models of SCARB2 in its neutral and acid conformations predicts that an alpha helix of SCARB2 moves towards VP1 residue N104 in its acid induced form (Figure 4.16). This indicates that N104 may play a role in binding to the acid-induced form, which is the conformation that is able to induce uncoating. These results, taken together with experiments performed by Dang et al 2014 that showed co-immunoprecipitation with SCARB2 and an EV71 peptide sequence containing residue N104, suggest that this residue is involved in SCARB2 binding. Given that the mutation is to a serine, which is smaller, it is possible that this serine is no longer able to bind SCARB2.

EV71A	NASDESMIETRCVLNSHSTAETTLDSFFSRAGLVGEIDLPLKGT	PNGYANWDIDITGY	116
EV71C4	116
EV71C1E.....	116
EV71B2	..T.....E.....	116
EV71B3	..T.....E.....	116
CVA16A	..QENL.....H.....IGN.....SI.TM.TT..Q.TD..V.....LM..	116
CVA16B	..KNL.....H...Q...AIGN.....SI.TM.TT..Q.TD..V.....LM..	116
CVA7	LV...KNM.....I.K...VE...SITN.Y.....VVNM.VQ...S...TE.F.K.E...M.F	115
CVA14	LV.....VNR...EE...VGH.....V.....Q...A.TG.F.S...VM..	115
EVA120	..T.KNM.....V.K...V.....TH.Y...SGL..V...TQS.H...V.F.T.T..VM..	114
EVA76	..TT..N.....A.I.K...E.T.IEH.....SM.S.LVSEKT-TQP.....VM..	115
EVA90	..T...N.L.....V.....VAE.SVSH.....GML.L.TSDE...I...FTT.....M.F	114
EVA89	..T...N.....A.V.K...V...SVEH.....A...MVE.LTSD...NI...T...VM..	115
EVA91	TT...N.....V.K...V...VSH.YGK..LV.W.Q.LTSTKN-NH.FK...V.VM.F	115
CVA92	VT.....H...HSV...S.EN...GRA...MAT.LTSEDS-A...FT..P...M..	116
SiEV46	TT.....V.R...V...SITN.YARA...YLK.LTSKD...FTNW...MAF	111
BaEV	T...N.....V.K.GV...TSIQH..A.SA...GMVT.LTSE...A...FT...M..	101
SiEV19	..T...G.....V.K...V...SIEH.YG...A...LVSILTSE-S-A...FT...V..M.F	107
SiEV43	..T.....V.K...V...SVEH.....A...Y.SILTST...A...FT...M..	108
CVA2	..T.NL.....V.KN.VE...SINH.....A...KVE.NDT..S-AT.FT...M.Y	116
CVA4	T.T.GNL.....V...G.R...HIEH.....S...VMEVDDT..A-GK.FS...MAF	116
CVA6	..NL.....M.RNGVN.ASVEH.Y.....VVEVKDS..S-LD..TV.P..VM.F	111
CVA3	..TT.....V.RNGVV..SV.H...S...VMNILDG...SK.FKT.E..VM.F	113
CVA8	..N.....RNGVV..S..H.....VINVQD...QK.FEV...VM.F	113
CVA10	..T...N.....I.KNGVL...INH...S...VVN.TDG..D-TT...T...IM.F	115
CVA12	..T.....V.K.GVS...SVEY...S..A.VVVVEDATA...NK...T.E..VM.F	114
CVA5	..T.....VNR.GVME.SVEH...S..AGILIIEDSGTS-TK...T.E..VM.F	115
EV71A	TVGSSKSEYSLVIRIYMRMKHVRRAWIPRPMRNQNYLFKSNPNYAGDSIKPTGTSRTAITT		296
EV71C4	...T...K.P...V.....A.....N.....A.....	296
EV71C1	...T...K.P...A.....N.....	296
EV71B2	...K.P...V.....A.....N.....N.....	296
EV71B3	...K.P...V.....A.....N.....	296
CVA16A	..TE..P...TL.V...I.....L...P...T...K.ND..C.S...DK..	295
CVA16B	..TE..PH.ITL.V...I.....L...P...T...K.ND..C.S...DK..	296
CVA7	MT.EG.PTQ.VT.....L..I...V...L.S...TMRNY...N.GA..C.AK..DK..	295
CVA14	I...EGAPSVHF.V.....V.....S.P.VAKNY...K.SE..CASS...S...	295
EVI20	II...GTPPT.LT.....L..I.G.....S.D.TARNY...N.SN..C.AV..QS...	294
EV76	V...GOLTEAV...F..I.....V...I.S.K.IVKNY..FDPAV-..HS...AS...	294
EV90	VL..E.LTEA.RVRIY..I.....L.S.R..L.NY..FD.AN.T..SA..AQ...	294
EV89	V...EQITDKITV..F..L...KT.V...L.S.K..L.NY..FD.ANLTMSA..AD.KN	295
EV91	V...GQITDQ.DV...I...K..L...L.S.P.ML.NY..FD.TKL.C.SK...S.K.	295
CVA92	V...ENITTK.TV...I.....S.P.I.L.NY..FN.ND.RHMAKD..S...S...	296
SiEV46	V...GSITSKIKV..F..I.....L.S.Q.MIRNY..FPT-TV.CLAA..NN...	290
BaEV	V...GSIKD.LIV...L..I...V...I.S.PYMLKNY..FD.NN..HVTNR-NS.K.	280
SiEV19	A...GNIKSNR..V.....I...V...F.S.P..L.NY..MD.TNL.CAST..AK...	287
SiEV43	A...GSITANR..V.....I.....L...P.VL.NY..FD.TN..CSS...QS...	288
CVA2	F..EEITNERIT.....L.....V...L.SEP.VL.NF...TAV-T-HVTAN..T..N	294
CVA4	V...KQITNQKFO...L.L.R...V...L.S.P.IYRNY.T.GTT-.QHLAKD.RK..E	295
CVA6	T..ESTTGKN/HV.V...I...K...V...L.S.A.MV..Y.T.SQT-.TNTA.D.AS...	290
CVA3	I..SKTPTERD.RV...KL.....V...I.S.PYVLKNY...D.AN.V.CAKD.DD.KN	293
CVA8	F..SKTPTARD.RV.V...L.....V...I.S.P.I.L.NY...D.TK.TS.SKD.QS.K.	293
CVA10	V.SREAPQLK.QT.V..KL.....I.S.P..L.NF...DSSK.TNSARD.SS.KQ	295
CVA12	T.SGEAPGKNITV..F..L.....V...I.S.L..L.NY..FDNTK.LNASHN..S..A	294
CVA5	M..GVSTGKDVTV..F.KL.....V...I.S.P..L.NY..FDKAN.IDASSN..S...	295

Figure 4.15 Sequence alignments of VP1 of Enterovirus A species. Alignments of SCARB2 dependent (EV71(genotypes/sub-genotypes; A, B2, B3, C1 and C4), CVA7, CVA14 and CVA16 (Genotypes; A and B)) and SCARB2 independent (CVA2, CVA3, CVA4, CVA5, CVA6, CVA8, CVA10 and CVA12) enterovirus A viruses as identified by (Yamayoshi et al 2012) and unknown receptor binding (EV76, EV89, EV90, EV91, EV120, CVA92, Simian enterovirus 19, Simian enterovirus 43, Simian enterovirus 46 and Baboon enterovirus). Conserved N104 residue is highlighted in yellow, conserved residues predicted to be involved in Cyclophilin A binding are highlighted in pink, Conserved N103 residue is highlighted in green. Cyclophilin A binding area of the HI loop found by Qing et al 2014 is highlighted in a green box. Only displaying partial alignments, full alignment can be found in the appendix.

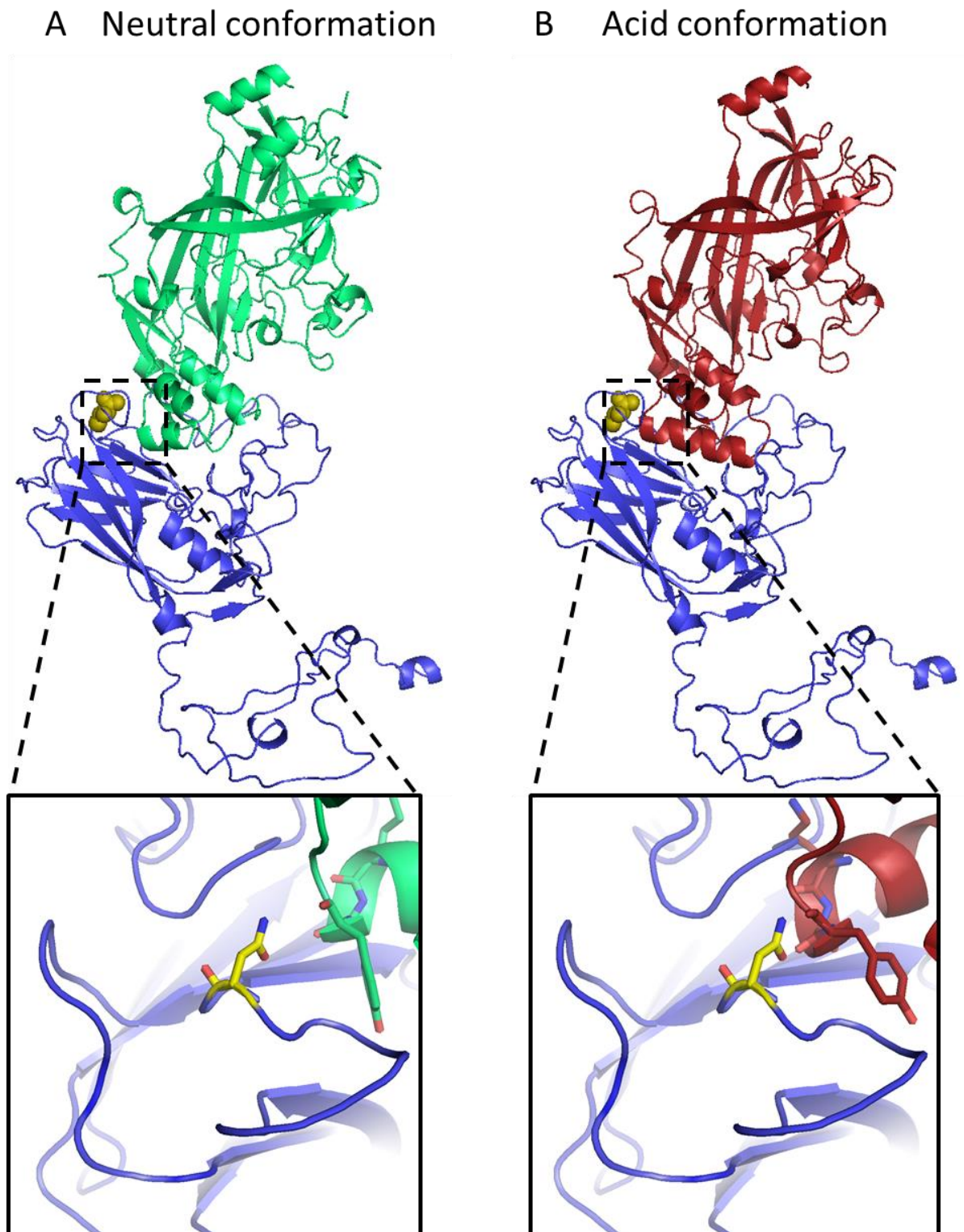


Figure 4.16 Acid induced conformational change in SCARB2 causes an alpha helix to move towards VP1 N104. Cartoon PyMol representation of docking model SCARB2 in its neutral conformation (A. green) and acid induced conformation (B. red) with EV71 VP1 (blue), N104 is highlighted in yellow.

Given the role of SCARB2 in cell entry and uncoating and the structural and co-immunoprecipitation data from Dang et al. 2014 indicating that N104 may interact with SCARB2, the cell entry and uncoating phenotypes of both WT and the acid-resistant mutant were compared.

To examine differences between cell entry, both isolates were used to infect cells that had been pre-treated with either chlorpromazine or gestin, which block the clathrin and caveolae-dependent endocytosis pathways, respectively at concentrations that have previously been shown to be effective against WT EV71 in RD cells (Lin et al. 2012; Lin et al. 2013) (work conducted by Amy Radcliffe). This revealed that both isolates were sensitive to chlorpromazine although the acid-resistant mutant was shown to be significantly more sensitive at the lowest concentration (10 μ M). This indicates that clathrin-dependent endocytosis is essential for both WT and the acid-resistant mutant, but the acid-resistant mutant is more sensitive to disruption of the clathrin-mediated endocytosis pathway (Figure 4.20). Both samples were also susceptible to the caveolar inhibitor gestin, although it was not possible to completely prevent infection. This indicates that the caveolar endocytosis is utilised by EV71 in Vero cells but is not essential for either WT or the acid-resistant mutant. It has previously been shown that gestin has no effect on cell lines expressing only SCARB2 as a functional receptor; this indicates another receptor on Vero cells may function in a caveolin-dependent manner (Figure 4.17).

A

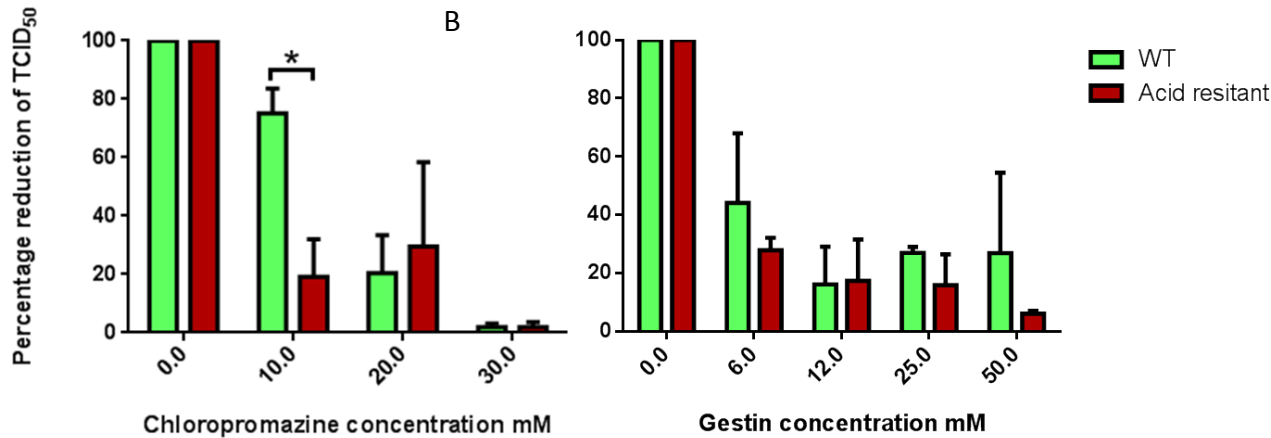


Figure 4.17 Analysis of the effect of inhibitors of cell entry. Vero cells were incubated in the presence of increasing concentrations of either chlorpromazine (A) or gestin (B) for two hours and then infected with either WT EV71 (Green) or the acid-resistant mutant (Red). After 24 hours samples were taken for titration via TCID₅₀ assay. Each bar represents an average of three measurements and error was measured using standard error * = $p \geq 0.01$. Experiments were conducted by Amy Radcliffe.

Now that it has been established that this mutant has an effect on cell entry, the effect on uncoating was further analysed. As a drop in pH is known to be essential for WT EV71 uncoating, the effect of endosome acidification inhibitors was analysed. Cells were incubated with a range of concentrations of endosome acidification inhibitors, ammonium chloride (NH₄Cl) or chloroquine for two hours prior to infection, with WT or acid-resistant virus isolates and were then titrated after 24 hours (work conducted by Amy Radcliffe). Both of these inhibitors have previously been shown to prevent infection by WT EV71 (Lin et al. 2012; Lin et al. 2013). Both the WT and the acid-resistant mutant were susceptible to inhibitors of endosome acidification, with the trend showing that the acid-resistant mutant appears to be less susceptible, although only one data point was shown to be significantly different (Figure 4.18). This suggests that the acid resistant mutant is less sensitive to inhibition of endosome acidification.

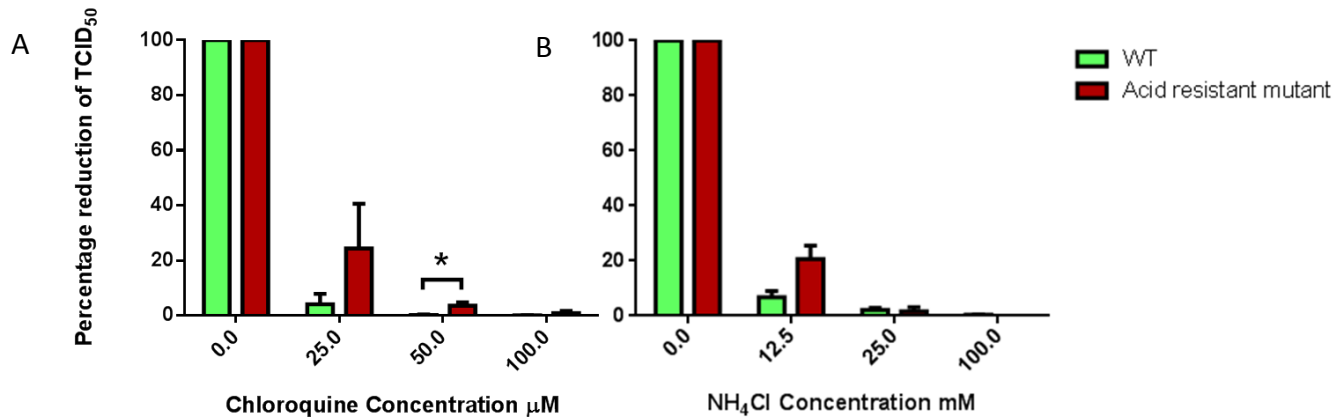


Figure 4.18 Endosome acidification plays an important role in WT EV71 and acid-resistant EV71. Vero cells were incubated in the presence of increasing concentrations of either Chloroquine (A) or NH₄Cl (B) for two hours and then infected with either WT EV71 (Green) or the acid resistant mutant (Red). After 24 hours samples were taken for titration via TCID₅₀. Experiments were performed in triplicate and error is measured by s.e.m, * = $p \geq 0.01$. Experiments were conducted by Amy Radcliffe.

Next the effect of the proline isomerase cyclophilin A was analysed (work conducted by Amy Radcliffe), which is the only known EV71 uncoating initiator other than SCARB2 (Qing et al. 2014). To analyse the effect of cyclophilin A both isolates were grown in Vero cells that had been treated with the cyclophilin A inhibitor, cyclosporine A. Cyclosporine A functions by binding to cyclophilin A making it less readily available in the cell for the virus to use. The Cyclosporine A analogue (HL051001P2) has previously been shown to inhibit EV71 infections (Qing et al. 2014). Here Vero cells were incubated in the presence of cyclosporine A for two hours prior to infection and incubated at 37 °C for 24 hours before samples were taken for titration (Figure 4.19). Titrations revealed that the acid-resistant mutant was significantly less susceptible to cyclosporine A.

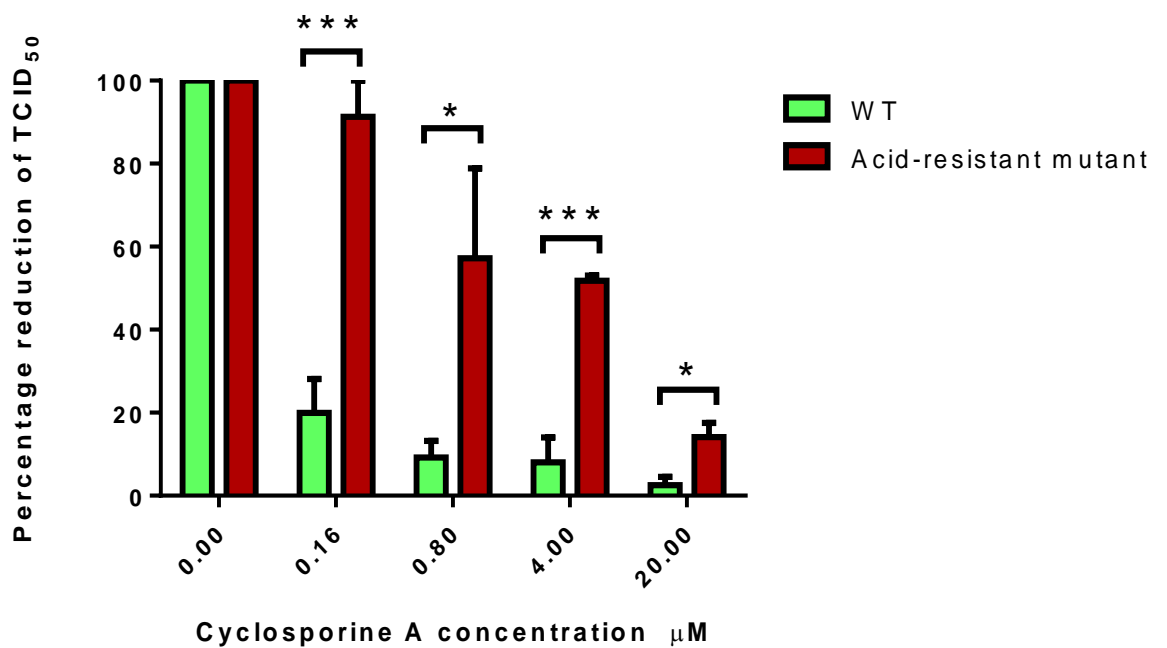


Figure 4.19 Cyclosporine A can prevent EV71 infection but is significantly less effective against the acid-resistant mutant. Vero cells were incubated in the presence of increasing concentrations cyclosporine A for two hours and then infected with either WT EV71 (Green) or the acid-resistant mutant (Red). After 24 hours samples were taken for titration via TCID₅₀ assay. Experiments were performed in triplicate and error is measured by s.e.m, * = $p \geq 0.01$, ** = ≥ 0.001 , * = $p \geq 0.0001$. Experiment was conducted by Amy Radcliffe.**

To gain a better understanding of the effect of mutation N104S has on the interaction with cyclophilin A, its location on the crystal structure was analysed in comparison to two previously identified cyclophilin A interaction sites (VP1; S243, P246) (Qing et al. 2014). This revealed that the site of the acid-resistance mutation N104S, is adjacent to the HI loop which has been shown to be a cyclophilin A interaction site (S243, P246) (Qing et al. 2014), meaning that N104 is present in an area that is involved in cyclophilin A interactions (Figure 4.20).

To determine whether the mutation may affect binding preferences for cyclophilin A this sequence was compared to known cyclophilin A target sequences. However,

no preference for either asparagine (N) or serine (S) was revealed and so it is unlikely that this residue directly effects cyclophilin A binding. However examination of residues neighbouring N104 revealed that residue 103 is a proline, which has been shown to be conserved across all EV71 genotypes (Figure 4.15). This is not found in other members of Enterovirus A species which also do not contain P246, a residue that has been shown to be important for cyclophilin A binding in EV71 (Figure 4.20) (Qing et al. 2014). So it is possible that VP1 residue 104 affects the availability of P103, and effects its interaction with cyclophilin A. Mutation of residue 243 to a proline has previously been shown to increase cyclophilin A binding while mutation of P246 has been shown to decrease cyclophilin A affinity (Qing et al. 2014). This demonstrates that prolines in this region are important for cyclophilin A interactions, and can increase capsid affinity towards cyclophilin A and reduce the effectiveness of cyclophilin A inhibitors. Given that N104S generates resistance to cyclosporine A and it is located next to a proline, it could be effecting the interaction between cyclophilin A and EV71 by affecting the availability of P103. If N104 blocks access to P103 then mutation to a smaller residue such as serine may release this blocking. Alternatively, if this mutation does indeed prevent interaction with SCARB2, then it is possible that SCARB2 usually blocks cyclophilin A interactions, and when it is not able to bind here, then it is not able to block cyclophilin A interactions.

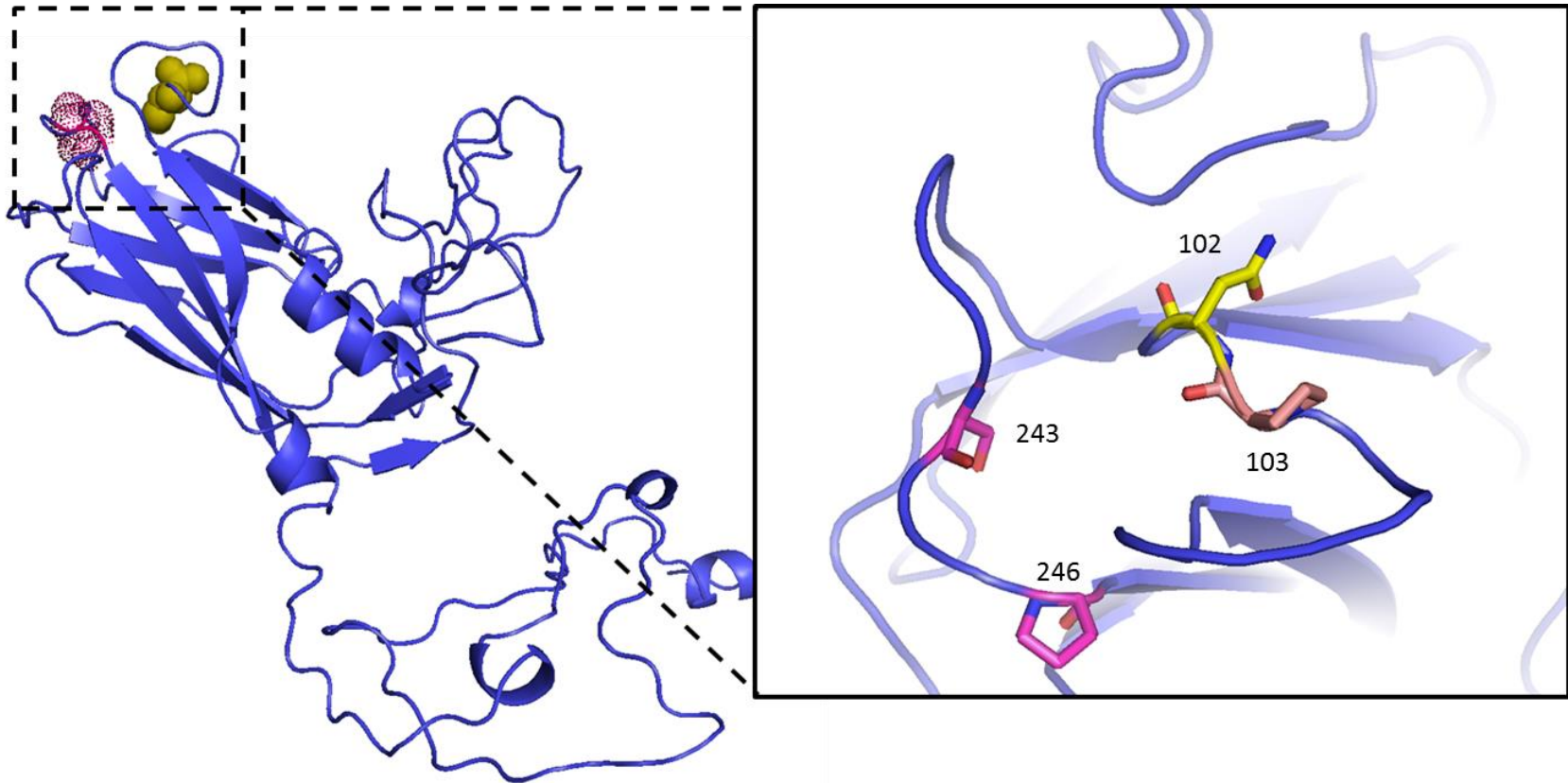


Figure 4.20 Potential role of cyclophilin A using crystal structure. Cartoon representation of VP1 (blue), acid-resistant mutation site is highlighted in yellow N104, residues that have previously been reported by Qing et al 2014 to be involved in cyclophilin A (S243, P246) interactions are represented in hot pink, and proline residue (P103) that we hypothesise could be involved in cyclophilin A interactions is highlighted in peach.

4.3 Discussion and future work

From, the work described in this Chapter it has been demonstrated that EV71 can grow in Vero or RD cells to reach titres of up to 1×10^8 TCID₅₀/ml and that growth in flasks was the most effective method of growing virus. Roller bottles and micro-carriers give no significant increase in virus yield and are more labour intensive to use.

Cell entry and uncoating has been studied in detail, showing that incubation of virus with cells in a low pH buffer can reduce the titre of the virus by 1×10^3 TCID₅₀/ml (three orders of magnitude). As EV71 uncoating is only induced when it binds to its receptor at a low pH it is likely that the reduction in virus titre is the result of the virus binding to the receptor and then uncoating outside the cell before endocytosis occurs. When EV71 is repeatedly exposed to these conditions, it evolves resistance and gains a mutation in VP1 (N104S). Immunoprecipitation and docking models have predicted N104 to be involved in binding SCARB2 the primary receptor and an uncoating initiator of EV71 (Dang et al. 2014). Further analysis of the docking model revealed that an alpha helix of SCARB2 is predicted to move towards N104 in its acid-induced conformation. The mutation N104S likely effects this interaction, which is potentially why the acid-resistant mutant is more sensitive to chlorpromazine, an inhibitor of the clathrin-dependent endocytosis pathway, which is the entry pathway SCARB2 utilizes. N104 was also shown to be in close proximity to residues previously shown by mutagenesis and immunoprecipitation to be involved in cyclophilin A interaction, which is a proline isomerase (Qing et al. 2014). This N104S mutant is less susceptible to cyclosporine A an inhibitor of

cyclophilin A. It is likely that this mutation reduces the binding capacity of EV71 to SCARB2 therefore leaving SCARB2 unable to induce uncoating even in the presence of low pH or unable to bind SCARB2 at all. A potential reason for increased binding capacity of cyclophilin A to the acid-resistant mutant could be that SCARB2 blocks access of cyclophilin A to P103 and if N104S cannot bind SCARB2, P103 is free to bind cyclophilin A, making it less susceptible to cyclosporine A. To further test this, uncoating assays, to detect if SCARB2 and cyclophilin A can induce conversion of mature particles to empty particles need to be performed, using the following isolates; EV71 WT, N104S and two additional mutants P103A and N104S/P103A. The susceptibility of the new mutants to cyclophilin A will also need to be assessed. Work to assess the toxicity of the inhibitors will also need to be done to confirm that the drop in titre observed is due to inhibition of virus entry and not due to a toxic effect on the cells.

In addition to greater knowledge of how EV71 uncoats/what residues it uses, greater insight into the timings of uncoating has also been gained. Figure 4.4-4.7 gives an insight into EV71 uncoating, from the viral growth curves there is a visible drop in titre after three hours which indicates that an uncoating event is occurring and from seven hours onwards titre begins to increase, this coincides with data from use with NLD inhibition which coincides with data previously seen in Lu et al 2011. NLD is known to prevent viral uncoating and from an inhibition time course it is evident that it is fully active until five hours post-infection. This indicates that between hours three and six EV71 is undergoing a prolonged uncoating event that causes the virion to become less infectious at three hours post infection, but six

hours post infection the virus become less susceptible to the uncoating inhibitor NLD, indicating that it the virus has undergone uncoating. From seven hours onwards the virus titre increases indicating that replication has occurred. Labelling experiments using an MOI of 10 for infection show that all proteins that become incorporated into mature virions are formed within nine to 12 hours and no virus capsid was detected to be produced after this point. However after this point virus titres continue to rise and make a sudden sharp increase at twenty hours post infection suggesting that virus replication is a multistep process infection.

This process differs from PV which undergoes a complete round of replication after nine hours and is known to complete uncoating and begin replication within one hour post-infection (Brandenburg et al. 2007). The long uncoating phase partially explains the reason for long life cycle of EV71 compared to PV.

In addition it was shown that standard sucrose gradients were not sufficient to purify EV71; this appeared to be in part due to a large population of enveloped particles. Use of Nycodenz gradients, which separates particles based on buoyant density, revealed two populations of particles; a high density population and a low density population. EM analysis revealed the high density particles were standard virus particles, but in the low density fractions there were what appeared to be black blobs. When the low density particles were treated with 1 v/v % NP40, and subjected to ultracentrifugation they sedimented at the same density as the high density particles. This suggests that treatment with detergent can disrupt the membranes to release naked particles. Western blot and SDS PAGE gel analysis revealed that both populations have standard EV71 protein profiles and were

detectable by a VP1 antibody. In HAV the enveloped particles were shown to have the VP1 precursor protein, VPX (Feng et al. 2013). Titrations revealed that the enveloped particles are more infectious than the non-enveloped particles. This is similar to what was observed for PV but differs from HAV where both particles were shown to be equally infectious (Chen et al 2015, Feng et al 2013). It was also demonstrated that EV71 enveloped particles may have a slightly different entry mechanism to non-enveloped viruses, as high density particles did not appear to be susceptible to chloroquine while low density particles were. The same observations were made in HAV (Feng et al. 2013). Further characterisation of these particles would be necessary as well as characterising the entry pathway and their susceptibility to neutralising antibodies.

Chapter 5

Chapter 5 Heat stability of EV71 and ways to increase it.

A major problem with some viral vaccines is their thermolability. This can be an issue for reasons such as a break in the cold chain, which can result in the vaccines undergoing structural re-arrangement that cause an antigenic shift. As a consequence they will no longer produce as powerful an appropriate immune response. This problem is especially exacerbated in picornavirus VLP vaccine candidates, which have been shown to be thermally unstable and lose native antigenicity at temperatures above 5 °C (Rombaut & Jore, 1997, personal communication with James Hogle, Harvard Medical School, described in more detail in sections 1.2.4, 1.4.3). These proposed vaccine candidates are produced in recombinant systems that express the viral structural protein P1 and viral protease 3C (described in more detail in section 1.4.3). When co-expressed, 3C cleaves P1 into its constituent structural proteins VP0, VP1 and VP3, which self-assemble into an empty capsid containing no viral RNA. In the absence of viral RNA VP0 does not undergo the cleavage into VP2 and VP4, which allows VP4 to rearrange and form an internal lattice that can improve virus stability (described in more detail in sections 1.2.4, 1.4.3). The thermal/antigenic instability of these vaccine candidates is an impediment to their development as practical products. Therefore to produce a viable EV71 VLP vaccine candidate, methods to improve its thermostability and assessment of its antigenicity need to be developed.

In this section different strategies to improve the EV71 stability and detect the antigenic shift are explored.

Several methods have previously been shown to improve capsid stability of picornaviruses. One is by mutagenesis, by selecting for mutations that stabilise the virus or by site-directed mutagenesis. Previously it has been shown that mutations identified by structural observation of the FMDV empty capsid crystal structure are able to improve the thermostability of FMDV VLPs (Porta et al. 2013).

Another strategy to improve VLP stability that is specific for enteroviruses, is to incubate in the presence of pocket-binding compounds that are able to enhance virus stability. Enteroviruses contain a structure in the VP1 structural protein known as the VP1 pocket. This naturally harbours a hydrophobic lipid known as the pocket factor, which is a virion stabiliser (Smith et al. 1986; Wang et al. 2012). The pocket factor binds here and it must be released before uncoating can occur (discussed in section 1.2.1, 1.2.4, Chapter 3). Certain compounds have been shown to displace the natural pocket factor due to higher binding affinities, and increase capsid stability so that it is unable to undergo structural rearrangements necessary for uncoating (discussed in section 1.3, chapter 3). These compounds have been shown to inhibit conformational changes and so improve the thermostability of a number of different enteroviruses, including EV71 (Katpally et al. 2007; Mosser et al. 1994; Shepard et al. 1993). They have also been shown to successfully increase the antigenic stability of PV VLPs produced in a recombinant system (Rombaut & Jore 1997). In Chapter 3, it was shown that the pocket-binding inhibitor NLD was able to increase the temperature at which mature EV71 particles were heat inactivated by ~ 3.5 °C (Figure 3.7), and an EV71 mutant resistant to NLD was shown to be resistant to NLD-mediated stabilisation. The mutations identified were predicted to prevent

NLD binding and as a result the mutant was more thermolabile than WT (Figure 3.7).

In addition to inhibitory compounds, natural pocket factors have also been shown to have a similar effect. In BEV1 it has been shown that a number of different fatty acids are able to function as natural pocket factors as identified by mass-spectroscopy (Ismail-Cassim et al. 1990; Smyth et al. 2003). Incubation with one natural pocket factor, lauric acid, was shown to improve the thermostability of BEV1 (discussed in section 1.2.1, Ismail-Cassim et al. 1990; Smyth et al. 2003). The natural pocket factor for other enteroviruses is unknown and all other data to date has been based upon predictions from crystal structures from the electron density filling the VP1 pocket. This data has often indicated that there could be a population of different sized fatty acids functioning as the pocket factor (discussed in section 1.2.1, Smyth et al. 1995). For EV71, the pocket factor has been predicted to be either sphingosine or lauric acid from two different crystal structures (Wang et al. 2012; Plevka et al. 2012).

Mutagenesis and/or pocket-binding compounds could be useful strategies to improve the capsid stability of EV71. However a method to detect EV71 native antigenicity also needs to be developed, so that the antigenic stability can be assessed.

Previous studies with PV have shown it is possible to develop antibodies that can distinguish between the antigenicity of native and heated forms (Rombaut et al. 1990; Rombaut & Jore 1997). Antibodies have been developed (mAbs D6 and A9) that have been shown to exclusively recognise EV71 full virions but not the

expanded empty capsids, indicating that they should only be able to recognise EV71 in its native antigenic form (Wang et al. 2012). In addition, it has been shown that certain receptors (e.g. SCARB2) are only able to bind the EV71 capsids in their native form (Qing et al. 2014).

In this section mutagenesis by artificial selection and the use of different pocket-binding compounds are assessed as methods to improve the thermostability of EV71. Also the available antibodies and receptors are used in IPs and ELISAs to analyse their capacity to detect native EV71 antigenicity.

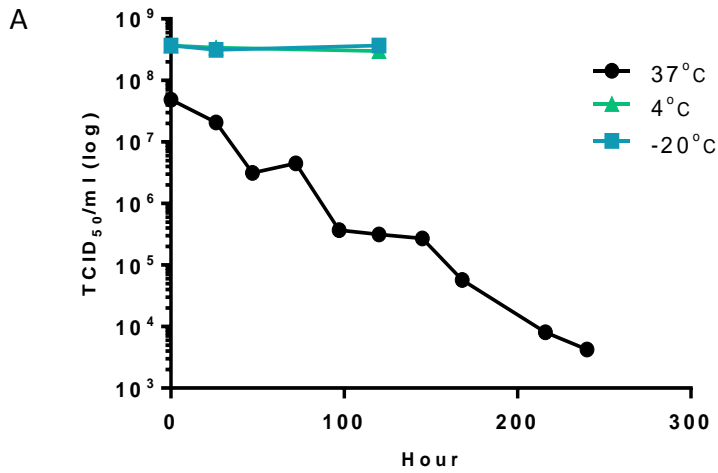
5.1 Capsid stability

5.1.1 Long term stability of EV71/CVA16

The long term stability of EV71 and CVA16 after storage at temperatures of 37 °C, 4 °C or -20 °C was assessed for 120-240 hours followed by titration via TCID₅₀ assay (Figure 5.1) (Work performed by Joseph Ward, an undergraduate under my supervision).

Stability for both viruses at 37 °C started to decrease after 23 hours. For CVA16 this continued until between 72 and 96 hours by which time the titre had dropped to 0, while that of EV71 had dropped by over 2 logs, although it was still viable. EV71 titres continued to drop by a further three logs over the next 150 hours, at which point the experiment was discontinued. Storage at 4 or -20 °C showed that CVA16 was very stable for over 196 hours and EV71 for over 120 hours, at which point the experiments were discontinued.

EV71 Stability



CVA16 Stability

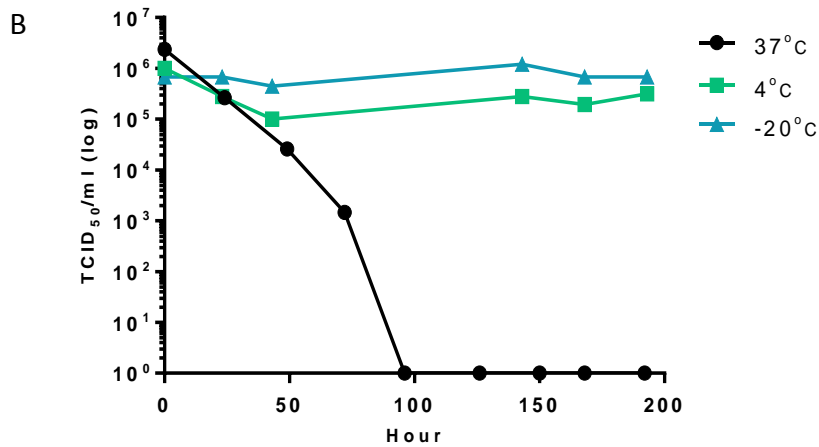


Figure 5.1 Long term stability of EV71 (A) and CVA16 (B). EV71 and CVA16 were stored at either 37 °C, 4 °C or -20 °C, and titrated every 24 hours. n = 1 (Performed by Joseph Ward)

5.1.2 Evolution of an EV71 isolate with increased thermal stability

One strategy to stabilise protein structures is the introduction of stabilising mutations. In an attempt to identify mutations that stabilise the EV71 capsid, an evolution experiment was carried out to select for stabilising mutations. The virus was repeatedly passaged at 37 °C after being heated between each passage. The selection temperature used was 50 °C as it was previously shown in chapter 3 that exposure to this temperature reduced the TCID₅₀/ml titre by over 99.9% (Figure 3.10 A, Figure 5.2). For the first passage, enough virus to infect a confluent T25 flask at an MOI of 10 TCID₅₀'s/cell post-heating, was used. The virus was first concentrated from cell culture medium by ultracentrifugation, and then re-suspended in a volume of 700 µl of serum-free medium (Figure 5.3). A 10 µl sample was taken for titration and the rest was heated to 50 °C for 30 minutes in a thermocycler. Another 10 µl of the heated virus was taken for titration and the rest was used to infect a confluent T25 flask of Vero cells. The flask was incubated at 37 °C until 100% cell death had occurred, and then harvested. Cell debris was removed and the cells were freeze-thawed three times in RIPA buffer, before being added to the tissue culture supernatant. This supernatant was then concentrated by ultracentrifugation and the resulting pellet was resuspended in 700 µl of serum-free media. The resuspended pellet was then heated to 50 °C and used to infect another T25 flask of Vero cells, this process was repeated until passage eight, at which less than a 10% drop in titre was observed for four consecutive passages (Figure 5.4). From analysing the effect of heating on each passage, it was apparent that over the first three passages there was initially a large drop in the post-heating titre, unusually at this point the virus actually appeared to become less heat stable. At

passage four there was a slight increase in titre indicating that the virus was becoming more heat stable. Then at passage five there was a large increase in titre and subsequently there was only a small difference between the post-heating and pre-heating titres, indicating that the virus was more heat stable than before.

Once it was established that the virus was able to tolerate a temperature of 50 °C, the thermostability of this isolate (now referred to as thermostable EV71) was assessed by creating a thermostability curve in the same manner as the WT heat stability curve generated in chapter 3. Figure 5.2 shows that WT virus could tolerate temperatures up to 45 °C before a loss in titre was observed and temperatures of 51 °C before complete inactivation occurred. The thermostable mutant could tolerate temperatures up to 51 °C before there was an observed loss in titre, and 56.5 °C before complete inactivation occurred. The growth kinetics of WT and thermostable EV71 were compared, revealing that thermostable EV71 did not achieve a titre equivalent to WT until 18 hour post infection, suggesting that thermostable EV71 has slower growth kinetics (Figure 5.5).

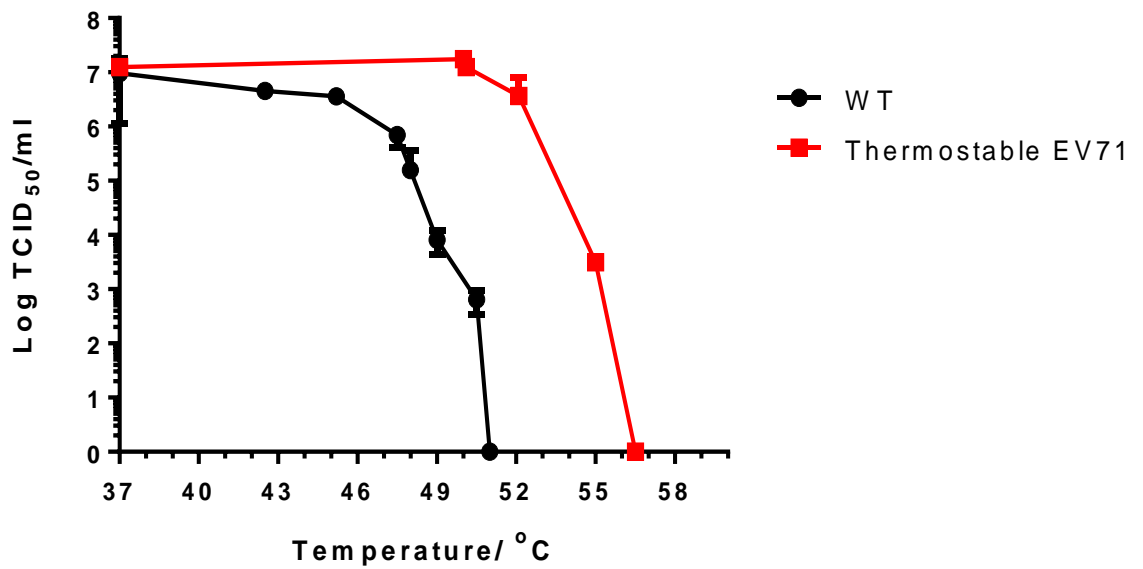


Figure 5.2 Heat stability curves of WT EV71 and thermostable EV71. WT (black circles) and thermostable EV71 (gray squares), were heated to a variety of temperatures for 30 minutes using a thermocycler and then titrated by TCID₅₀ assay. WT curve is previously shown in figure 3.7 and is included for comparison.

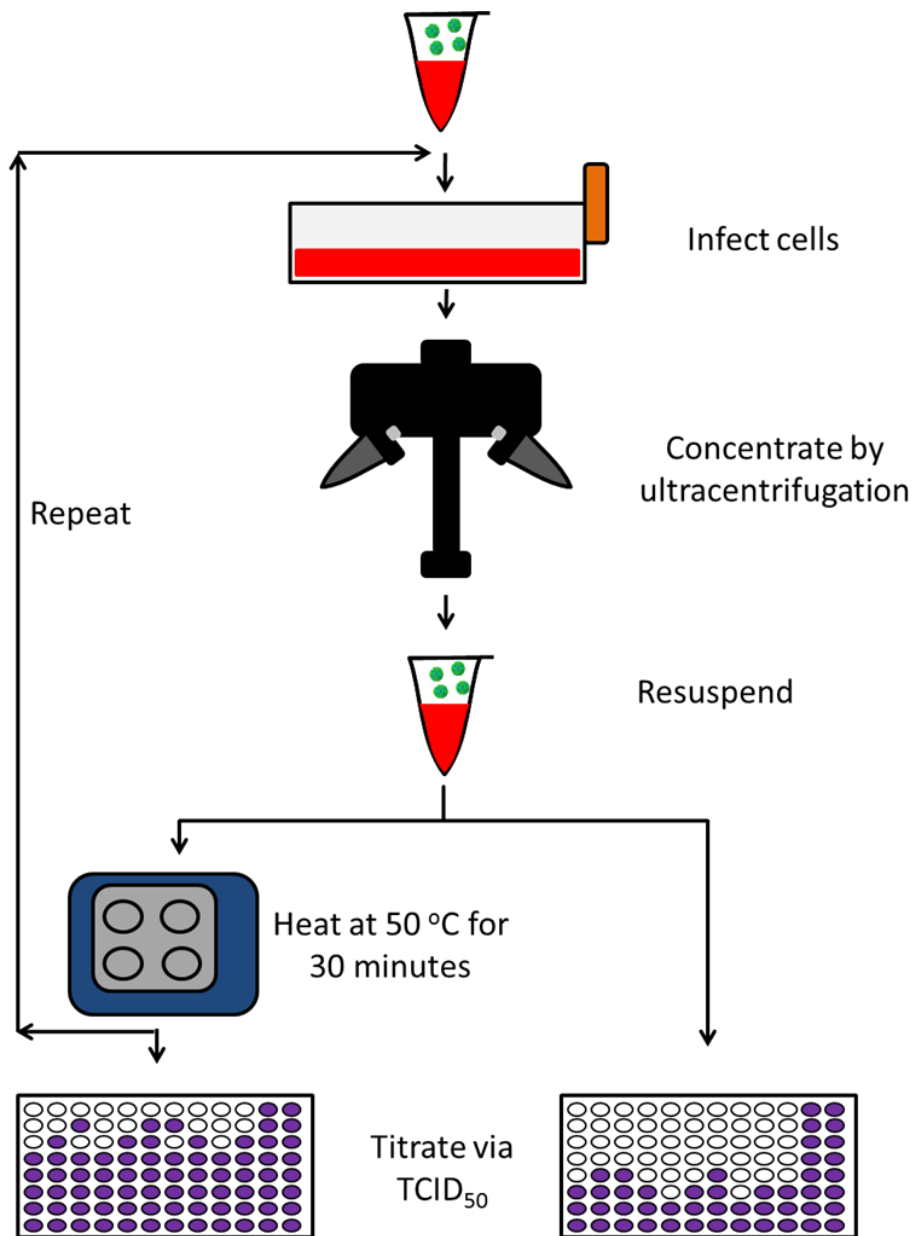


Figure 5.3 Selection of a thermostable EV71 isolate. A T25 was infected with EV71, after 100% cell death. The virus was then concentrated from cell culture medium by ultracentrifugation, and then re-suspended in a volume of 700 μ l of serum-free medium. A 10 μ l sample was taken for titration and the rest was heated to 50 oC for 30 minutes in a thermocycler. Another 10 μ l of the heated virus was taken for titration and the rest was used to infect a confluent T25 flask of Vero cells. The flask was incubated at 37 oC until 100% cell death had occurred, and then harvested. Cell debris was removed and the cells freeze-thawed three times in RIPA buffer, before being added to the tissue culture supernatant. This supernatant was then concentrated by ultracentrifugation and the resulting pellet was resuspended in 700 μ l of serum-free media. The resuspended pellet was then heated to 50 oC and used to infect another T25 flask of Vero cells, this process was repeated until passage eight

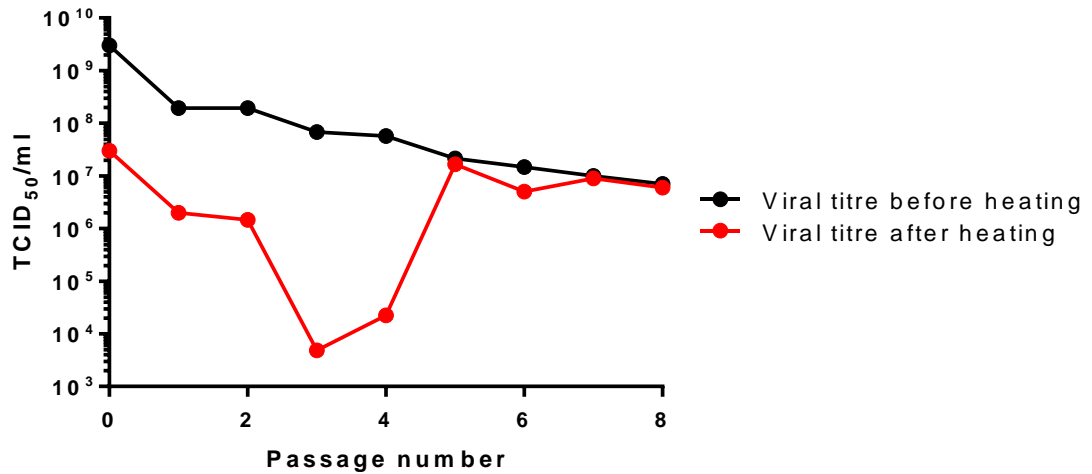


Figure 5.4 Difference in titres between EV71 thermostable mutants before and after heating. EV71 was repeatedly passaged in cell culture after being heated to 50 °C for 30 minutes each time using a thermocycler. Viral titres were determined before and after heating by TCID₅₀ assay (n=1).

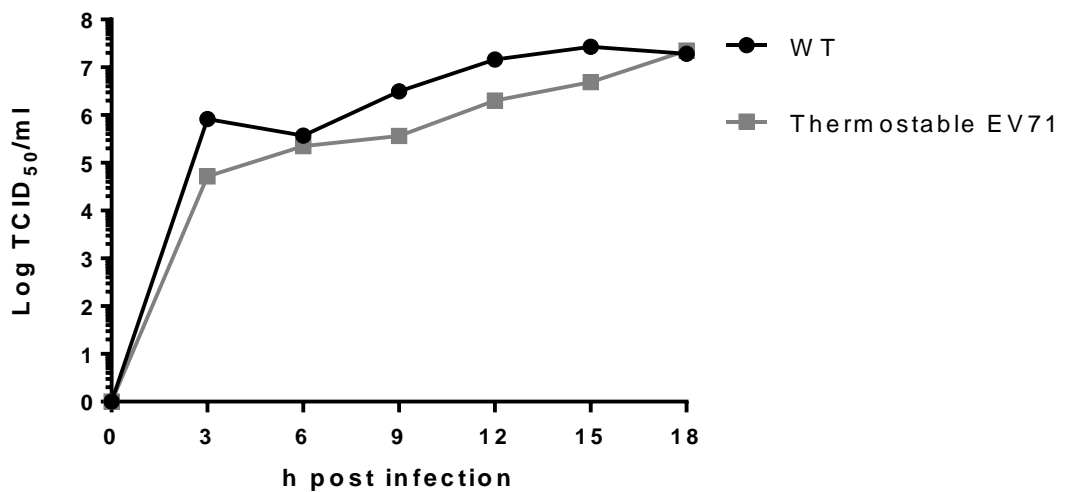


Figure 5.5 Grow kinetics of WT EV71 and thermostable EV71. WT and thermostable virus were used to infect wells in a six well plate at MOI 1 TCID₅₀'s/cell and whole cell samples were taken every three hours for 18 hours. Samples were then titrated via TCID₅₀ assay. WT curve is previously shown in figure 3.8 and is included for direct comparison.

5.1.3 Determination of heat stability mutations

In order to determine the mechanism of increased thermostability, the entire capsid coding region of thermostable EV71 was sequenced using the methods described in the materials and methods (section 2.4.5 - 2.4.7). This revealed two point mutations located on VP1 (V179A and L183V). Mapping the mutations onto the crystal structure of VP1 using PyMol showed that they were located towards the end of the inside of the VP1 pocket (Figure 5.6). The VP1 pocket is the site of binding of the pocket factor, a fatty acid known to act as an enterovirus capsid stabiliser (discussed in sections 1.2.1, 1.2.4). Predictive modelling of the mutations into the virus capsid, not taking into account the effect of pocket factor stability, were performed by Luigi De Colibus (Oxford University). These models did not predict any significant increase in the inherent stability of the virus capsid (personal communication with Luigi De Colibus). This suggests that the mutations could improve stability by affecting the virus' interaction with the pocket factor (Figure 5.6). Both mutations, V179A and L183V are to smaller amino acids, which indicate that they could cause an increase in the size of the VP1 pocket. Using PyMol to substitute the amino acids gives further indication that these mutations could affect the size of the pocket. In WT EV71 V179 is at the upper edge of the hydrophobic space that represents the pocket. However when mutated to an alanine residue, it no longer touches this hydrophobic area, which could result in an increase in the size of the pocket (Figure 5.6). Most of the other molecules lining the space around the VP1 pocket appear to point directly out of the space, indicating that they do not fill the pocket. The other heat-stabilising mutation L183V, is much higher up and at the edge of the space that pocket could potentially occupy, therefore a mutation to

a smaller amino acid could allow for an increase in pocket size (Figure 5.6). This potentially indicates that these mutations allow for a larger pocket factor to bind, or that the mutations allow the pocket factor to bind deeper into the pocket.

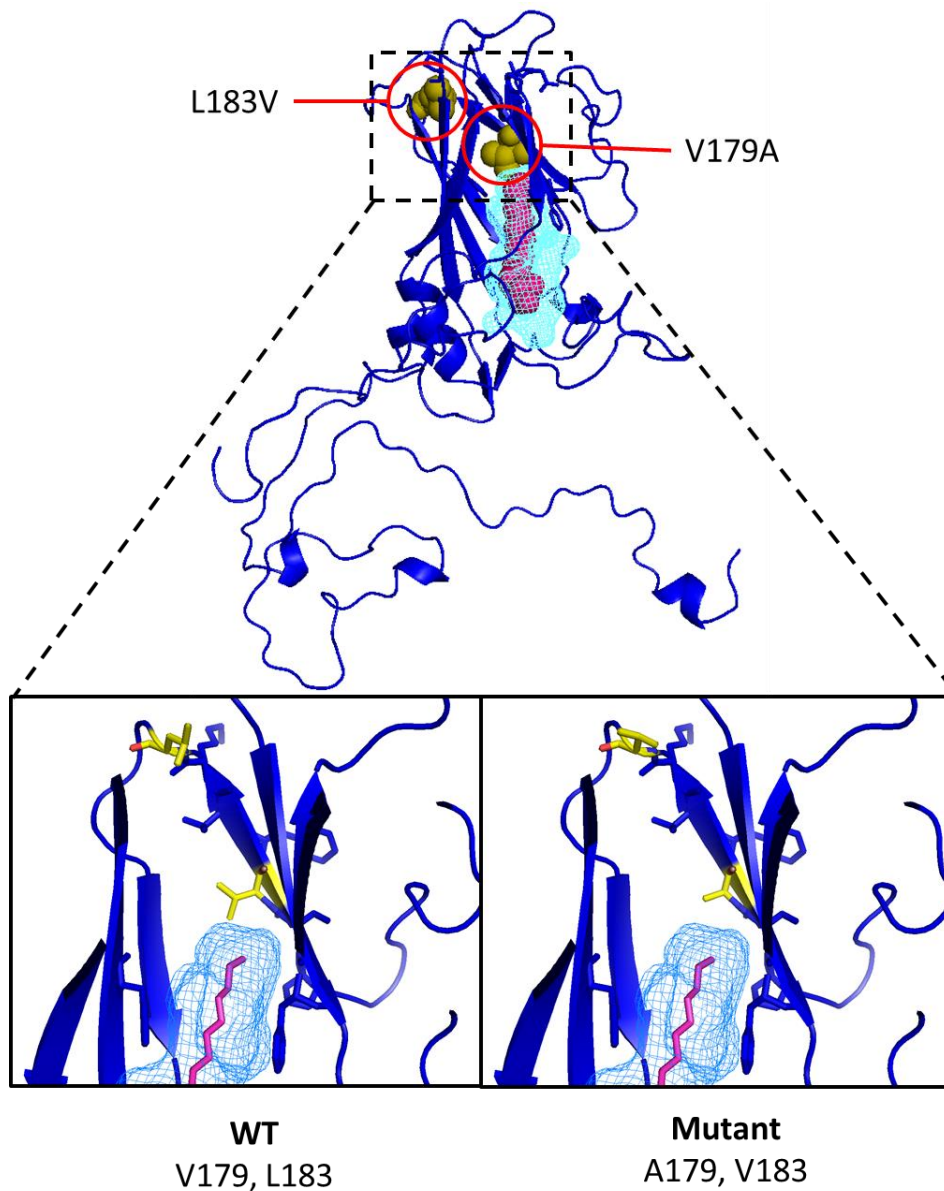


Figure 5.6 Location of thermostabilising mutations. Crystal structure of WT EV71, VP1 is blue, pocket factor is represented in hot pink, pocket is represented by blue mesh and mutations (L183V, V179A) highlighted as yellow spheres. The lower panels show a close up view of top of VP1 pocket, all residues lining the pocket are presented as sticks, with mutations highlighted in yellow. In the right hand side panel, mutated residues have been inserted using PyMol mutagenesis tool for illustration purposes.

5.1.4 Effect of different pocket factors on the thermostability of WT EV71 and isolates with VP1 pocket mutations

Previous work performed in chapter 3 showed that the EV71 inhibitor NLD is able to bind the VP1 pocket to displace the natural pocket factor and increase virus thermostability (Figure 3.8, 5.6). Mutations that allow resistance to NLD reduce the thermostability of EV71 (Figure 3.8, 5.6). These mutations are predicted to prevent NLD and the natural pocket factor from binding and, accordingly, NLD was unable to improve the thermostability of this mutant. In addition to this, previous work in BEV1 shows that one of its pocket factors (lauric acid) can function as an inhibitor in the same manner as NLD and improve the thermostability of BEV1 (Ismail-Cassim et al. 1990; Smyth et al. 2003). Mutations that were observed in thermostable EV71 are within the VP1 pocket and could affect the way the virus interacts with the pocket factor. Together, this indicates that which pocket factor binds and how it interacts with the pocket is important for capsid stability.

To get a better understanding of the role the pocket factor plays, the effect of different potential pocket factors on virus stability was studied by comparing WT EV71 to thermolabile (NLD resistant, I113M, V123L) and thermostable (V179A, L183V) EV71, which are predicted to have altered interactions with the pocket factor. To perform this, heat-stability curves of the three different isolates in the presence of different pocket factors were carried out (Figure 5.6). The pocket factors used were the fatty acids, acetic acid, lauric acid, palmitic acid, stearic acid, sphingosine and arachidic acid, along with NLD as a pocket-binding inhibitor (De Colibus et al. 2014, Chapter 3) (table 5.1). The main difference between the fatty

acids is that they are different sizes with carbon backbones ranging from C2 to C20. NLD is a pocket-binding inhibitor (described in more detail in chapter 3) that was shown to improve the heat stability of WT EV71 while having no effect on the heat stability of the thermolabile/inhibitor-resistant EV71 (Figure 3.7, 5.6). This data provided evidence that incubation of WT EV71 in the presence of the mentioned fatty acids caused a reduction in thermostability, except for sphingosine which had no effect, while incubation in the presence of NLD (as previously shown in chapter 3, figure 3.7) caused an increase (Figure 5.7, 5.8A). Incubation of thermostable EV71 in the presence of these fatty acids, including sphingosine, caused a dramatic decrease in thermostability (Figure 5.7). Incubation with NLD still caused an increase in heat stability but not as dramatic as in WT. Incubation of thermolabile/inhibitor-resistant EV71 in the presence of any of the fatty acids or NLD did not affect thermostability (Figure 5.8). This was expected as structural modelling in chapter 3 predicted that the mutations present prevented both NLD and (likely) the natural pocket factor from binding.

A possible reason for the reduction in heat stability observed when incubated in the presence of different fatty acids at a high concentration is that this caused the natural pocket factor to be displaced, and these now bound fatty acids function less effectively at improving heat stability.

Interestingly, these alternative pocket factors are only able to decrease the temperature at which the virus begins to inactivate but does not affect the final inactivation temperature. Incubation in the presence of NLD, however, increases both the temperature at which the virus begins to lose infectivity and the

temperature at which complete inactivation occurs. The differences in responses to the different pocket factors between the three isolates show that mutations in the virus pocket do affect the way EV71 interacts with pocket factors. It should be noted that the concentration of compound the virus was incubated at was very at a very high concentration (1000 nM).

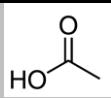
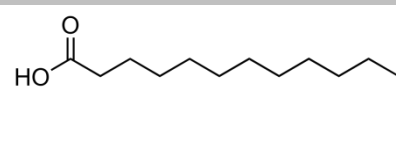
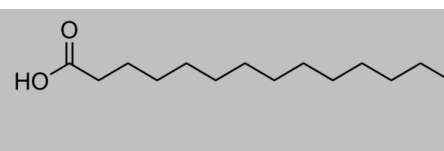
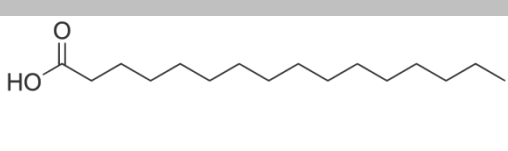
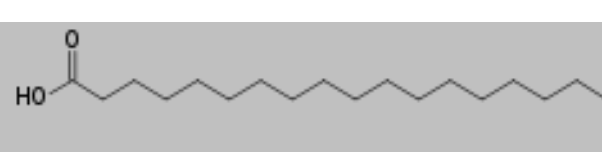
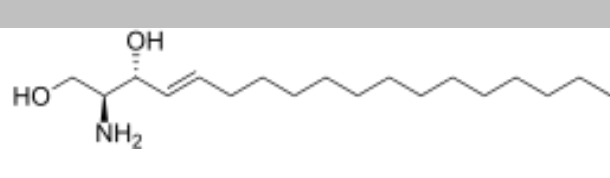
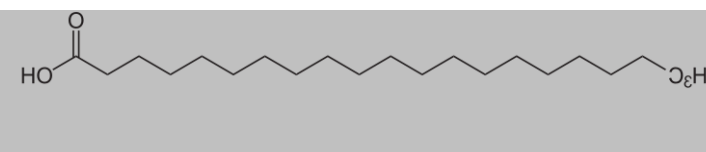
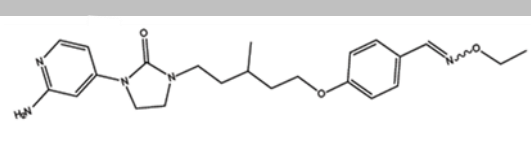
Name	Structure
Acetic acid C:2	
Lauric acid C:12	
Myristic acid C:14	
Palmitic acid C:16	
Stearic acid C:18	
Sphingosine C:18X	
Arachidic acid C:20	
NLD	

Table 5.1 Pocket factor table. This table lists the different pocket factors used in stability experiments and shows their chemical structures.

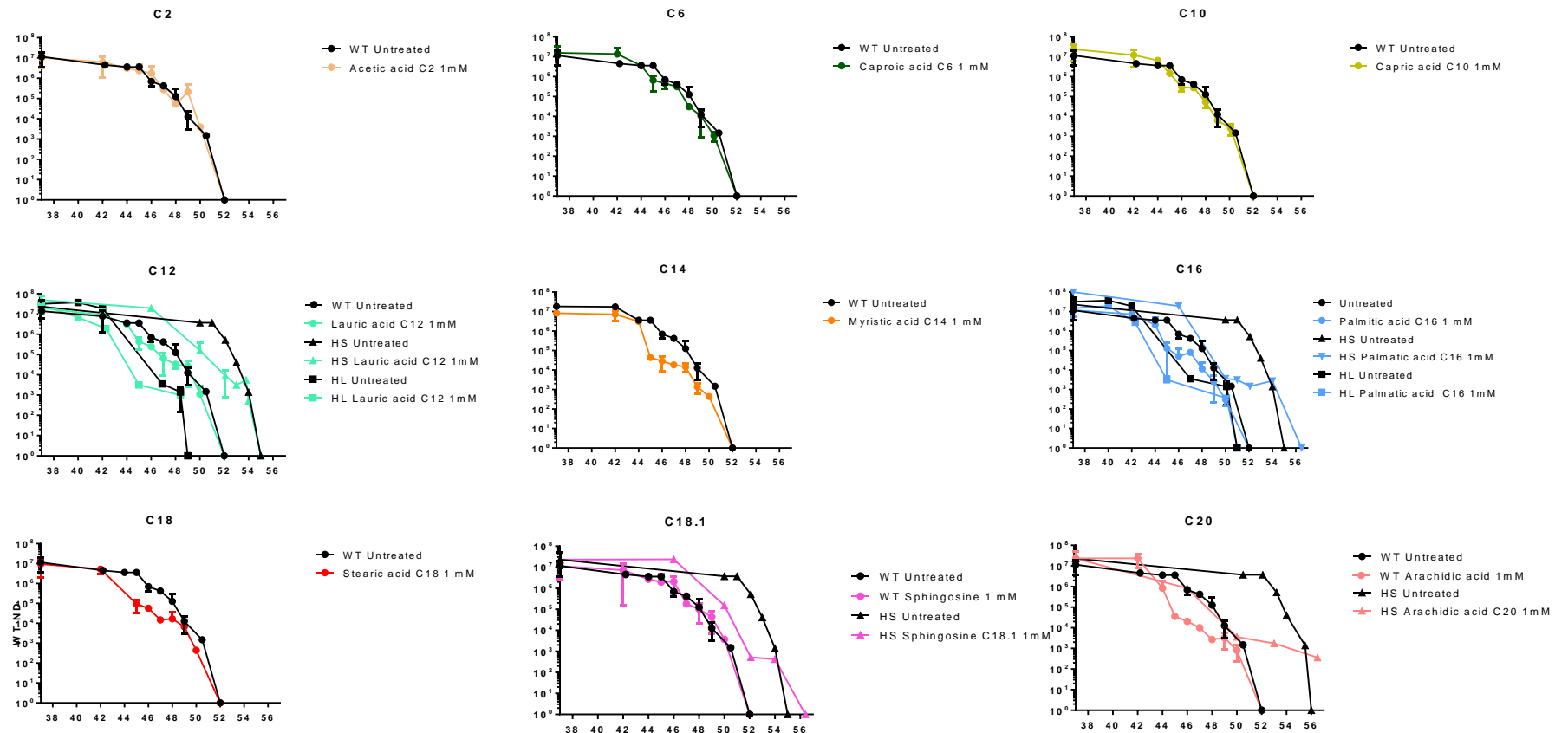


Figure 5.7 Effect of fatty acids on heat stability of EV71 isolates with different pocket mutations. Heat stability curves of WT EV71, Thermostable (VP1; V179A, L183V), (HS) EV71 and Thermolabile/Inhibitor-resistant (VP1; I113M, V123L) (HL) EV71 after incubation in the presence of either PBS (untreated) after incubation in the presence of 1 mM of different fatty acids. Samples in PBS and fatty

acids were incubated at 37 °C for one hour, prior to heating while samples incubated in NLD were heated within 10 minutes of addition. After heating, samples were titrated by TCID₅₀ assay and values plotted. The data for samples of WT and thermolabile, untreated and NLD-treated were previously depicted in figure 3.7 of chapter 3 and the data for thermostable untreated was previously depicted in figure 5.2, these are included here for comparison.

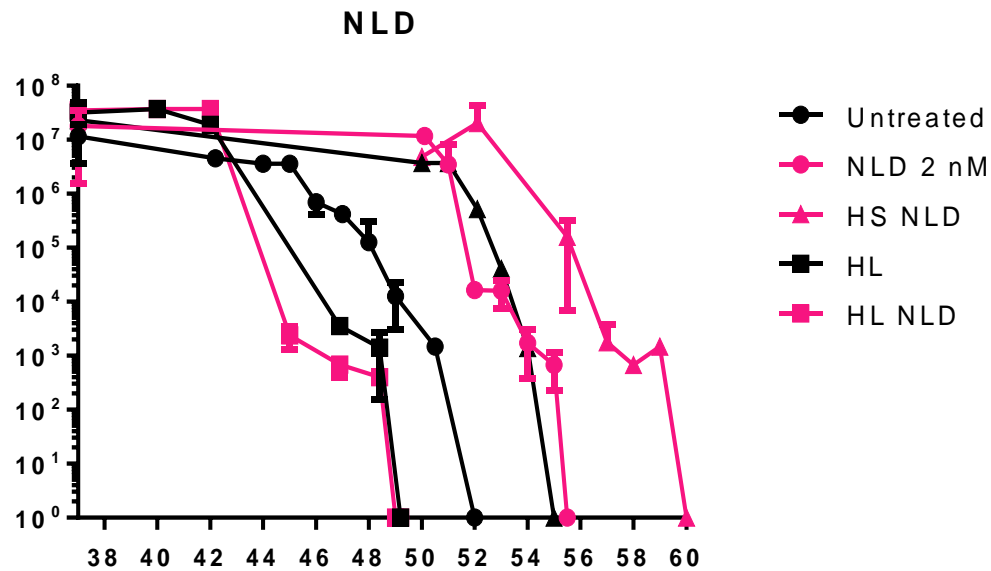


Figure 5.8 Effect of a pocket-binding inhibitor on heat stability of EV71 isolates with different pocket mutations. Heat stability curves of WT EV71, Thermostable (VP1; V179A, L183V), (HS) EV71 and Thermolabile/Inhibitor-resistant (VP1; I113M, V123L) (HL) EV71 after incubation in the presence of either PBS (untreated) in the presence of 2 nM NLD.

5.1.5 Binding of pocket factors to virus

It is predicted that thermolabile/inhibitor-resistant EV71 is unaffected by incubation in the presence of pocket factors and is thermolabile due to mutations that prevent pocket factors from binding.

To test this, the ability of WT and thermolabile/inhibitor-resistant EV71 to associate with NLD or palmitic acid was evaluated. Palmitic acid is a candidate pocket factor and is available as a labelled molecule. It was shown to reduce WT EV71 thermostability but not affect thermolabile/inhibitor-resistant EV71 stability (shown in section 5.1.4, Figure 5.7). Virus was purified and concentrated through a sucrose cushion and then incubated in the presence of ^3H labelled palmitic acid. This was then subjected to ultracentrifugation through a nycodenz gradient. The gradients were then fractionated and each fraction was analysed by scintillation counting to assess where ^3H palmitic acid was sedimenting in relation to where EV71 was shown to sediment in section 4.1.3. Because of the concentration of the material supplied, it was not possible to incubate the virus in the presence of $1000\ \mu\text{M}$ ^3H palmitic, as was done in the thermostability curve experiments, and instead the isolates were incubated in $20\ \mu\text{M}$ ^3H palmitic acid. When co-incubated for 1 hour at $37\ ^\circ\text{C}$ no association between palmitic acid with either WT or thermolabile/inhibitor-resistant EV71 was observed (Data not shown), however when incubated overnight at $4\ ^\circ\text{C}$ palmitic acid was shown to associate with both isolates (Figure 5.9A and B, black lines). The ability of NLD to displace ^3H palmitic acid was assessed by incubating in the presence of NLD for two minutes prior to nycodenz gradient ultracentrifugation. This revealed that NLD consistently reduced

the amount of palmitic acid associated with the WT virus (Figures 5.9A, hot pink lines). However when added to the thermolabile/inhibitor-resistant virus the results were inconsistent, with one experiment showing that incubation with NLD had no effect on palmitic acid association (Figure 5.7B, left-hand graph), and another showing it to be as effective at preventing palmitic acid association as in WT (Figure 5.7B, right-hand graph).

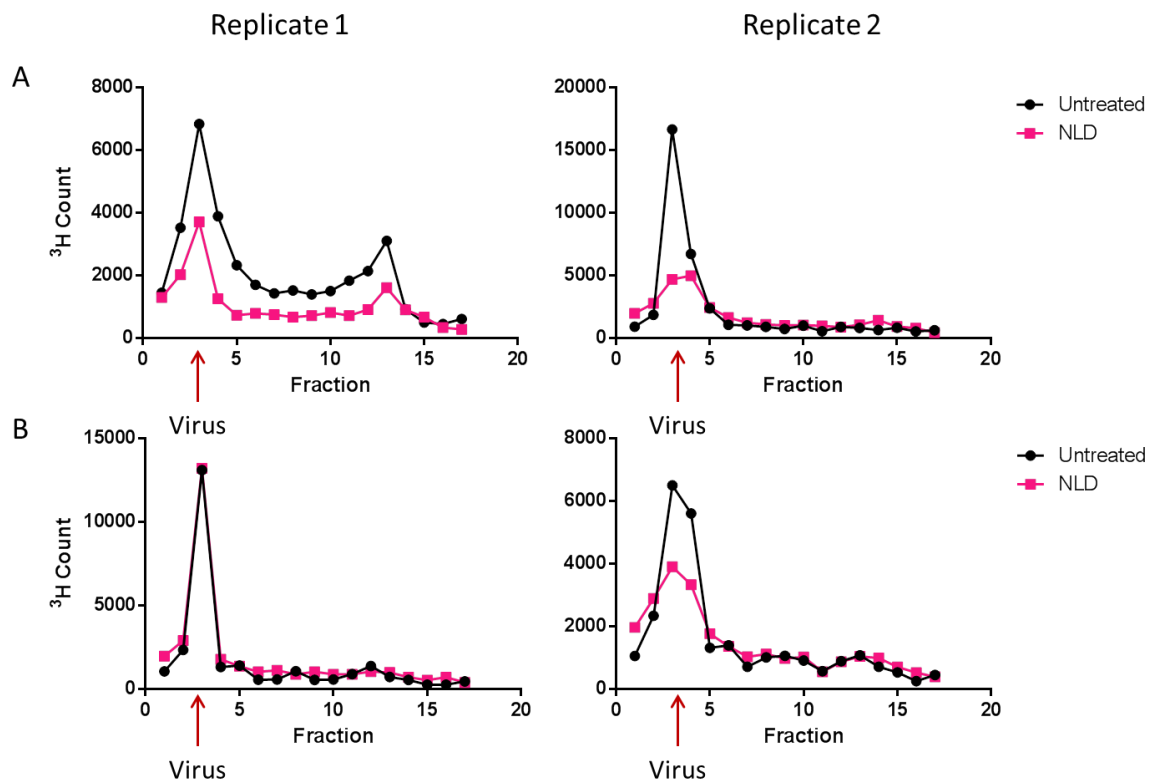


Figure 5.9 Nycodenz gradient profiles of WT EV71 (A) and NLD resistant EV71 (B) to separate the virus particles based upon the buoyant density. The positions of virus peaks are indicated by red arrows. Virus was subjected to ultracentrifugation through a 30% sucrose cushion and resuspend in PBS overnight in the presence of ^3H palmitic acid. Samples were then incubated in either the presence (hot pink) or absence (black) of 2 nM NLD before being subjected to ultracentrifugation through a self-forming 40% nycodenz gradient. Post-centrifugation, samples were fractionated and each fraction was analysed by scintillation counting.

5.1.6 Effect of pocket factors in other enteroviruses

In the previous section it was demonstrated that incubation of EV71 in the presence of different fatty acids was able to reduce its thermostability (Figure 5.8). This is in contrast to previous data for BEV1 where incubation in the presence of lauric acid, one of its predicted pocket factors, was shown to improve thermostability (Ismail-Cassim et al. 1990; Smyth et al. 2003).

As it has been shown that BEV1 can be stabilised by lauric acid, experiments were conducted to test the effect of lauric acid and other fatty acids on the stability of BEV2. A comparison of BEV1 and BEV2 VP1 pockets reveals that BEV2 is predicted to harbour a larger pocket factor due to having a larger pocket, therefore it would be expected that they behave differently in the presence of different fatty acids (Figure 5.10, produced by Jingshan Ren at Oxford University).

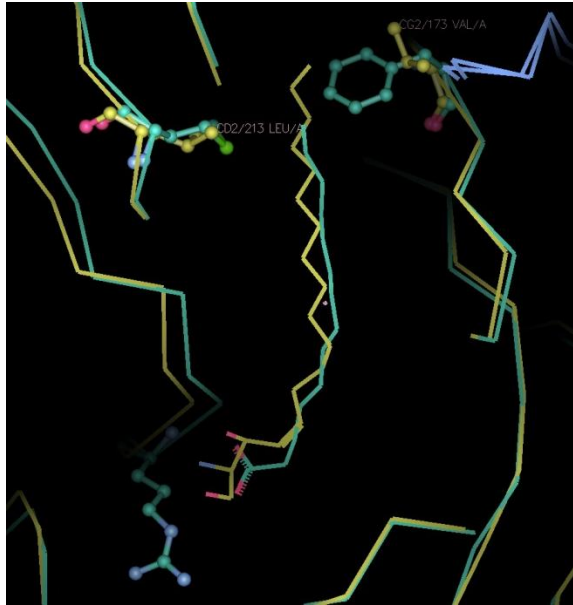


Figure 5.10 *Crystal structures reveal BEV1 and BEV2 have different sized VP1 pockets. Crystal structure overlay of BEV1 (green) and BEV2 (yellow) pockets and predicted pocket factors lauric acid and palmitic acid produced by Jingshan Ren at Oxford University.*

Initially BEV2 was incubated either in PBS or the different fatty acids which were shown to be able to reduce the stability of EV71 (Figure 5.8 and Table 5.1). Samples were then titrated by TCID₅₀ assay before and after heating to 50 °C (Figure 5.11A). This revealed that the titre of BEV2 was dramatically reduced when heated in the presence of any of the fatty acids tested, compared to heating in the presence of PBS. This demonstrated that incubation in the presence of different fatty acids, including lauric acid, was able to decrease the thermostability of BEV2. The destabilising effect was also more dramatic than that observed for WT EV71. In EV71 the reduction in titre of the WT virus was generally between 0.5 and 2 orders of magnitude, however for BEV2 it was between 4 and 5 orders of magnitude (Figure 5.11A).

Following confirmation that incubation of BEV2 in the presence of fatty acids reduced the thermostability when measured via TCID₅₀, the effect on conversion of 160S particles to 80S particles was analysed, as this was the mode of assessment used to show lauric acid could improve the heat stability of BEV1 (Ismail-Cassim et al. 1990). This was to ensure it was not affecting titre by any other mode of action.

In this experiment ³⁵S-labelled BEV2 from crude cell lysate was purified through a sucrose gradient and resuspended in PBS. This was split into three separate samples, one was left untreated, the other was heated to 50 °C and the final sample was incubated in the presence of lauric acid for one hour and subsequently heated to 50 °C. All three samples were then subjected to centrifugation through a sucrose gradient which separates particles based upon their density. Each gradient was then fractionated and each fraction was analysed by scintillation counting to detect the amount of ³⁵S-labelled BEV2. When the untreated virus was subjected to centrifugation through a gradient, a peak was visible at fractions 10-12 (Figure 5.11B), which has previously been identified as the point at which mature BEV 160S particles sediment in 15-45% sucrose gradient (shown in section 4.1.3). A peak at the same position was also identified in the sample heated to 50 °C, but there was no observable peak in the sample heated in the presence of lauric acid and there does appear to be a shift towards a peak at the 80S position (Figure 5.11B). This indicated that heating BEV2 to 50 °C was not sufficient to destabilise the capsid, but heating to 50 °C after incubation in the presence of lauric acid disrupted the virus. This complements what was observed in the titration experiments where heating BEV2 in the presence of PBS only caused a small reduction in titre of less than one

order of magnitude, but incubation in the presence of pocket factors was able to reduce the titre by over four orders of magnitude (Figure 5.11 A). This indicates that incubation in the presence of different pocket factors can reduce virus stability as well as improve it. Work should, however, be repeated with BEV1 alongside to confirm the observation made previously (Ismail-Cassim et al. 1990).

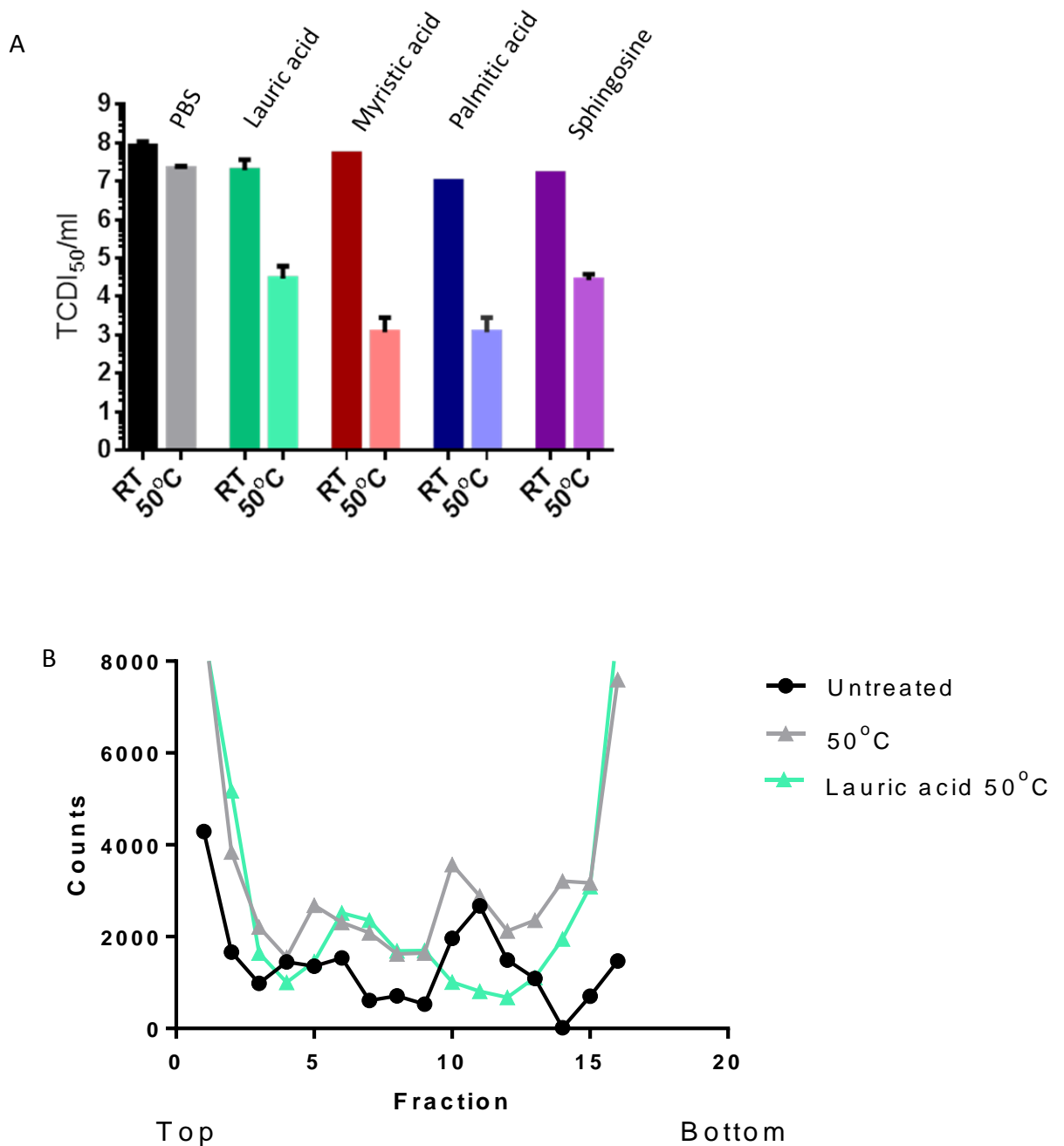


Figure 5.11 Effect of heating on BEV2 after incubation in the presence of short chain fatty acids. (A) BEV2 was incubated in the presence of either PBS, *lauric acid* (green), *myristic acid* (red), *palmitic acid* (blue), *sphingosine*(purple) for one hour at 37 °C prior to heating to 50 °C for 30 minutes in a thermocycler. Samples were then titrated before and after heating by TCID₅₀ assay (B) Sample of ³⁵S-labelled BEV that was either untreated, heated to 50 °C for 30 minutes or incubated in the presence of *lauric acid* for one hour prior to heating to 50 °C for 30 minutes and were subjected to ultracentrifugation through a 15-45% sucrose gradient. The gradient was fractionated and each sample was analysed by scintillation counting to detect the sedimentation position of each sample. n = 1

5.2 The potential use of antibodies and/or purified receptor to distinguish between heated and native empty particles

Now that methods to stabilise the virus capsid had been established, methods to distinguish between native and non-native antigenicity were required. Previous work had shown that an antibody known as D6 was discriminatory between empty and full virus particles (Wang et al. 2012). Purified receptors PSGL1 or SCARB2 were also tested as reagents to detect conformational changes as they had previously been shown to be specific to non-expanded virus particles (Qing et al. 2014).

5.2.1 Immunoprecipitation of EV71 using capsid antibodies D6 and A9

Initially antibodies that had been shown to bind natively antigenic EV71 were tested using immunoprecipitation.

The antibodies used were monoclonal antibodies D6 and A9 that had been shown to only be able to interact with natively antigenic EV71 (Wang et al. 2012). Initially both antibodies were used in immunoprecipitation assays to establish if they could distinguish between virus in heated and non-heated (native) crude lysates (Figure 5.12). Immunoprecipitations were performed with ³⁵S-methionine/cysteine radiolabeled EV71 crude lysate and analysed by SDS-PAGE and autoradiography. It was evident from this that both antibodies recognised native EV71 but not the heated EV71 (“heated antigenicity”). The autoradiograph shows VP0, VP1, VP2 and VP3 bands, with a lower intensity observed for VP2 than VP0. This lower intensity could be due to differences in methionine and cysteine residues in the VPs, as VP1 has 13, VP3 has 12 and VP0 has 10, whereas VP2 has 9. However it is more likely that this sample contains as high proportion of empty capsids compared to mature

virions. As empty capsids contain uncleaved VP0 and in mature virions VP0 is cleaved into VP2 and VP4. Both antibodies were also tested by Western blot, however nothing was detected, suggesting that they recognise conformational epitopes only.

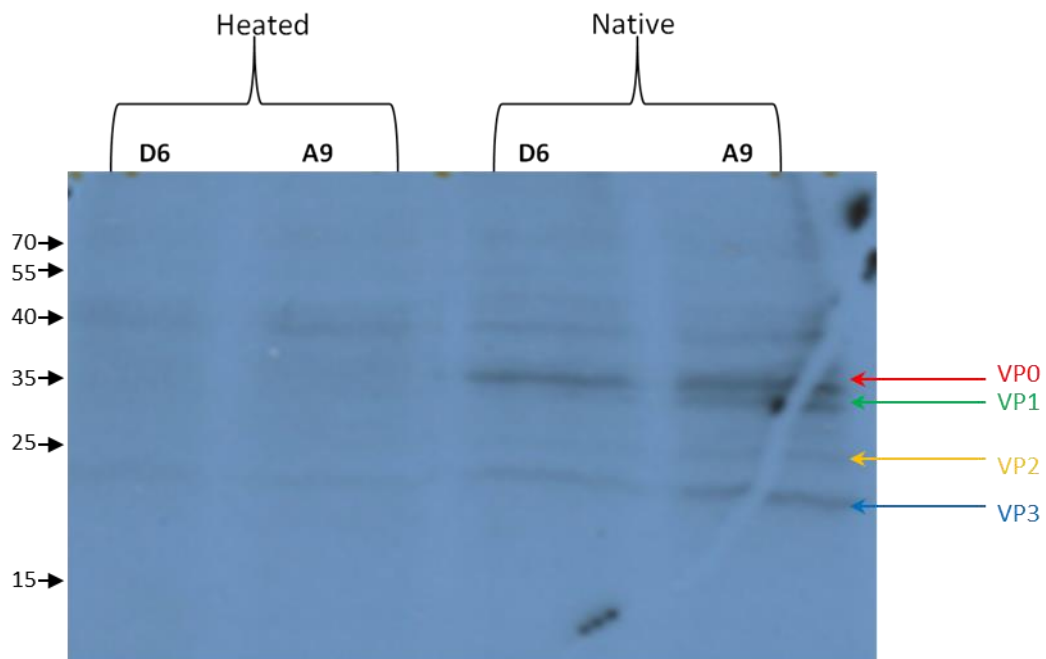


Figure 5.12 Antibodies recognise native virus particles but not heated virus particles. Immunoprecipitations (See materials and methods section 2.6) were performed with ³⁵S labelled EV71 crude lysate that had either been heated to 50 °C for 30 minutes or was untreated. The resulting immunoprecipitation was then analysed by SDS PAGE and autoradiography. D6 and A9 are only able to detect native antigenicity (Wang et al. 2012).

5.2.2 Use of ELISA in combination with EV71 receptors and antibodies to detect native EV71 antigenicity

As it was established that antibodies D6 and A9 could distinguish between native and heated antigenicity, it was attempted to use the antibodies in an ELISA using purified receptor as a capture molecule.

ELISA plates were coated with one of two EV71 purified receptors (PSGL1 or SCARB2, supplied by Prof Ian Jones, University of Reading) overnight at 4 °C. The following day the plates were incubated with either EV71 crude lysate, heated EV71 crude lysate (50 °C), EV71 VLPs produced in a baculovirus system (provided by Ian Jones, University of Reading) or control non-infected Vero cell crude lysate. After washing the plates, samples were then incubated with either A9 or D6, followed by an HRP-conjugated anti-mouse secondary antibody and developed with OPD substrate. The OD 492 nm values showed the untreated EV71 crude lysate sample to have a significantly higher reading than VLPs and Vero cell lysate, indicating that WT antigenicity was detected (Figure 5.13). Although a higher reading was generally observed in the untreated EV71 compared to heated, a significant difference was only seen in one of the receptor antibody combinations against heated EV71 (SCARB2/A9), the error bars were very large in the other samples. All readings were quite low therefore this appears to be an ineffective method of detecting EV71 antigenicity.

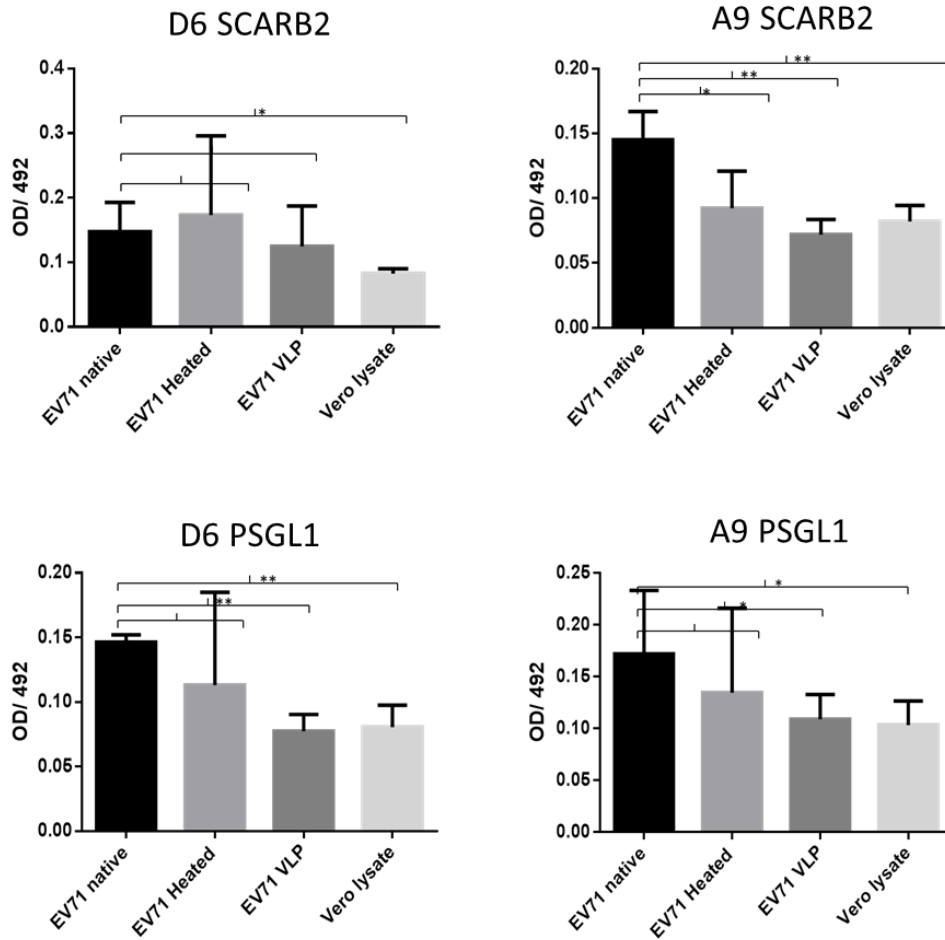


Figure 5.13 Graphs to illustrate ELISA results of EV71 captured with purified receptor (SCARB2 or PSGL1) and detected using antibodies raised against the whole capsid (D6 or A9). * = $p \geq 0.01$, ** = ≥ 0.001 .

5.3 Discussion

In this section methods for increasing thermostability and detecting antigenic stability of EV71 were explored. This work has highlighted the role of the VP1 pocket in enterovirus stability, and that compounds which bind residues within this structure were shown to have dramatic effects on the thermostability of both EV71 and BEV.

Initially, attempts to improve the thermostability of EV71 used natural selection by heating the virus between each passage to 50 °C, a temperature which was shown to reduce the titre by over 99.9% (Figure 5.3, 5.4). This resulted in identification of a mutant of EV71 with increased thermostability (Figure 5.2), which possessed two mutations in the VP1 pocket (V179A, L183V). Observations of the WT crystal structure indicated that these mutations could increase the pocket size (Figure 5.6, 5.10). This could have two possible effects; it could allow the pocket factor to bind deeper into the pocket, it could allow it to bind to a larger pocket factor, or both. It was also shown that inhibitors that bind the VP1 pocket can improve enterovirus stability, and mutations that give resistance to these inhibitors reduce thermostability (Figure 5.14). Work described in Chapter 3 showed that the pocket-binding inhibitor NLD was able to improve the thermostability of WT EV71, but had no effect on thermolabile/inhibitor-resistant EV71. The same effect is seen in other enteroviruses, with pocket-binding inhibitors improving thermostability, while thermolabile/inhibitor-resistant mutants with bulky residues filling the pocket were unaffected by the inhibitor (Groarke & Pevear 1999; Heinz et al. 1989; Lacroix et al. 2014; Liu et al. 2012; Mosser et al. 1994; Salvati et al. 2004). In addition, it has also

previously been demonstrated that natural pocket factors improve thermostability and function as inhibitors to prevent infection in BEV1 (Ismail-Cassim et al. 1990; Smyth et al. 2003).

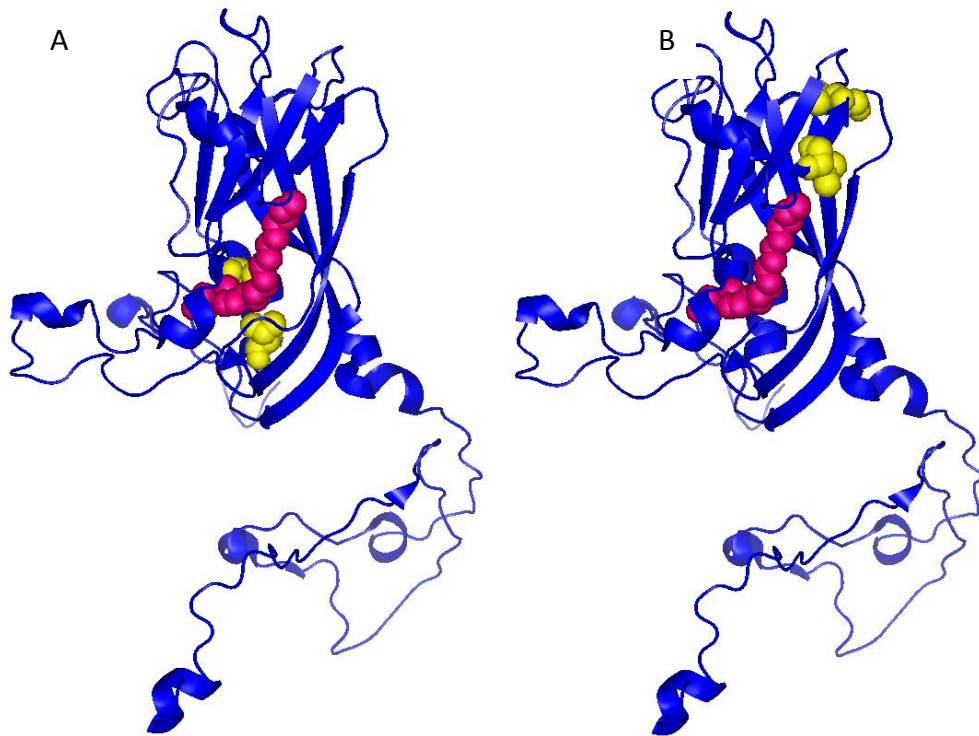


Figure 5.14 Comparison of location of mutations in (A) inhibitor-resistant/thermolabile EV71 and (B) thermostable. Crystal structure of WT EV71 with mutations of thermolabile/inhibitor resistant EV71 and thermostable EV71 highlighted by yellow spheres, VP1 is in blue and the pocket factor is represented as hot pink spheres. Modelled using PyMol.

Together, this work shows that pocket factor binding is important for enterovirus stability. To test how the different mutations in the pocket affected pocket factor interactions, the effect of different compounds that are able to bind and occupy the pocket have on the thermostability of the different EV71 mutants was compared (Figure 5.6).

Here, virus was incubated in the presence of fatty acids at a very high concentration (1000 nM) for a prolonged period of time to displace the natural pocket factor. NLD has a high binding affinity so can displace the natural pocket factor at low concentrations (Discussed in section 1.3, chapter 3). Incubation in the presence of NLD was able to improve the thermostability of both WT and thermostable EV71. NLD-binding increased the temperature at which WT began to lose titre from ~46 °C to ~51 °C and increased the temperature at which thermostable EV71 began to lose titre from ~52 °C to ~54 °C (Figure 5.8). Incubation of WT EV71 in the presence of different fatty acids reduced thermostability to varying degrees, with the exception of sphingosine, which has a more bulky head that potentially allows it to bind better because it can make more contacts (Figure 5.7). In thermostable EV71 all of the fatty acids tested, including sphingosine, were shown to decrease thermostability to a more dramatic degree than for WT EV71 (Figure 5.7). The reason for the increase in stability when the two isolates are incubated in NLD is postulated to be that the compound displaced the natural pocket factor due to a higher binding affinity. This stabilised the virus by making it more difficult to release this unnatural pocket factor due to a higher binding affinity and therefore was unable to undergo conformational changes associated with loss of native antigenicity. However, in the case of the fatty acids reducing virus stability, it is likely that because the virus had been incubated in such high concentrations of these pocket factors the natural pocket factor had been displaced by mass action. These compounds do not bind with a higher affinity and are therefore more easily displaced, causing the thermostability to be reduced. The potential reasons for sphingosine having no effect on the stability of WT virus capsid, are either because it is the natural pocket

factor or it binds with the same affinity as the natural pocket factor, therefore incubation in its presence has no visible effect. This suggests that the mode of action of these mutations is to change the affinity for pocket factors. As in WT, sphingosine had no effect on thermostability, but reduced the thermostability of the thermostable isolate. This indicates that thermostable EV71 no longer uses sphingosine as its natural pocket factor. It is not possible to tell whether the mutations do affect the size of the pocket factor, as a pocket factor has not yet been identified which has no effect on the thermostability of the thermostable mutant. More fatty acids could be tested to determine this.

Pocket factor preference, however, cannot be the only effect on thermostability due to the effect observed for NLD. Thermostable EV71 was more stable than WT in the presence of NLD and NLD was still able to further increase the thermostability of thermostable EV71. If pocket factor preference was the only reason for an increase in thermostability then both isolates would have the same thermostability in the presence of NLD as it is not available in the cell. Therefore, it appears that thermostable EV71 interacts with NLD with a higher affinity. If the mutations were merely affecting which pocket factor binds, and what pocket factor binds was the sole determinant of capsid stability then the thermostability of both isolates would be the same when incubated in same pocket factor.

This work so far has shown that the pocket factor is important for enterovirus stability and that binding of certain pocket factors is able to reduce virus stability. The role of the pocket factor and its ability to destabilise enteroviruses is further demonstrated using BEV. Lauric acid was previously shown to improve the

thermostability of BEV1 (Ismail-Cassim et al. 1990; Smyth et al. 2003), while in this work it was shown to reduce thermostability in BEV2, along with several other fatty acids of different sizes (Figure 5.11). It would be useful to repeat this experiment with BEV1 to observe the effects of other fatty acids on heat stability and to confirm the effects of lauric acid. It would also be useful to test the effect of a larger range of fatty acids to see if it was possible to find one that was able to improve the heat stability of EV71. It would also be useful to test a wide range of concentrations.

To further demonstrate the importance of pocket factor binding on enterovirus stability, the thermolabile/inhibitor-resistant EV71 isolate was incubated in the presence of different pocket factors and its thermostability was then assessed revealing that the presence of different pocket factors and NLD had no effect on its thermostability (Figure 5.7 C). It is predicted that the mutations fill the entrance of the pocket with bulky side chains so that NLD and the natural pocket factor cannot bind the pocket, which causes a reduction in stability. To test if these mutations do prevent the pocket factor from binding WT virus and the thermolabile/inhibitor-resistant virus, these samples were incubated in the presence of ^3H palmitic acid overnight. Palmitic acid is a pocket factor that was shown to reduce WT stability and have no effect on the stability of the thermolabile/inhibitor-resistant EV71 (Figure 5.7). When the association of ^3H palmitic acid and the two virus isolates was assessed by analysis on nycodenz gradients, it was revealed that palmitic acid was able to associate with both isolates (Figure 5.9). This is unexpected as it was predicted that palmitic acid would be unable to bind the thermolabile/inhibitor-

resistant isolate, it should be noted that the incubation time of this experiment was overnight, in contrast to experiments detailed in section 5.1.4 where incubations were one hour. The experiments here therefore need to be repeated over the same time range. However, these results do appear to establish that palmitic acid can still bind thermolabile/inhibitor-resistant EV71. The effects of NLD remain unclear.

When this incubation experiment was repeated in the presence of NLD for two minutes, it was shown that NLD was able to prevent palmitic acid from associating with WT, but for the thermolabile/inhibitor-resistant mutant, NLD prevented palmitic acid binding in one experiment but had no effect in another (Figure 5.9). These observations require further investigation.

Finally, strategies to detect an antigenic shift away from native antigenicity have been developed. It has been demonstrated that two different antibodies (D6 and A9) are only able to detect EV71 in its native non-heated form using IPs (Figure 5.12). ELISAs using these antibodies and purified receptors as capture molecules were also shown to be able to detect the difference between native and heated antigenicity, although it was not very sensitive (Figure 5.13). It would be useful to further optimise this method to make it more sensitive. It would be useful to use these antibodies to produce an EV71 antigenicity curve to see if it was possible to detect the actual point of a shift away from native antigenicity and to correlate with infectivity.

In the future this work would need to be carried out with EV71 VLPs to see if the strategies used here were able to improve the antigenic stability of VLPs

Chapter 6

Chapter 6 Concluding remarks and future perspective

The virus capsid plays many important roles in the virus life cycle such as; host cell recognition, cell entry, uncoating and protection of viral RNA from degradation. In this thesis artificial selection, inhibitory compounds and structural analysis have been combined to further understand aspects of these multiple roles.

One aspect studied here was cell entry of EV71 in Vero cells. It was revealed that incubation of EV71 in a low pH buffer on Vero cells causes a reduction in titre (discussed in section 4.2). Given that incubation of the virus in the presence of its receptor SCARB2 is known to induce uncoating (Chen et al. 2012; Dang et al. 2014) it was hypothesised that the prolonged treatment at a low pH on the cell surface in the presence of SCARB2 induced the virus to uncoat outside of the cell, which caused the observed reduction in titre. Repeated exposure to these conditions resulted in a mutant, termed the acid-resistant mutant (VP1 N104S) (discussed in section 4.2). Structural data and comparisons of susceptibility of WT and the acid-resistant mutant phenotypes to different inhibitors, indicated that the acid-resistant mutant (VP1 N104S) may not undergo SCARB2-mediated uncoating and is instead reliant on another EV71 uncoating initiator, the proline isomerase cyclophilin A. As the acid-resistant mutant is less susceptible to the cyclophilin A inhibitor cyclosporine A, it was predicted that the acid-resistant mutant has a higher binding affinity for cyclophilin A, as has been demonstrated for other EV71 isolates resistant to cyclosporine A analogues (Qing et al. 2014). It was speculated that the mechanism by which N104S causes an increased affinity for cyclophilin A is by making residue P103 more accessible/available than in the WT. We predicted that N104 blocks cyclophilin A interaction with P103, either directly or indirectly by allowing interactions with SCARB2. To confirm this proposed mode of action several things must be established such as the role of binding to SCARB2/cyclophilin A, the

ability of SCARB2/cyclophilin A to induce uncoating at neutral pH and low pH and how the acid-resistant mutant (N104S) interacts with SCARB2 and cyclophilin A in cells. Initially this work would require the creation of the following mutants to act as controls for the inhibitor experiments; VP1 P103A, VP1 P103A/N104S. This work would be needed to confirm that P103 is involved in cyclophilin A interactions. To assess the roles that N104 and P103 play in binding to SCARB2 and cyclophilin A, co-immunoprecipitation of SCARB2/cyclophilin A with the following EV71 isolates WT, VP1 N104S, VP1 P103A, VP1 N104S/P103A could be performed and compared. Mature virions or small peptide sequences (Dang et al. 2014) could be used in these experiments. The same approach could be used to assess how binding of SCARB2 and cyclophilin A mutually influence each other by pre-treating with one uncoating initiator and observing the binding of the other. Such experiments would show whether the mutations are able to either increase or decrease binding. The structures of each mutant in combination with both SCARB2 and cyclophilin A would need to be solved using either crystallography and/or cryo-EM to determine how each residue interacts with the uncoating initiators.

This would help to determine how the mutations affect binding, but further work would need to be done to determine their functionality. To determine if N104S affects SCARB2-mediated cell entry, infectivity experiments could be carried out comparing WT and the acid-resistant mutant using a cell line that is artificially expressing SCARB2 but no other EV71 receptors (Yamayoshi et al. 2009). This would confirm that virus could only have entered via SCARB2 and no other unknown receptors which are present in Vero cells.

To elucidate the role of these residues in uncoating, uncoating assays of each mutant in the presence and absence of acidic conditions with both purified SCARB2 and cyclophilin A would need to be performed. This could be done by tracking conversion of mature 160S

particles into uncoating intermediate 135S or empty 80S particles by use of a sucrose gradient (described in sections 1.2.1, 1.2.4, Chen et al 2012, Dang et al 2014).

Finally toxicity experiments (such as MTT assays) of the compounds used would need to be performed to ensure that the observed effects were not due to the cell death (Mosmann 1983).

Further knowledge of this could aid strategies to prevent the interactions between SCARB2/cyclophilin A and could potentially lead to structure-based design of inhibitors that are able to bind the virus capsid and block these interactions.

Further to the role of certain residues in cell entry and uncoating, this thesis has demonstrated that EV71 takes an unusually long time to uncoat in comparison to other picornaviruses (Section 4.1.2). In most picornaviruses, cell entry and uncoating occurs within 30 minutes of infection (Brandenburg et al. 2007). Here using an infectivity time course, where EV71 samples were taken for titration every hour post-infection it was shown that the virus titre dropped in the first three hours post-infection. This reduction in infectivity suggests that the virus has undergone uncoating, as reported by Lu et al 2011. However, another time course experiment examining the time at which EV71 lost susceptibility to the uncoating inhibitor NLD, revealed that this did not occur until five hours post-infection (Section 4.1.2). Therefore the virus cannot have completed uncoating until after five hours post-infection. Together, these data indicate that EV71 begins to uncoat three hour post-infection, but does not complete it until six hours post-infection. It is possible that initial structural rearrangements occur by three hours post-infection, which reduces its infectivity, but the virus then takes a further two hours to releases its RNA. To confirm what is occurring between three and five hours post-infection, a further time course should be carried out to assess what uncoating stage the virus particle is at each time point, e.g. mature 160S, uncoating intermediate 135S or empty 80S (described in

1.2.1, 1.2.4). This could be achieved by analysing samples from each time point on a sucrose gradient, which is able to separate these three particle types based upon their density. If it is confirmed that viral particles undergo structural rearrangements, to uncoating intermediate particles (135S) before they uncoat at five hours post-infection, it would need to be tested if these particles are less infectious and still susceptible to NLD. This would reveal what is happening to the EV71 capsid during its unusually long uncoating time, but it would not reveal why it takes so long. To get a better understanding of what is happening to the virus at each stage and what induces uncoating, a time course of compounds that affect cell entry, uncoating, virus trafficking, endosome acidification and endosome maturation could be carried out. This would aid in annotating exactly when certain events occur and give an idea of when the virus interacts with different uncoating factors. Live cell and confocal imaging, staining for EV71 and different cellular markers could be used to determine where it is in the cell and what it is associating with at each time point. This would be very useful in terms of further understanding the virus life cycle, which could have implications in therapeutic strategies.

This work discussed so far has focused on how uncoating effects the virus in relation to the cell. Another major focus of the work in this thesis has been on the effect compounds that bind the VP1 pocket have on enterovirus capsid stability (Chapters 3 & 5). The VP1 pocket is a hydrophobic cavity that harbours a lipid that must be ejected before uncoating can occur (Discussed in section 1.2.4). Previous work has shown that compounds that bind this pocket with high affinity and displace the natural pocket factor can increase the capsid stability. This stabilising effect can make the virus unable to uncoat and these compounds can therefore act as inhibitors. Both novel synthetic compounds and natural pocket factors are able to do this (Discussed in section 1.3). Here it was established that two novel compounds NLD and ALD were able to inhibit EV71 infection *in vitro* and NLD was shown to improve the virus thermostability (sections 3.1, 3.3). NLD was shown to be more than an order of

magnitude more potent than the previous most powerful EV71 pocket-binding inhibitor (GPP3) and was not toxic to cells at inhibitory concentrations. In addition, the effects of EV71 resistance towards these three compounds (NLD, GPP3 and ALD) were studied. WT virus was repeatedly passaged in their presence, until the titre of virus grown in the presence of the compounds was equivalent to WT grown without inhibitors. These resistant isolates were shown to be genetically and thermally unstable and thermostability could not be increased by incubation with NLD. Sequencing revealed that they all possessed the same two mutations in the VP1 pocket (I113M and V123L). Modelling predicted that these mutations fill the pocket and prevent binding of NLD and the natural pocket factor. Experiments conducted to test if the mutations did prevent NLD and pocket factor binding were inconclusive and need to be repeated. Natural fatty acids were not shown to be able to inhibit uncoating.

This work has demonstrated the potential effectiveness of NLD as an EV71 therapeutic. However further work needs to be carried out before it could be used in humans, such as testing its efficacy against other enteroviruses, the efficiency of the compounds at preventing disease in animal models, virulence of the resistant virus and further characterisation of the action of NLD and resistance.

It would be useful to test the efficiency of NLD at inhibiting other enteroviruses, given that HFMD is caused by a broad range of viruses and it is impossible to tell if EV71 is the causative agent without either serum testing or sequencing. NLD would be a better therapeutic if it was able to treat a wider variety of viral infections. Work so far has shown NLD is able to inhibit CVA16 (De Colibus et al. 2014) and PV (Adeyemi, University of Leeds, unpublished, Neyts, KU Leuven, unpublished), but not CVB4 (Neyts, KU Leuven, unpublished). Viruses that should be tested with high priority are CVA6 and CVA10, which

are the next largest causative agents of HFMD after EV71 and CVA16, and also CVA7 which, like EV71, can be neurotropic (Table 1.1).

While establishing if NLD has a broad range effect, it will be essential to test if it is effective and non-toxic *in vivo* as well as *in vitro*. Further to the testing of the *in vivo* efficiency of the compound, the virulence and rate at which resistance evolves must be further evaluated. It would be useful to establish if resistance would evolve *in vivo*. Work with PV has shown that it takes much more time for resistance to evolve *in vivo* than *in vitro* (Tanner et al. 2014). This could be investigated by PCR analysis of mouse faeces or blood after infection with EV71 and treatment with NLD.

Finally it would be good to confirm the exact mechanism action of NLD. Work by Dang et al 2014 confirmed that it prevents uncoating as measured by preventing conversion from 160S particles to 135S or 80S particles (section 4.1.2). However, some pocket-binding inhibitors in other enteroviruses can also prevent receptor binding (Mckinlay et al. 1992). This experiment could be conducted using co-immunoprecipitation with EV71 to investigate if receptors bind EV71 in the presence of NLD. Further to this, live cell imaging could be used to assess if NLD can prevent endocytosis, by measuring the distance travelled into the cell as performed in Brandenburg et al. 2007.

The work described above has highlighted the role of the pocket factor in capsid stability and the use of compounds such NLD as enterovirus inhibitors. To further study capsid thermostability a selection experiment was carried out by repeatedly exposing the virus to 50 °C, a temperature which reduced the WT titre by over 99.9% (Figure 3.7, Section 5.1.2). This resulted in selection of an isolate that tolerated a temperature 5.5 °C higher than WT. Sequencing revealed two mutations in the VP1 pocket (V179A, L183V) which appear to increase the size of the pocket. In an attempt to better understand the effect of these heat stabilising mutations and the role of the pocket factor, the effect of different fatty acids on

heat stability was compared between WT, thermostable and inhibitor-resistant/thermolabile EV71. This work showed that all fatty acids tested (other than sphingosine) lowered the thermostability of WT, indicating that sphingosine could be the natural pocket factor. All fatty acids tested reduced the stability of thermostable EV71 and to a higher degree than the WT, indicating that none of these are the natural pocket factor. Therefore the mutations change the pocket factor preference. In addition to this the mutations also appear to make the capsid more sensitive to changes in pocket factor. This work has given further insight into how the “wrong” pocket factor effects heat stability, however work in BEV1 has shown that this virus naturally associates with multiple different pocket factors and that some natural pocket factors can have a stabilising effect. To better determine the role of the pocket factor, the exact pocket factor population must be examined and the way in which virus interacts with each pocket factor must be determined.

To determine the natural pocket factor population, purified virus could be analysed by mass-spectrometry as was previously done for BEV1 (Smyth et al. 2003) or by NMR. It would be useful to investigate virus produced from several different cell lines as well, to see if this made an impact on the pocket factor population. Recently, structural analysis has indicated that different cell lines can affect which pocket factor binds (Ren et al. 2015). Further screening of different fatty acids could be employed; a suggested list is in the appendix 2. A pocket factor that was able to stabilise EV71 could potentially be used as an inhibitor or aid inhibitor design.

To understand the interactions occurring with the different pocket factors, predictive modelling or solving the structure of the viruses in the presence of different pocket factors would need to be carried out. This would give information about exactly what interactions form between the pocket and the different pocket factors.

Another way to study the interactions of different pocket factors would be to perform a series of artificial selection experiments in the presence of different pocket factors at elevated temperatures. This could select for a change in pocket factor. The mutations identified could give further information about how pocket factor preference is formed.

The work described here has provided information about how the VP1 pocket is involved in structural stability, if it was desired to select for further heat stabilising mutations that are not involved in pocket factor binding, a heat stability selection experiment could be set up using the inhibitor resistant mutant, which it is hypothesised not to harbour a pocket factor.

Now that heat stabilising strategies have been established, the question remains regarding whether incubation with NLD and/or the mutations V179A and L183V are able to also improve the stability of VLPs. First the antigenic stability of untreated WT virus and VLPs produced in a recombinant system would need to be evaluated and then compared to the various different stabilising strategies. This could be done by creating heat stability curves in the same manner as previous experiments but instead of assessing titre, the native antigenicity could initially be assessed using antibodies D6 and A9. Section 5.1.2 showed that D6 and A9 were able to distinguish between native and heated antigenicity. This could be done via IP or ELISA, but ELISA would require further optimisation. Although these antibodies will be useful in assessing the virus antigenicity, further antibodies that could bind other sites on the capsid would need to be developed. This would enable further assessment of the antigenicity of a variety of epitopes on the capsid and therefore give a fuller view of the capsids antigenicity. Once a method to maintain VLP antigenic stability is established it would be required to test their efficacy as a vaccine in an animal model. There are several different animal models available for EV71 such as the suckling mouse model described in section 1.4.3, murine-adapted EV71 virus model (Johan Neyts, KU Leuven, personal communication), transgenic line of mice that have been engineered to express

human SCARB2 (Y. W. Lin et al. 2013). It would also be useful to test if the same techniques could be used to improve efficacy of other enterovirus VLPs. A further potential method of improving VLP stability would be to over-express a natural pocket factor that has a stabilising effect in the recombinant system.

A final observation made during this thesis is that two distinct types of viable virus particles exist in EV71, non-enveloped and enveloped particles, which can be distinguished by their buoyant densities and the enveloped particles are sensitive to detergent treatment (section 4.1.3). As picornaviruses have traditionally been considered to be non-enveloped viruses this is interesting but not completely unexpected as similar observations have been made for HAV and PV (Feng et al. 2013; Chen et al. 2015). Studies with these viruses have indicated that these two particles have different entry and/or uncoating strategies. Similar observations were made here, although only in an n = 1 experiment and so it would be necessary to undertake a more comprehensive analysis. The presence of two particles with different entry pathways would have implications on our understanding on EV71 cell entry. The work presented here and that reported by others to annotate different cell entry pathways by EV71 has been performed on a population of the two different particles present in cell lysates, which appears to be predominantly enveloped virus. It would be useful to understand the pathways of both particles and look at receptor binding in different cells to assess if there is a difference. Different pathways could have implications in pathogenesis and potentially affect disease treatment. In HAV it has been demonstrated that enveloped particles could be used as a form of immune evasion, therefore testing the neutralising capacity of a panel of different antibodies, such as D6 and A9, against both the enveloped and non-enveloped form would be useful. Determining the structure of the enveloped virus would be useful as it could give a greater insight into how enveloped virus enters a cell and if key areas of the capsid are covered by the envelope, and potentially give an idea of how the envelope is attached to the capsid. In addition to this it would be useful

to use the techniques (buoyancy, EM and detergent treatment) used to determine that EV71 was enveloped, to screen the rest of the picornavirus family to assess if there are other members of the picornavirus family able to produce enveloped particles.

In conclusion, this thesis has produced a body of work that has contributed to a greater understanding of EV71 uncoating and could have implications in the design of future vaccines and antiviral

Chapter 7

Bibliography

Chapter 7 Bibliography

- Acharya, R. et al., 1989. The three-dimensional structure of foot-and-mouth disease virus at 2.9 Å resolution. *Nature*, 337(6209), pp.709–716.
- Ansardi, D.C. & Morrow, C.D., 1995. Amino acid substitutions in the poliovirus maturation cleavage site affect assembly and result in accumulation of provirions. *Journal of virology*, 69(3), pp.1540–1547.
- Ansardi, D.C., Porter, D.C. & Morrow, C.D., 1991. Coinfection with recombinant vaccinia viruses expressing poliovirus P1 and P3 proteins results in polyprotein processing and formation of empty capsid structures. *Journal of virology*, 65(4), pp.2088–2092.
- Arita, M. et al., 2008. Cooperative effect of the attenuation determinants derived from poliovirus sabin 1 strain is essential for attenuation of enterovirus 71 in the NOD/SCID mouse infection model. *Journal of virology*, 82(4), pp.1787–1797.
- Arita, M. et al., 2005. Temperature-sensitive mutants of enterovirus 71 show attenuation in cynomolgus monkeys. *The Journal of general virology*, 86, pp.1391–401.
- Ashraf, S. et al., 2013. Biological characteristics and propagation of human rhinovirus-C in differentiated sinus epithelial cells. *Virology*, 436, pp.143–146.
- Basavappa, R. et al., 1994. Role and mechanism of the maturation cleavage of VP0 in poliovirus assembly: structure of the empty capsid assembly intermediate at 2.9 Å resolution. *Protein science : a publication of the Protein Society*, 3(10), pp.1651–1669.
- Baxt, B., 1987. Effect of lysosomotropic compounds on early events in foot-and-mouth disease virus replication. *Virus research*, 7(3), pp.257–271.
- Berryman, S. et al., 2005. Early Events in Integrin alpha v beta 6-Mediated Cell Entry of Foot-and-Mouth Disease Virus. *Journal of virology*, 79(13), pp.8519–8534.
- Bostina, M. et al., 2011. Poliovirus RNA is released from the capsid near a twofold symmetry axis. *Journal of virology*, 85(2), pp.776–783.
- Le Bouvier, G.L., 1955. The modification of poliovirus antigens by heat and ultraviolet light. *Lancet*, 269(6898), pp.1013–1016.
- Brandenburg, B. et al., 2007. Imaging Poliovirus Entry in Live Cells. *PLoS Biology*, 5(7), p.e183.

- Bubeck, D., Filman, D.J. & Hogle, J.M., 2005. Cryo-electron microscopy reconstruction of a poliovirus-receptor-membrane complex. *Nature structural & molecular biology*, 12(7), pp.615–618.
- Chang, J.-Y. et al., 2012. Selection and characterization of vaccine strain for Enterovirus 71 vaccine development. *Vaccine*, 30(4), pp.703–711.
- Chen, P. et al., 2012. Molecular determinants of enterovirus 71 viral entry: a cleft around Q172 on VP1 interacts with a variable region on scavenger receptor B2. *The Journal of biological chemistry*, 287(10), pp.6406–6420.
- Chen, Y.-H. et al., 2015. Phosphatidylserine Vesicles Enable Efficient En Bloc Transmission of Enteroviruses. *Cell*, 160(4), pp.619–630.
- Chern, J.-H. et al., 2004. Design, synthesis, and structure-activity relationships of pyrazolo[3,4-d]pyrimidines: a novel class of potent enterovirus inhibitors. *Bioorganic & medicinal chemistry letters*, 14(10), pp.2519–2525.
- Chou, A.H. et al., 2013. Formalin-inactivated EV71 vaccine candidate induced cross-neutralizing antibody against subgenotypes B1, B4, B5 and C4A in adult volunteers. *PLoS ONE*, 8(11), e79783.
- Chou, A.H. et al., 2012. Immunological Evaluation and Comparison of Different EV71 Vaccine Candidates. *Clinical and Developmental Immunology*, 2012, p.831282.
- Chou, A.-H. et al., 2012. Pilot scale production of highly efficacious and stable enterovirus 71 vaccine candidates. *PloS one*, 7(4), p.e34834.
- Chow, M. et al., 1987. Myristylation of picornavirus capsid protein VP4 and its structural significance. *Nature*, 327(6122), pp.482–486.
- Chung, C. et al., 2010. Enterovirus 71 virus-like particle vaccine : Improved production conditions for enhanced yield. *Vaccine*, 28(43), pp.6951–6957.
- Chung, Y.-C. et al., 2006. Expression, purification and characterization of enterovirus-71 virus-like particles. *World journal of gastroenterology*, 12(6), pp.921–927.
- Chung, Y.-C. et al., 2008. Immunization with virus-like particles of enterovirus 71 elicits potent immune responses and protects mice against lethal challenge. *Vaccine*, 26(15), pp.1855–1862.
- Clarke, P., Kitchin, N. & Souverbie, F., 2001. A randomised comparison of two inactivated hepatitis A vaccines, AvaximTM and VaqtaTM, given as a booster to subjects primed with AvaximTM. *Vaccine*, 19(31), pp.4429–4433.
- Clarke, T., 2001. Polio's last stand. *Nature*, 409(6818), pp.278–280.

- De Colibus, L., Wang, X., Spyrou, J.A.B., et al., 2014. More-powerful virus inhibitors from structure-based analysis of HEV71 capsid-binding molecules. *Nature structural & molecular biology*, 21(3), pp.282–288.
- De Colibus, L., Wang, X., Spyrou, J. a B., et al., 2014. More-powerful virus inhibitors from structure-based analysis of HEV71 capsid-binding molecules. *Nature structural & molecular biology*, 21(3), pp.282–288.
- Colonno, R.J. et al., 1988. Evidence for the direct involvement of the rhinovirus canyon in receptor binding. *Proceedings of the National Academy of Sciences of the United States of America*, 85(15), pp.5449–5453.
- Coyne, C.B. & Bergelson, J.M., 2006. Virus-induced Abl and Fyn kinase signals permit coxsackievirus entry through epithelial tight junctions. *Cell*, 124(1), pp.119–131.
- Coyne, C.B. et al., 2007. Coxsackievirus entry across epithelial tight junctions requires occludin and the small GTPases Rab34 and Rab5. *Cell Host Microbe*, 2, pp. 181-192
- Curry, S. et al., 1997. Dissecting the roles of VP0 cleavage and RNA packaging in picornavirus capsid stabilization: the structure of empty capsids of foot-and-mouth disease virus. *Journal of virology*, 71(12), pp.9743–9752.
- Dang, M. et al., 2014. Molecular mechanism of SCARB2-mediated attachment and uncoating of EV71. *Protein Cell*, 5(9), pp.692–703.
- Danthi, P. et al., 2003. Genome delivery and ion channel properties are altered in VP4 mutants of poliovirus. *Journal of virology*, 77(9), pp.5266–5274.
- Davis, M.P. et al., 2008. Recombinant VP4 of human rhinovirus induces permeability in model membranes. *Journal of virology*, 82(8), pp.4169–4174.
- Dimmock, N.J. & Tyrrell, D.A.J., 1963. Some physico-chemical properties of rhinoviruses. *Br J Exp Pathol*, 45, pp.271–280.
- Doherty, G.J. & McMahon, H.T., 2009. Mechanisms of endocytosis. *Annual review of biochemistry*, 78, pp.857–902.
- Du, N. et al., 2014. Cell Surface Vimentin Is an Attachment Receptor for Enterovirus 71. *Journal of virology*, 88(10), 5816-5833.
- Feil, S.C. et al., 2012. An Orally Available 3-Ethoxybenzoxazole Capsid Binder with Clinical Activity against Human Rhinovirus. *ACS Med Chem Lett*, 3(4), pp.303–307.
- Feng, Z. et al., 2013. A pathogenic picornavirus acquires an envelope by hijacking cellular membranes. *Nature*, 496(7445), pp.367–371.

- Filman, D.J. et al., 1989. Structural factors that control conformational transitions and serotype specificity in type 3 poliovirus. *The EMBO journal*, 8(5), pp.1567–1579.
- Foo, D.G.W., Alonso, S., Phoon, M.C., et al., 2007. Identification of neutralizing linear epitopes from the VP1 capsid protein of Enterovirus 71 using synthetic peptides. *Virus Research*, 125(1), pp.61–68.
- Foo, D.G.W., Alonso, S., Chow, V.T.K., et al., 2007. Passive protection against lethal enterovirus 71 infection in newborn mice by neutralizing antibodies elicited by a synthetic peptide. *Microbes and Infection*, 9(11), pp.1299–1306.
- Fowler, D.M. et al., 2010. High-resolution mapping of protein sequence- function relationships. *Nature methods*, 7(9), pp.741–746.
- Fricks, C.E. & Hogle, J.M., 1990. Cell-induced conformational change in poliovirus: externalization of the amino terminus of VP1 is responsible for liposome binding. *Journal of virology*, 64(5), pp.1934–1945.
- Fry, E.E. et al., 2003. Crystal structure of Swine vesicular disease virus and implications for host adaptation. *Journal of virology*, 77(9), pp.5475–5486.
- Geller, R. et al., 2007. antiviral approach refractory to development of drug resistance Evolutionary constraints on chaperone-mediated folding provide an antiviral approach refractory to development of drug resistance. *Genes & Development*, 21, pp.195–205.
- Gong, M. et al., 2014. Cryo-electron microscopy study of insect cell-expressed enterovirus 71 and coxsackievirus a16 virus-like particles provides a structural basis for vaccine development. *Journal of virology*, 88(11), pp.6444–6452.
- Grant, R. a et al., 1994. Structures of poliovirus complexes with anti-viral drugs: implications for viral stability and drug design. *Current biology : CB*, 4(9), pp.784–797.
- Groarke, J.M. & Pevear, D.C., 1999a. Attenuated Virulence of Pleconaril-Resistant Coxsackievirus B3 Variants. *Journal of Infectious Diseases*, 179, pp.1538–1541.
- Groarke, J.M. & Pevear, D.C., 1999b. Attenuated Virulence of Pleconaril-Resistant Coxsackievirus B3 Variants. *JID*, 179, pp.1538–1541.
- Groppelli, E., Tuthill, T.J. & Rowlands, D.J., 2010. Cell entry of the aphthovirus equine rhinitis A virus is dependent on endosome acidification. *Journal of virology*, 84(12), pp.6235–6240.
- Gulland, A., 2014. World has been slow to act on polio outbreak in Syria, charity warns. *BMJ*, 348, p.1947.

- Guo, J. et al., 2015. Immunodeficiency-related vaccine-derived poliovirus (iVDPV) cases: A systematic review and implications for polio eradication. *Vaccine*, 33(10), pp.1235–1242.
- Guttman, N. & Baltimore, D., 1977. Morphogenesis of poliovirus. IV. existence of particles sedimenting at 150S and having the properties of provirion. *Journal of virology*, 23(2), pp.363–367.
- Halsey, N.A. et al., 2004. Search for poliovirus carriers among people with primary immune deficiency diseases in the United States, Mexico, Brazil, and the United Kingdom. *Bulletin of the World Health Organization*, 82(1), pp.3–8.
- Heinz, B.A., Rueckert, R.R., Shepard, D.A., Dutko, F.J., Mckinlay, M.A., Fancher, M., et al., 1989. Genetic and molecular analyses of that are resistant to an antiviral compound . Genetic and Molecular Analyses of Spontaneous Mutants of Human Rhinovirus 14 That Are Resistant to an Antiviral Compound. *Journal of virology*, 63(6), pp.2476-2485.
- Hertzler, S., Luo, M. & Lipton, H.L., 2000. Mutation of Predicted Virion Pit Residues Alters Binding of Theiler’s Murine Encephalomyelitis Virus to BHK-21 Cells. *Journal of virology*, 74(4), pp.1994–2004.
- Hoey, E.M. & Martin, S.J., 1974. A possible precursor containing RNA of a bovine enterovirus: the provirion 11. *Journal of General Virology*, 24(3), pp.515–524.
- Hu, Y.-C. et al., 2003. Formation of enterovirus-like particle aggregates by recombinant baculoviruses co-expressing P1 and 3CD in insect cells. *Biotechnology Letters*, 25(12), pp.919–925.
- Huang, S.-W. et al., 2012. Mutations in VP2 and VP1 capsid proteins increase infectivity and mouse lethality of enterovirus 71 by virus binding and RNA accumulation enhancement. *Virology*, 422(1), pp.132–143.
- Ismail-Cassim, N., Chezzi, C. & E, N.J.F., 1990. Inhibition of the uncoating of bovine enterovirus by short chain fatty acids. *Journal of General Virology*, 71, pp.2283–2289.
- Johansson, S. et al., 2002. Molecular analysis of three Ljungan virus isolates reveals a new, close-to-root lineage of the Picornaviridae with a cluster of two unrelated 2A proteins. *Journal of virology*, 76(17), pp.8920–8930.
- John, J., 2009. Role of injectable and oral polio vaccines in polio eradication. *Expert review of vaccines*, 8(1), pp.5–8.
- Katpally, U., Smith, T.J. & Rhinovirus, H., 2007. Pocket Factors Are Unlikely To Play a Major Role in the Life Cycle of Human Rhinovirus Pocket Factors Are Unlikely To Play a Major Role in the Life Cycle of. *Journal of virology*, 81(12), pp.6307-6315.

- Kattur Venkatachalam, A.R. et al., 2014. Concentration and purification of enterovirus 71 using a weak anion-exchange monolithic column. *Virology journal*, 11(1), p p.99-108.
- Ke, Y. & Lin, T., 2006. Modeling the Ligand - Receptor Interaction for a Series of Inhibitors of the Capsid Protein of Enterovirus 71 Using Several Three-Dimensional Quantitative Structure - Activity Relationship Techniques. *J. Med. Chem*, 49, pp.4517–4525.
- Kellogg, E.H., Leaver-fay, A. & Baker, D., 2011. Role of conformational sampling in computing mutation-induced changes in protein structure and stability. *Proteins*, 79(3), pp.830–838.
- Kew, O.M. et al., 2005. Vaccine-derived polioviruses and the endgame strategy for global polio eradication. *Annual review of microbiology*, 59, pp.587–635.
- Kok, C.C., 2015. Therapeutic and prevention strategies against human enterovirus 71 infection. *World Journal of Virology*, 4(2), pp.78-95.
- Kolpe, A.B. et al., 2012. Display of enterovirus 71 VP1 on baculovirus as a type II transmembrane protein elicits protective B and T cell responses in immunized mice. *Virus Research*, 168(1-2), pp.64–72.
- Kouivaskaia, D. V et al., 2011. Original article Immunological and pathogenic properties of poliovirus variants selected for resistance to antiviral drug V-073. *Antiviral Therapy*, 16(7), pp.999–1004.
- Ku, Z. et al., 2013. Neutralizing Antibodies Induced by Recombinant Virus-Like Particles of Enterovirus 71 Genotype C4 Inhibit Infection at Pre- and Post-attachment Steps. *PLoS ONE*, 8(2), pp.1–8.
- Kuo, R.-L. & Shih, S.-R., 2013. Strategies to develop antivirals against enterovirus 71. *Virology journal*, 10(1), pp.28-36.
- Lacroix, C. et al., 2014. A novel benzonitrile analogue inhibits rhinovirus replication. *Journal of Antimicrobial Chemotherapy*, 69(June), pp.2723–2732.
- Lee, W.M., Monroe, S.S. & Rueckert, R.R., 1993. Role of maturation cleavage in infectivity of picornaviruses: activation of an infectosome. *Journal of virology*, 67(4), pp.2110–2122.
- Lehtinen, M. et al., 2012. Overall efficacy of HPV-16/18 AS04-adjuvanted vaccine against grade 3 or greater cervical intraepithelial neoplasia: 4-year end-of-study analysis of the randomised, double-blind PATRICIA trial. *The lancet oncology*, 13(1), pp.89–99.
- Li, C. et al., 2012. In Vitro Assembly of an Empty Picornavirus Capsid follows a Dodecahedral Path. *Journal of Virology*, 86(23), pp.13062–13069.

- Li, H. et al., 2013. Virus-like particles for enterovirus 71 produced from *Saccharomyces cerevisiae* potentially elicits protective immune responses in mice. *Vaccine*, 31(32), pp.3281–3287.
- Li, X. et al., 2001. The C-terminal residues of poliovirus proteinase 2Apro are critical for viral RNA replication but not for cis- or trans-proteolytic cleavage. *Journal of General Virology*, 82(2), pp.397–408.
- Lin, H.-Y. et al., 2013. Caveolar Endocytosis Is Required for Human PSGL-1-Mediated Enterovirus 71 Infection. *Journal of virology*, 87(16), pp.9064–9076.
- Lin, S.-Y. et al., 2014. Evaluation of the stability of enterovirus 71 virus-like particle. *Journal of bioscience and bioengineering*, 117(3), pp.366–371.
- Lin, Y.-L. et al., 2011. Enterovirus type 71 neutralizing antibodies in the serum of macaque monkeys immunized with EV71 virus-like particles. *Vaccine*, 30, pp 1305-1312
- Lin, Y.W. et al., 2013. Human SCARB2 Transgenic Mice as an Infectious Animal Model for Enterovirus 71. *PLoS ONE*, 8(2), p.e57591.
- Lin, Y.-W. et al., 2009. Enterovirus 71 infection of human dendritic cells. *Experimental biology and medicine (Maywood, N.J.)*, 234(10), pp.1166–1173.
- Lin, Y.-W. et al., 2012. Human SCARB2-Mediated Entry and Endocytosis of EV71. *PloS one*, 7(1), p.e30507.
- Liu, C.-C. et al., 2007. High immunogenic enterovirus 71 strain and its production using serum-free microcarrier Vero cell culture. *Vaccine*, 25(1), pp.19–24.
- Liu, F. et al., 2012. Research in Veterinary Science Virus-like particles : potential veterinary vaccine immunogens. *Research in Veterinary Science*, 93(2), pp.553–559.
- Liu, H. et al., 2012. Characterization of Poliovirus Variants Selected for Resistance to the Antiviral Compound V-073. *Antimicrobial agents and chemotherapy*, 56(11), pp.5568–5574.
- Liu, J. et al., 2011. Lycorine reduces mortality of human enterovirus 71-infected mice by inhibiting virus replication. *Virology Journal*, 8(1), pp.483-500.
- Liu, Y. et al., 2015. Structure and inhibition of EV-D68, a virus that causes respiratory illness in children. *Science*, 347(6217), pp.71–74.
- Logan, D. et al., 1993. Structure of a major immunogenic site on foot-and-mouth disease virus. *Nature*, 362(6420), pp.566–568.

- Lokugamage, K.G. et al., 2008. Chimeric coronavirus-like particles carrying severe acute respiratory syndrome coronavirus (SCoV) S protein protect mice against challenge with SCoV. *Vaccine*, 26(6), pp.797–808.
- López-Macías, C. et al., 2011. Safety and immunogenicity of a virus-like particle pandemic influenza A (H1N1) 2009 vaccine in a blinded, randomized, placebo-controlled trial of adults in Mexico. *Vaccine*, 29(44), pp.7826–7834.
- Luo, M. et al., 1987. The atomic structure of Mengo virus at 3.0 Å resolution. *Science*, 235(4785), pp.182–191.
- Macadam, A.J. et al., 2006. Rational design of genetically stable, live-attenuated poliovirus vaccines of all three serotypes: relevance to poliomyelitis eradication. *Journal of virology*, 80(17), pp.8653–8663.
- Macejak, D.G. & Sarnow, P., 1992. Association of heat shock protein 70 with enterovirus capsid precursor P1 in infected human cells. *Journal of virology*, 66(3), pp.1520–1527.
- Mao, Q. et al., 2013. The cross-neutralizing activity of enterovirus 71 subgenotype C4 vaccines in healthy chinese infants and children. *PLoS ONE*, 8(11), pp.16–20.
- Marongiu, M.E. et al., 1981. Poliovirus morphogenesis. I. Identification of 80S dissociable particles and evidence for the artifactual production of procapsids. *Journal of virology*, 39(2), pp.341–347.
- Martín-Acebes, M. a et al., 2009. Internalization of swine vesicular disease virus into cultured cells: a comparative study with foot-and-mouth disease virus. *Journal of virology*, 83(9), pp.4216–4226.
- Martín-Acebes, M.A. et al., 2011. Foot-and-mouth disease virus particles inactivated with binary ethylenimine are efficiently internalized into cultured cells. *Vaccine*, 29(52), pp.9655–9662.
- Mckinlay, M.A. et al., 1992. Treatment of the picornavirus common cold by inhibitors of viral uncoating and attachment. *Annual review of microbiology*, 46, pp.635–654.
- McMinn, P. et al., 2001. Neurological manifestations of enterovirus 71 infection in children during an outbreak of hand, foot, and mouth disease in Western Australia. *Clinical infectious diseases*, 32(2), pp.236–242.
- Mcminn, P.C., 2003. Enterovirus 71 in the Asia-Pacific region : An emerging cause of acute neurological disease in young children. *Neurol J Southeast Asia*, 8, pp.57–63.
- McMinn, P.C., 2012. Recent advances in the molecular epidemiology and control of human enterovirus 71 infection. *Current opinion in virology*, 2(2), pp.199–205.

- Meng, T. et al., 2011. Display of VP1 on the surface of baculovirus and its immunogenicity against heterologous human enterovirus 71 strains in mice. *PloS one*, 6(7), p.e21757.
- Mosmann, T., 1983. Rapid colorimetric assay for cellular growth and survival: application to proliferation and cytotoxicity assays. *Journal of immunological methods*, 65(1-2), pp.55–63.
- Mosser, A.G., Sgro, J. & Rueckert, R.R., 1994. Distribution of drug resistance mutations in type 3 poliovirus identifies three regions involved in uncoating functions . Distribution of Drug Resistance Mutations in Type 3 Poliovirus Identifies Three Regions Involved in Uncoating Functions. *Journal of virology*, 68(12), pp.8193-8201.
- Mulcahy, L.A., Pink, R.C. & Carter, D.R.F., 2014. Routes and mechanisms of extracellular vesicle uptake. *Journal of extracellular vesicles*, 3, pp.1–14.
- Mulder, A.M. et al., 2012. Toolbox for Non-Intrusive Structural and Functional Analysis of Recombinant VLP Based Vaccines: A Case Study with Hepatitis B Vaccine. *PloS one*, 7(4), p.e33235.
- Mutsvunguma, L.Z. et al., 2011. Theiler’s murine encephalomyelitis virus infection induces a redistribution of heat shock proteins 70 and 90 in BHK-21 cells, and is inhibited by novobiocin and geldanamycin. *Cell Stress and Chaperones*, 16(5), pp.505–515.
- Nishimura, Y. et al., 2013. Enterovirus 71 Binding to PSGL-1 on Leukocytes: VP1-145 Acts as a Molecular Switch to Control Receptor Interaction. *PLoS Pathogens*, 9(7), p.e1003511.
- Nishimura, Y. et al., 2009. Human P-selectin glycoprotein ligand-1 is a functional receptor for enterovirus 71. *Nature medicine*, 15(7), pp.794–797.
- Nishimura, Y., Wakita, T. & Shimizu, H., 2010. Tyrosine sulfation of the amino terminus of PSGL-1 is critical for enterovirus 71 infection. *PLoS pathogens*, 6(11), p.e1001174.
- Olson, N.H. et al., 1993. Structure of a human rhinovirus complexed with its receptor molecule. *Proceedings of the National Academy of Sciences of the United States of America*, 90(2), pp.507–511.
- Panjwani, A. et al., 2014. Capsid Protein VP4 of Human Rhinovirus Induces Membrane Permeability by the Formation of a Size-Selective Multimeric Pore. *PLoS pathogens*, 10(8), p.e1004294.
- Paul, Y., 2009. Oral polio vaccines and their role in polio eradication in India. *Expert review of vaccines*, 8(1), pp.35–41.

- Pevear, D.C. et al., 1999. Activity of Pleconaril against Enteroviruses Activity of Pleconaril against Enteroviruses. *Antimicrobial agents and chemotherapy*, 43(9), pp.2109-2115.
- Pevear, D.C. et al., 2005a. Relationship of Pleconaril Susceptibility and Clinical Outcomes in Treatment of Common Colds Caused by Rhinoviruses. *Antimicrobial agents and chemotherapy*, 49(11), pp.4492–4499.
- Pevear, D.C. et al., 2005b. Relationship of Pleconaril Susceptibility and Clinical Outcomes in Treatment of Common Colds Caused by Rhinoviruses Relationship of Pleconaril Susceptibility and Clinical Outcomes in Treatment of Common Colds Caused by Rhinoviruses. *Antimicrobial agents and chemotherapy*, 49(11), pp.4492–4499.
- Plevka, P., Perera, R., Cardoso, J., et al., 2012. Crystal Structure of Human Enterovirus 71. *Science*, 336(6086), p.1274.
- Plevka, P. et al., 2013. Structure of human enterovirus 71 in complex with a capsid-binding inhibitor. *Proceedings of the National Academy of Sciences*, 110, pp.3–7.
- Plevka, P., Perera, R. & Rossmann, M.G., 2012. Structure determination of enterovirus 71 research papers. *Biological Crystallography*, 68, pp.1217–1222.
- Porta, C. et al., 2013. Rational Engineering of Recombinant Picornavirus Capsids to Produce Safe, Protective Vaccine Antigen. *PLoS Pathogens*, 9(3), p.e1003255.
- Praefcke, G.J.K. et al., 2004. Identification of residues in the human guanylate-binding protein 1 critical for nucleotide binding and cooperative GTP hydrolysis. *Journal of Molecular Biology*, 344(1), pp.257–269.
- Premanand, B. et al., 2012. Induction of protective immune responses against EV71 in mice by baculovirus encoding a novel expression cassette for capsid protein VP1. *Antiviral research*, 95, pp. 311-315.
- Qing, J. et al., 2014. Cyclophilin A Associates with Enterovirus-71 Virus Capsid and Plays an Essential Role in Viral Infection as an Uncoating Regulator. *PLoS Pathogens*, 10(10), p.e1004422.
- Ren, J. et al., 2013. Picornavirus uncoating intermediate captured in atomic detail. *Nature Communications*, 4, pp.1927–1929.
- Ren, J. et al., 2015. Structures of coxsackievirus A16 capsids with native antigenicity, implications for particle expansion, receptor binding and immunogenicity. *Journal of Virology*, 4343, pp 1102–1115.
- Rombaut, B. et al., 1990. Creation of an antigenic site in poliovirus type 1 by assembly of 14 S subunits. *Virology*, 174(1), pp.305–307.

- Rombaut, B. & Jore, J.P., 1997. Immunogenic, non-infectious polio subviral particles synthesized in *Saccharomyces cerevisiae*. *The Journal of general virology*, 78 (Pt 8), pp.1829–1832.
- Rossmann, M.G.; et al., 1985. Structure of a human common cold virus and functional relationship to other picornaviruses. *Nature*, 317, pp. 145–153
- Rotbart, H.A., 2002. Treatment of picornavirus infections. *Antiviral Research*, 53, pp.83–98.
- Rotbart, H.A., Connell, J.F.O. & Mckinlay, M.A., 1998. Treatment of human enterovirus infections. *Antiviral research*, 38, pp.1–14.
- Salvati, A.L. et al., 2004. Mechanism of Action at the Molecular Level of the Antiviral Drug 3 (2H) -Isoflavene against Type 2 Poliovirus Mechanism of Action at the Molecular Level of the Antiviral Drug 3 (2H) -Isoflavene against Type 2 Poliovirus. *Antimicrobial agents and chemotherapy*, 48(6), p.2233-2243.
- Schmid, E.M. et al., 2006. Role of the AP2 β -Appendage Hub in Recruiting Partners for Clathrin-Coated Vesicle Assembly. *PLoS Biology*, 4(9), pp.1532–1548.
- Shafren, D.R., Williams, D.T. & Barry, R.D., 1997. A decay-accelerating factor-binding strain of coxsackievirus B3 requires the coxsackievirus-adenovirus receptor protein to mediate lytic infection of rhabdomyosarcoma cells. *Journal of virology*, 71(12), pp.9844–9848.
- Shang, L., Xu, M. & Yin, Z., 2013. Antiviral drug discovery for the treatment of enterovirus 71 infections. *Antiviral Research*, 97(2), pp.183–194.
- Shepard, D. a, Heinz, B. a & Rueckert, R.R., 1993. WIN 52035-2 inhibits both attachment and eclipse of human rhinovirus 14. *Journal of virology*, 67(4), pp.2245–2254.
- Shia, K. et al., 2002. Design, Synthesis, and Structure- Activity Relationship of Pyridyl Imidazolidinones: A Novel Class of Potent and Selective Human Enterovirus 71. *J. Med. Chem*, 45, pp.1644–1655.
- Shih, S. et al., 2004. Mutation in Enterovirus 71 Capsid Protein VP1 Confers Resistance to the Inhibitory Effects of Pyridyl Imidazolidinone Mutation in Enterovirus 71 Capsid Protein VP1 Confers Resistance to the Inhibitory Effects of Pyridyl Imidazolidinone. *Antimicrobial agents and chemotherapy*, 48(9), pp.3523–3529.
- Shingler, K.L. et al., 2013. The Enterovirus 71 A-particle Forms a Gateway to Allow Genome Release: A CryoEM Study of Picornavirus Uncoating. *PLoS Pathogens*, 9(3), p.e1003240.

- Shingler, K.L. et al., 2015. The Enterovirus 71 Procapsid Binds Neutralizing Antibodies and Rescues Virus Infection In Vitro. *Journal of Virology*, 89(3), pp.1900–1908.
- Smith, T.J. et al., 1986. The site of attachment in human rhinovirus 14 for antiviral agents that inhibit uncoating. *Science*, 233(4770), pp.1286–1293.
- Smyth, M. et al., 2003. Identification of the pocket factors in a picornavirus. *Archives of Virology*, 148, pp.1225–1233.
- Smyth, M. et al., 2003. Identification of the pocket factors in a picornavirus. *Archives of Virology*, 148(6), pp.1225–1233.
- Smyth, M. et al., 1995. Implications for viral uncoating from the structure of bovine enterovirus. *Structural biology*, 2, pp.224–231.
- Solomon, T. et al., 2010. Virology, epidemiology, pathogenesis, and control of enterovirus 71. *The Lancet infectious diseases*, 10(11), pp.778–790.
- Strauss, M. et al., 2013. RNA transfer from poliovirus 135S particles across membranes is mediated by long umbilical connectors. *Journal of virology*, 87(7), pp.3903–3914.
- Su, P.-Y. et al., 2015. Cell Surface Nucleolin Facilitates Enterovirus 71 Binding and Infection. *Journal of Virology*, 89, pp.4527–4538.
- Suomalainen, M. & Greber, U.F., 2013. Uncoating of non-enveloped viruses. *Current Opinion in Virology*, 3(1), pp.27–33.
- Superti, F. et al., 1987. The effect of lipophilic amines on the growth of hepatitis A virus in Frp/3 cells. *Archives of Virology*, 96(3-4), pp.289–296.
- Tan, C.W. et al., 2013. Enterovirus 71 Uses Cell Surface Heparan Sulfate Glycosaminoglycan as an Attachment Receptor. *Journal of virology*, 7(7), p e41381.
- Tanner, E.J. et al., 2014. Dominant drug targets suppress the emergence of antiviral resistance. *eLife*, 3, pp.1–16.
- Tesar, M. et al., 1993. Analysis of a potential myristoylation site in hepatitis A virus capsid protein VP4.pdf. *Virology*, 194, pp.616–626.
- Thibaut, H.J., De Palma, A.M. & Neyts, J., 2012. Combating enterovirus replication: State-of-the-art on antiviral research. *Biochemical Pharmacology*, 83(2), pp.185–192.

- Tijmsma, a. et al., 2014. The Capsid Binder Vapendavir and the Novel Protease Inhibitor SG85 Inhibit Enterovirus 71 Replication. *Antimicrobial Agents and Chemotherapy*, 58(11), pp.6990–6992.
- Toth, K.S. et al., 1993. Crystallization and preliminary X-ray diffraction studies of Theiler's virus (GDVII strain). *Journal of Molecular Biology*, 231, pp.1126–1129.
- Tuthill, T.J. et al., 2009. Equine Rhinitis A Virus and Its Low pH Empty Particle : Clues Towards an Aphthovirus Entry Mechanism ? *PLoS pathogens*, 5(10), p.e1000620.
- Tuthill, T.J. et al., 2010. Picornaviruses. *Current topics in microbiology and immunology*, 343, pp.43–89.
- Tyka, M.D. et al., 2011. Landscape Mapping. *J Mol Biol*, 405(2), pp.607–618.
- Wang, X. et al., 2012. A sensor-adaptor mechanism for enterovirus uncoating from structures of EV71. *Nature structural & molecular biology*, 19(4), pp.424–429.
- Wang, X. et al., 2012. Characterization of full-length enterovirus 71 strains from severe and mild disease patients in northeastern China. *PloS one*, 7(3), p.e32405.
- Wang, X. et al., 2015. Hepatitis A virus and the origins of picornaviruses. *Nature*, 517(7532), pp.85–88.
- Wildenbeest, J.G. et al., 2012. Pleconaril revisited: Clinical course of chronic enteroviral meningoencephalitis after treatment correlates with in vitro susceptibility. *Antiviral Therapy*, 17(3), pp.459–466.
- Xing, W. et al., 2014. Hand , foot , and mouth disease in China , 2008 – 12 : an epidemiological study. *Lancet Infect Dis*, 14(April), pp.308–318.
- Xu, L. et al., 2014. Protection against Lethal Enterovirus 71 Challenge in Mice by a Recombinant Vaccine Candidate Containing a Broadly Cross-Neutralizing Epitope within the VP2 EF Loop. *Theranostics*, 4(5), pp.498–513.
- Yamayoshi, S. et al., 2013. Functional comparison of SCARB2 and PSGL1 as receptors for enterovirus 71. *Journal of virology*, 87(6), pp.3335–3347.
- Yamayoshi, S., Iizuka, S., et al., 2012. Human SCARB2-Dependent Infection by Coxsackievirus A7, A14, and A16 and Enterovirus 71. *Journal of virology*, 86(10), pp.5686–5696.
- Yamayoshi, S. et al., 2009. Scavenger receptor B2 is a cellular receptor for enterovirus 71. *Nature medicine*, 15(7), pp.798–801.

- Yamayoshi, S., Fujii, K. & Koike, S., 2012. Scavenger receptor b2 as a receptor for hand, foot, and mouth disease and severe neurological diseases. *Frontiers in microbiology*, 3, pp.32-40.
- Yang, B., Chuang, H. & Yang, K.D., 2009. Sialylated glycans as receptor and inhibitor of enterovirus 71 infection to DLD-1 intestinal cells. *Virology journal*, 6, p0.141-146.
- Yang, S.-L. et al., 2011. Annexin II binds to capsid protein VP1 of enterovirus 71 and enhances viral infectivity. *Journal of virology*, 85(22), pp.11809–118020.
- Ye, X. et al., 2014. Chimeric Virus-Like Particle Vaccines Displaying Conserved Enterovirus 71 Epitopes Elicit Protective Neutralizing Antibodies in Mice through Divergent Mechanisms. *Journal of Virology*, 88(1), pp.72–81.
- Ypma-Wong, M.R. et al., 1988. Protein 3CD is the major Poliovirus proteinase responsible for cleavage of the P1 capsid precursor. *Virology*, 270(1988), pp.265–270.
- Zhang, F. et al., 2014. Oral immunization with recombinant enterovirus 71 VP1 formulated with chitosan protects mice against lethal challenge. *Virology Journal*, 11(1), p.80-85.
- Zhang, L. et al., 2012. Vaccination with coxsackievirus B3 virus-like particles elicits humoral immune response and protects mice against myocarditis. *Vaccine*, 30(13), pp.2301–2308.
- Zhang, Y. et al., 2011. Pathogenesis study of enterovirus 71 infection in rhesus monkeys. *Laboratory investigation; a journal of technical methods and pathology*, 91(9), pp.1337–1350.
- Zhao, D. et al., 2015. Enterovirus71 virus-like particles produced from insect cells and purified by multistep chromatography elicit strong humoral immune responses in mice. *Journal of Applied Microbiology*, 6, pp.12922-12930.
- Zhao, M. et al., 2013. Immunization of N terminus of enterovirus 71 VP4 elicits cross-protective antibody responses. *BMC microbiology*, 13(289), pp.1–9.

Website

WWW, nhs.uk 2012. Available at: <http://www.nhs.uk/Conditions/Hand-foot-and-mouth-disease/Pages/Introduction.aspx> Accessed: 09/03/2016

WWW picornaviridae 2015. Available at; <http://www.picornaviridae.com/>
Accessed: 09/03/2016

WWW,bbcnews 2007, Available; <http://news.bbc.co.uk/1/hi/uk/6930684.stm>,
Accessed; 09/03/2016

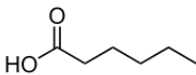
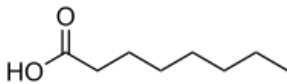
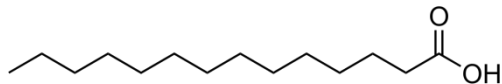
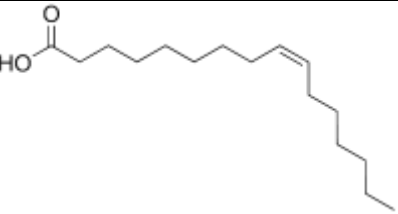
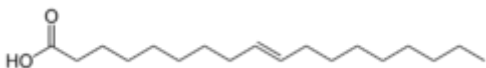
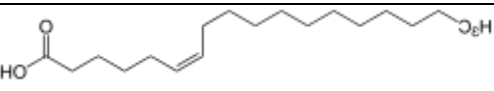
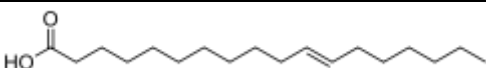
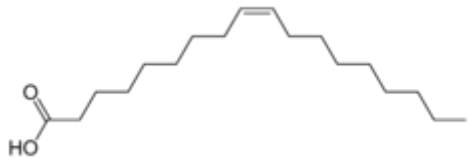
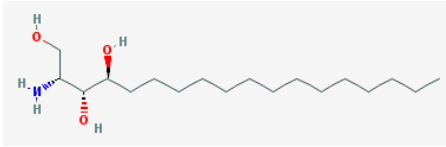
WWW,globalresearch 2015, Available;
<http://www.globalresearch.ca/pharmaceutical-giant-glaxosmithkline-accidentally-released-45-liters-of-concentrated-live-polio-virus-in-the-environment/5405801>,
Accessed: 09/03/2016

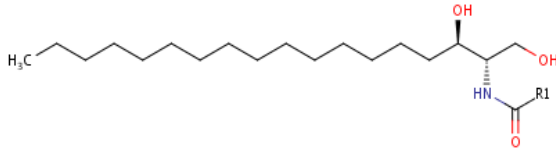
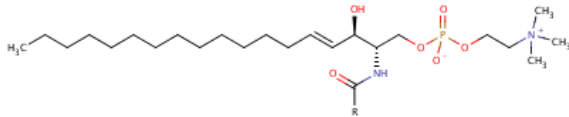
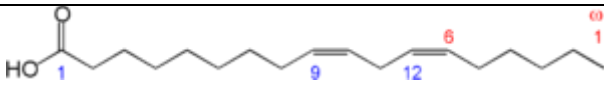
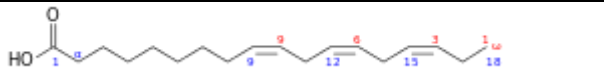
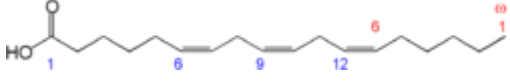
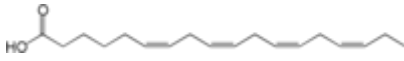
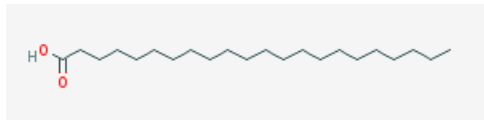
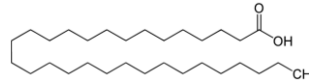
Appendix

Virus	Mutation	Inhibitor	Ref
EV71	I1113M	NLD	
	I1113L	NLD	
	I1113M/L1123V	NLD,GPP3,ALD	
	V1192M	BPROZ-194	Shih et al. 2004
CVA16	L1113F	GPP3	
Polio 1	A1088T/A3024V	V-073	Liu et al 2012
	P1161S	V-073	Liu et al 2012
	I1183T	V-073	Liu et al 2012
	I1194M	V-073	Liu et al 2012
	I1194F	V-073	Liu et al 2012
	A3024V	V-073	Liu et al 2012
Polio 2	D1131V	3(2H)-Isoflavene	Salvati et al 2004
	I1194M	3(2H)-Isoflavene/V073	Salvati et al 2004 /Liu et al 2012
	I1194F	V073	Liu et al 2012
	N1053S	3(2H)-Isoflavene	Salvati et al 2004
	K4058G	3(2H)-Isoflavene	Salvati et al 2004
Polio 3b	M1105T	WIN51711	Mosser et al. 1994
	F1237L	V-073	Mosser et al. 1994/Liu et al 2012
	D1129V	WIN51711	Mosser et al. 1994
	I1192M	V-073	Mosser et al. 1994/Liu et al 2012
	I1192F	WIN51711/V-073	Mosser et al. 1994/Liu et al 2012
	V1194L	WIN51711	Mosser et al. 1994
	M1260L	WIN51711	Mosser et al. 1994
	A3024V	V-073	Liu et al 2012
	S4046L	WIN51711	Mosser et al. 1994
	P1052S	WIN51711	Mosser et al. 1994
	N1051S	WIN51711	Mosser et al. 1994
	A1049V	WIN51711	Mosser et al. 1994
	A2205V	WIN51711	Mosser et al. 1994
	V2208I	WIN51711	Mosser et al. 1994
I3049M	WIN51711	Mosser et al. 1994	
T4053A	WIN51711	Mosser et al. 1994	

HRV14	N1100S	WIN 52035-2	Shepard et al 1993
	N1105S	WIN 52035-2	Shepard et al 1993
	A1150T	LPCRW_0005	Lacroix et al. 2014
	A1150V	LPCRW_0005	Lacroix et al. 2014
	Y1152F	Pleconaril	Ledford et al. 2005
	V1153	WIN 52035-2	Shepard et al 1993
	V1191L	Pleconaril	Ledford et al. 2005
	C1199Y	WIN 52084	Heinz et al 1989
	C1199A	WIN 52084	Heinz et al 1989
	C1199W	WIN 52084	Heinz et al 1989
	C1199F	WIN 52084	Heinz et al 1989
	C1119TC	WIN 52035-2.	Shepard et al 1993
	V1188M	WIN 52084/ WIN 52035-2	Heinz et al 1989/ Shepard et al 1993
	V1188L/L1112F	WIN 52084	Heinz et al 1989
	V1188L	WIN 52084	Heinz et al 1989 Shepard et al 1993
	S1223G	WIN 52084, WIN 52035- 2	Heinz et al 1989
	N1105S/V1176A	WIN 52084	Heinz et al 1989
	N1219S	WIN 52084	Heinz et al 1989
	V1188M/C1119W		
	CVB3	I1092M	Pleconaril
I1092L		Pleconaril	Groarke and Pevear 1999
I1092L/L1207V		Pleconaril	Groarke and Pevear 1999
Echovirus 11	V117I	Pleconaril	Benschop et al 2015
	V119M	Pleconaril	Benschop et al 2015
	I183M	Pleconaril	Benschop et al 2015
	I188L	Pleconaril	Benschop et al 2015

Appendix 1 Table of mutations that give enteroviruses resistance towards pocket binding inhibitors.

Name	Structure
Hexanoic acid C:6	
CAPRYLIC ACID C:8	
C:14	
Palmitoleic acid C16.1	
Elaidic acid C18:1(9trans)	
Petroselinic Acid 6c-18:1	
Vaccenic acid 18:1 <i>cis</i> -11 -11	
Oleic acid C18:1(9cis)	
Phytosphingosine t18:0	
Dihydroceramide C2-C20	

	
Sphingomyelin	
Linoleic Acid 18:2 <i>cis,cis</i> -9,12	
<i>alpha</i> -Linolenic acid C18:3	
Gamma- Linolenic acid 18:3 ω-6	
Stearidonic acid 18:4 W3 C ₁₈ H ₂₈ O ₂	
Behenic acid C:22	
Melissic acid C:30	

Appendix 2. Other fatty acids that could be tested